

ID 1268
20/8/2001

COMPUTERIZED



NATIONAL CHEMICAL LABORATORY
REFERENCE BOOK
(NOT TO BE ISSUED)

**STUDY OF PHASE TRANSITIONS IN
THERMOSENSITIVE POLYMERS**

A THESIS
SUBMITTED TO THE
UNIVERSITY OF PUNE
FOR THE DEGREE OF
DOCTOR OF PHILOSOPHY
(IN CHEMISTRY)

By
VAISHALI S. SHINDE

POLYMER SCIENCE & ENGINEERING GROUP
CHEMICAL ENGINEERING DIVISION
NATIONAL CHEMICAL LABORATORY
PUNE-411 008, INDIA

TH-1284

AUGUST 2001

CERTIFICATE

Certified that the work incorporated in the thesis entitled "Study of Phase Transitions in Thermosensitive Polymers" submitted by Mrs. Vaishali S. Shinde, was carried out under my supervision. Such material as has been obtained from sources has been duly acknowledged in the thesis.

National Chemical Laboratory
Pune 411008.

Dr. R. A. Mashelkar
(Research Guide)

TH-1284

Dedicated to my beloved parents

11-1584

Acknowledgements

I would like to express my sincere thanks and indebtedness to my research guide, Dr. R. A. Mashelkar, FRS, DG, Council of Scientific and Industrial Research (CSIR, India) for his valuable guidance and constant encouragement which he had given me throughout the course of this doctoral research. As an outstanding teacher and scientist, he has given me the benefit of his excellent training in abundant measure. I am also inspired by his commitment and dedication to the science.

Mere words cannot express my gratitude to Dr. M. V. Badiger, since he is one who introduced me to this challenging field. He taught, criticized, encouraged and advised me with patience during my research work and preparation of thesis. I will be always indebted to this outstanding gentleman.

It was great pleasure to discuss some of the work with Dr. A. K. Lele. His suggestions and critical comments carried me in the right direction.

I am thankful to Dr. P. Ratnaswamy, Director, NCL for permitting me to present this work in the form of thesis.

I would like to acknowledge the financial support received from CSIR in the form of senior research fellowship.

I am especially very grateful to Dr. M. G. Kulkarni, Head of PSE Division for fruitful discussions among us during this work. I am also thankful to Dr. P. Rajamohanam, Dr. R. N. Karmalkar, Dr. B. S. Lele, Dr. V. P. Joshi, Mr. M. J. Thaker, Mr. S. S. Patil for their suggestions and cooperation during important stages of my work.

It gives me a great pleasure to thank all my friends in NCL who shared all kinds of moments with me. I enjoyed their company and learnt many things from them.

There are some debts in the world, which cannot be paid off. Whatever I could achieve in my life, has been the dream of my parents, the constant pursuit of which has made my life extremely meaningful and full of happiness. I am very grateful to my brother, Sachin and sisters, Manisha, Savita for their love and unstinted support.

A special thanks to my parent-in-law for their immense cooperation and encouragement which enabled to complete this work.

Mere presence of my son, Suvid who has arrived in this world at the time of compiling of the thesis, has helped to neutralize all my work pressures.

Finally, I am especially very grateful to my husband, Sanjay for his constant encouragement and inspiration during the course of my research work.



Vaishali S. Shinde

CONTENTS

	Page No.
List of Figures	vi
List of Tables	ix
Abbreviations	x
Abstract	xi

CHAPTER I

Literature Survey

1.1	Introduction	1
1.2	Stimuli-responsive polymers	2
1.3	Gels	2
1.4	Hydrogels	5
1.5	Classification of hydrogels	5
1.5.1	Naturally occurring hydrogels	5
1.5.2	Synthetic hydrogels	5
1.5.3	Conventional hydrogels	6
1.6	Stimuli-responsive hydrogels	6
1.6.1	pH-sensitive hydrogels	6
1.6.2	Light-sensitive hydrogels	9
1.6.3	Electric field-sensitive hydrogels	9
1.6.4	Magnetic field-sensitive hydrogels	10
1.6.5	Biochemically-sensitive hydrogels	10
1.6.6	Thermosensitive hydrogels	11
1.7	Phase transition in thermosensitive hydrogels	14
1.8	Experimental technique for studying phase transition in thermosensitive Polymers	15
1.8.1	Cloud-point determination	17
1.8.2	Light scattering study	18
1.8.3	Differential scanning calorimetry	19

1.8.4	Viscometry	19
1.8.5	Fluorescence	21
1.8.6	NMR-spectroscopy	21
1.9	Theory	22
1.10	Effect of solvent on phase transition of thermosensitive polymers	26
1.11	Effect of additives on phase transition of thermosensitive polymers	27
1.12	Fundamental interaction for volume phase transition	28
1.12.1	van der-waals interaction	28
1.12.2	Hydrophobic interaction	30
1.12.3	Hydrogen bonding interaction	31
1.12.4	Electrostatic interaction	31
1.13	Applications of thermosensitive polymers	32
1.13.1	Switches and actuators	32
1.13.2	Separations	34
1.13.3	Tissue culture technique	36
1.13.4	Drug delivery system	36
1.13.5	Immunoassays and enzyme reactions	39
1.13.6	Enhanced oil recovery	40
1.13.7	Thermoassociative polymers	42
1.14	Concluding remarks	43
1.15	References	44

Chapter 2

Objectives and scope of work

2.1	Objectives and scope of work	50
2.2	References	52

Chapter 3

Molecular tailoring of thermosensitive hydrogels

3.0	Introduction	53
-----	--------------	----

Part A: Synthesis of hydrophobically modified thermosensitive hydrogels

3.1	Introduction	54
3.1.1	Theory	56
3.1.2	Experimental section	60
3.1.3	Materials	60
3.1.4	Synthesis of monomers	60
3.1.4.1	Acryloyl chloride	60
3.1.4.2	Acryloyl-4-amino butyric acid[X3]	61
3.1.4.3	Acryloyl-6-amino caproic acid [X5]	61
3.1.4.4	Acryloyl-11, ω -amino undecanoic acid [X10]	62
3.1.5	Synthesis of copolymer gels	62
3.1.6	Characterization of gels	65
3.1.7	Results and discussions	66
3.1.7.1	Copolymer structure	66
3.1.7.2	Swelling behaviour and LCST	66
3.1.8	Conclusions	79
3.1.9	References	81

Part B: Synthesis of thermosensitive gels by γ -radiation technique

3.2	Introduction	82
3.2.1	Mechanism of Radiation polymerization and crosslinking	83
3.2.2	Experimental section	85
3.2.3	Materials	85
3.2.4	Synthesis homopolymer and copolymer gels	86
3.2.5	Swelling ratio measurements	86
3.2.6	^{13}C NMR measurements	87
3.2.7	Results and discussions	87
3.2.7.1	Structure and composition of copolymers	87
3.2.7.2	Swelling ratios of copolymer gels	90
3.2.7.3	Effect of molecular weight of PEO on the swelling ratios of copolymer gels	90

3.2.7.4	Thermoreversibility of the copolymer gel	94
3.2.8	Conclusions	94
3.2.9	References	95

Chapter 4

Effect of surfactants on the phase transition of poly(acryloyl aminoacids) based thermosensitive hydrogels

4.1	Introduction	96
4.2	Experimental Section	97
4.3	Materials	97
4.4	Synthesis of monomers	97
4.4.1	Acryloyl chloride	97
4.4.2	<i>N</i> -Acryloyl-L-phenylalanine [APA]	98
4.4.3	<i>N</i> -Benzylacrylamide [NBAm]	98
4.4.4	<i>N</i> -Acryloyl-6-amino caproic acid [A6ACA]	99
4.5	Synthesis of polymers	99
4.6	Swelling ratio measurements	99
4.7	¹³ C NMR measurements	102
4.8	Results and discussions	102
4.8.1	Composition of copolymer gels by solid-state ¹³ C NMR Spectroscopy	102
4.8.2	Swelling characteristics of gels in SDS solution	104
4.8.3	Core-shell morphology in copolymer gels	106
4.8.4	Effect of degree of ionization of -COOH groups on the equilibrium swelling ratios of the copolymer gels	111
4.9	Conclusions	112
4.10	References	114

Chapter 5

The Influence of experimental conditions on the mesoscopic morphologies developed during the phase transition of thermosensitive polymer

5.1	Introduction	115
-----	--------------	-----

5.2	Theory	116
5.2.1	Phase diagram	116
5.2.2	Polymerization kinetics	118
5.3	Experimental section	120
5.4	Materials	120
5.5	Preparation of PNIPAm gel films	120
5.6	Morphology studies	121
5.7	Swelling ratio measurements	121
5.8	Results and discussion	121
5.9	Conclusions	138
5.10	References	139

Chapter 6

Conclusions and directions for future work

6.1	Conclusions	140
6.2	Directions for the future work	142

List of figures

Figure No.	Title of Figure	Page No.
Chapter 1		
Figure 1.1	Schematic diagrams of Phase transition of thermosensitive polymer system in solution and as hydrogel	12
Figure 1.2	Phase transition temperature by cloud point determination	18
Figure 1.3	Phase transition temperature by DSC measurement	20
Figure 1.4	Schematic representation showing of four fundamental molecular Interactions which induces phase transition in gels	29
Figure 1.5	Intelligent polymeric bi-layers	33
Figure 1.6	Separation process based on thermosensitive gels	35
Figure 1.7	Tissue recovery by low temperature treatment	37
Figure 1.8	On-off switching mechanism of drug release	38
Figure 1.9	Thermally induced immunoassay scheme for thermosensitive gels	41
Chapter 3		
Figure 3.1	Sequence of swelling and collapse in the LFHB model	59
Figure 3.2	Reaction scheme for the synthesis of hydrophobic monomers and the copolymer gels	64
Figure 3.3	Comparison of ^{13}C NMR spectra of homopolymer and copolymer gels	67
Figure 3.4	Effect of alkyl chain length on swelling behavior of copolymer gels. Experimental data: (○) PNIPAm; (▲) X3-1; (■) X5-1; (●) X10-1. Lines are theoretical fits	68
Figure 3.5	DSC heating scans of copolymer gels	70
Figure 3.6	Effect of concentration of hydrophobic comonomer on swelling behavior of copolymer gels. Experimental data: (■) X5-1; (▲) X5-3; (●) X5-5. Lines are theoretical fits	71
Figure 3.7	Correlation between LCSTs, ζ and length of alkyl group (X) of the comonomer	76

Figure 3.8	^{13}C NMR Spectra of PEO homopolymer gel VE (a) and copolymer gels VA-2 (b), VA-3 (c), VA-4 (d)	88
Figure 3.9	Swelling ratios of gels as a function of temperature	91
Figure 3.10	Temperature dependent swelling ratios of PEO-PNIPAm copolymer gels prepared from PEO of different molecular weights	92
Figure 3.11	Kinetics of swelling-deswelling of PEO-PNIPAm copolymer gel	93

Chapter 4

Figure 4.1	Chemical structures of gels	101
Figure 4.2	Comparison of ^{13}C CP-MASS spectra of homopolymer [PNIPAm](2C) and copolymer gels [PNIPAm-co-PAPA] [95:5 (2B); 80:20 (2A)]	103
Figure 4.3	Swelling ratios of PNIPAm homopolymer gel as a function of temperature in different concentration of SDS solutions	105
Figure 4.4	Temperature-dependent swelling ratios of PNIPAm-co-PAPA [80:20] copolymer gel in different concentrations of SDS solutions	107
Figure 4.5	Pictures of swollen homopolymer and copolymer gels. (a)PNIPAm homopolymer gel (left) and PNIPAm-co-PNBAm [80:20] copolymer gel (right) swollen in 1.0% SDS solution at 40 °C (b)PNIPAm-co-PAPA [80:20] copolymer gel (left) and PNIPAm-co-P6ACA [80:20] copolymer gel (right) swollen in 1.0% SDS solution at 40 °C. (c)PNIPAm-co-PAPA [95:5] copolymer gel swollen in 1.0% SDS solution at 10 °C (left) and at 40 °C (right)	108
Figure 4.6	Influence of ionization time of -COOH groups on swelling ratios of PNIPAm-co-PAPA [80:20] copolymer gels in 1.0% SDS solution	113

Chapter 5

Figure 5.1	Predicted phase diagram of PNIPAm of different molecular weights	125
Figure 5.2	Tc-MW phase diagram superimposed on reaction paths showing phase separation	126
Figure 5.3	Various reaction paths entering the phase diagram in different regions	129
Figure 5.4	Scanning Electron Microscopy of PNIPAm gel films prepared at different initial conditions. (a) $T_0=6^\circ\text{C}$, $M_0=10\%$ by wt, (b) $T_0=27^\circ\text{C}$, $M_0=10\%$ by wt, (c) $T_0=6^\circ\text{C}$, $M_0=20\%$ by wt, (d) non-adiabatic with one side of the film at 10°C and other side exposed to air	131-132
Figure 5.5	Prediction of temperature rise in a non-adiabatic polymerization process in a film with one side cooled and the other exposed to air	133
Figure 5.6	Swelling capacities of gels having different heterogeneous morphologies	133
Figure 5.7	Swelling kinetics of gels showing heterogeneous morphologies	135
Figure 5.8	Optical transition of P6 gel during swelling	135
Figure 5.9	Absorbance of PNIPAm versus time measured in UV-Vis-spectrophotometer (Shimadzu, UV-1601PC) at constant $\lambda=555\text{ nm}$	137

List of Tables

Table No.	Title of Table	Page No.
Chapter 1		
Table 1.1	Environmental stimuli and their possible responses	3
Table 1.2	Molecular mechanisms of sharp transition	4
Table 1.3	Thermal properties of aqueous polyacrylamide derivatives	7
Table 1.4	Some examples of polymers and surfactants which show LCST behavior in aqueous solutions	13
Table 1.5	Monomers used in pH-sensitive hydrogels	16
Chapter 3		
Table 3.1	Feed compositions of copolymer gels	63
Table 3.2	Molecular parameters.	73
Table 3.3	Hydrogen bonding parameters.	73
Table 3.4	Binary interaction parameters and crosslink density	74
Table 3.5	Comparison between experimentally measured heat of demixing (DSC) and theoretical predictions from equation (3.12)	78
Table 3.6	Feed compositions for the preparation of hydrogels	86
Table 3.7	Chemical shift assignments for ^{13}C peaks in the copolymer	89
Table 3.8	Copolymer composition by ^{13}C NMR spectroscopy	89
Chapter 4		
Table 4.1	Feed composition of homopolymer and copolymer gels	100
Table 4.2	Composition of copolymer gels by ^{13}C NMR spectroscopy	104
Chapter 5		
Table 5.1	Pure component characteristic parameters	123
Table 5.2	Hydrogen bonding parameters	123
Table 5.3	Parameters for kinetics of polymerization	127

Abbreviations

ΔG_{el}	Elastic free energy
v_e	Moles of elastically active chains in the gel
V	Volume of the gel.
V_o	Volume at synthesis at a given temperature and pressure.
ϕ	Volume fraction.
r_i	Number of lattice sites occupied by a molecule of component i.
v_i^*	Characteristic mer volume of component i.
ϵ_i^*	Characteristic mer-mer interaction energy for component i.
ζ_{12}	Binary interaction parameter between components 1 and 2.
$\tilde{\rho}$	Reduced density of the mixture.
\tilde{P}	Reduced pressure.
\tilde{T}	Reduced temperature.
ΔH	Heat of volume transition.
E_{ij}^o, S_{ij}^o and V_{ij}^o	Changes in the energy, entropy and volume due to the formation of an i-j hydrogen bond.
(v_e/V_o)	Cross-link density.
q	Swelling ratio.
k_p	Rate constant of propagation.
k_d	Rate constant of dissociation (of initiator).
k_t	Rate of termination reactions.
f	Efficiency of the initiator.
C_M	Chain transfer coefficient to monomer,
C_S	Chain transfer coefficient solvent
C_I	Chain transfer coefficient to initiator.
R_p	Rate of propagation
K	Thermal conductivity,
ρ	Density
C_p	Specific heat of the reaction mass.

ABSTRACT

Introduction

Recently, the phenomenon of phase transition in polymers has attracted a great deal of attention because of the scientific interest and technological significance. In polymeric hydrogels the discontinuous reversible volume transitions between the swollen and the collapsed phases have been induced by using the trigger of an external stimuli such as temperature, pH, solvent composition, ionic composition, electric field etc.¹ The exciting aspects of these stimuli-responsive hydrogels is that their stimuli responses are smartly and intelligently manifested in changes in shape, phase, optics, mechanics, surface energies, permeation rates, recognition etc. These hydrogels have shown promising applications in gel-based actuators, valves, molecular sensors, controlled-release systems for drugs and other substances, artificial muscles for robotic devices, optical shutters and molecular separation systems.² In view of the emerging practical applications in various fields as far-flung as in medicine and in robotics, these hydrogels have been considered as the materials of 21st century.³

Of the various stimuli mentioned above, temperature is one of the most significant and extensively studied stimuli, which affects the phase transitions. The polymers, which undergo phase transitions as a function of temperature, are called as "thermosensitive or thermoreversible polymers". The phase transition is a manifestation of the competition between two forces acting on the polymer chain. Affinity between the polymer segments tends to shrink the polymer, while the entropic interactions due to the thermal motion of the individual segments tends to expand it. In general, at higher temperature, the entropic interactions dominate the segmental affinity, and the polymer is expanded. At lower temperature the segmental affinity is dominant, and the polymer collapses and the phases separate. The temperature at which a polymer solution separates into two or more phases is known as the phase separation temperature (T_{ps}). Polymer solutions exhibit a great variety of temperature induced phase transitions. It is well known that in general the solubility of a polymer in a solvent increases with an increase in temperature. However, there is a certain class of polymers, which exhibit the thermodynamic lower critical solution temperature (LCST), show an inverse solubility behavior with an increase in

temperature. The classical example is the solution of poly(N-isopropylacrylamide) [PNIPAm]⁴ in water which shows an LCST in the range of 31-33 °C. Below LCST, the polymer is completely soluble in water while it becomes insoluble and it phase-separates above its LCST. With an LCST that approached the normal body temperature made PNIPAm an attractive system for studies related to pharmaceutical and biomedical applications.^{5,6}

Crosslinked hydrogels obtained from these thermosensitive polymers undergo a first order volume transition at the LCST. Thus, the gels are highly swollen below LCST and completely collapsed or shrunk above the LCST. These volume transitions are attributed to the hydrophobic interactions and polymer-polymer/polymer-solvent H-bonding interactions. Thermosensitive polymers find a wide range of applications in separations, controlled drug delivery, biotechnology and robotics. Commercially, these polymers can be used in various processes such as oil-dewatering, food protein separations, metal removal, chromatography, patch drug delivery, flavor release, waste dewatering, etc.⁷⁻⁹

In view of the increasing demand for thermosensitive polymers for various applications, there is a need to develop newer thermosensitive polymers. The present work, therefore, focuses on the design and synthesis of new hydrophobic comonomers and consequent development of novel thermosensitive polymers by incorporating these new comonomers. The structural elucidation of these polymers has been carried out by various spectroscopic techniques. The influence of chemical structure and various additives on the transition properties of these polymers has been corroborated. The entire work is presented in seven chapters. A brief out line of the work is given below,

Chapter 1: Literature Survey

The introductory chapter provides an overview of various aspects of hydrogels pertaining to the fundamental causes of phase transitions, the concept of LCST, molecular interactions, synthesis, characterization, swelling of hydrogels and applications in different fields. The major emphasis, however, is given to thermosensitive polymers, which is the subject of this thesis. A wide variety of experimental methodologies such as UV-turbidimetry and visual observation of macroscopic phase transition, calorimetry, light

scattering, fluorescence, viscometry, IR spectroscopy and NMR spectroscopy which are to study thermosensitive polymers are also discussed in this chapter.

A large number of theoretical models have been proposed in the literature to explain the first order volume transition in non-ionic thermosensitive gels.¹⁰⁻¹³ A brief account of this work is given in this chapter. This chapter also discusses the effect of additives on the transition temperature of the thermosensitive polymers.

Chapter 2: Objective and scope of the work

The present investigation was undertaken to design and synthesize new thermosensitive polymers, especially hydrogels having flexible hydrophobic groups and to study their volume phase transitions as a function of temperature. New hydrophobically modified monomers based on aminoacids were synthesized and copolymerized with PNIPAm. The characterization of the copolymer gels was made by swelling ratio measurement, IR and NMR-spectroscopy. The influence of surfactants such as SDS on the swelling of hydrophobically modified polymer gels was also studied. Such polymer-surfactant interactions have potential applications in controlled release technology and rheology. Therefore, the rheological investigation of the hydrophobically modified polymer-surfactant system was also undertaken.

Chapter 3: Molecular tailoring of thermosensitive hydrogels

In order to develop a thermosensitive polymer for a specific end-application, its LCST has to be tailor made. This can be achieved by changing the chemical structure of the hydrogel by introducing hydrophobic and hydrophilic groups in the chain. Hydrophobic and hydrogen bonding interactions play an important role in determining the transition temperature of the hydrogel. The degree of swelling and the transition temperature of an hydrogel can be modulated by adding co-solutes or co-solvents in the medium or by copolymerization with comonomers, which are more or less hydrophobic in nature. This chapter describes the strategies of changing the chemical structure of hydrogels and the results of our consequent investigations.

Part A: Synthesis of hydrophobically modified thermosensitive hydrogels

This part deals with the synthesis of hydrophobic comonomers containing varying lengths of alkyl groups and a terminal carboxylic acid group. These monomers were copolymerized with poly(N-isopropylacrylamide) to give hydrophobically modified copolymer gels. These hydrogels showed lower LCST and lower heat of transition when compared to pure PNIPAm gel. The reduction in the transition temperature was found to increase with the length of the alkyl group and the concentration of the hydrophobic comonomers. The experimental results were compared with the theoretical calculations based on a lattice-fluid-hydrogen-bond [LFHB] model. A linear correlation between the transition temperature and the number of alkyl groups was found to exist in these gels. Such a correlation could be useful in designing gels with specific transition temperatures. The presence of the terminal carboxylic acid group on the hydrophobic side chain of the comonomer is believed to prevent the association of water molecules around the hydrophobic groups thereby causing a reduction in the heat of transition.

Part B: Synthesis of thermosensitive hydrogels by γ -radiation technique

This part describes the synthesis of copolymer gels based on poly(ethylene oxide) and poly(N-isopropylacrylamide) by γ -radiation technique.¹⁴ The choice of poly(ethylene oxide) [PEO] is mainly due to its excellent biocompatibility and good aqueous swelling characteristics. Although, PEO belongs to a class of LCST polymers its transition temperature is not in the observable range. Therefore, by copolymerising PEO with other LCST polymers the desired transition temperature can be obtained. Furthermore, since these copolymer gels are synthesized by γ -radiation technique, they are free from impurities and can have potential biomedical applications. The structure and composition of the copolymer gels have been studied by ¹³C NMR spectroscopy. The temperature dependent swelling ratio measurements of PEO homopolymer gels do not exhibit a well-defined first order transition. However, the copolymer gels of PEO and PNIPAm showed clear LCST behavior.

Chapter 4: Effect of Surfactants on the Phase transition of poly(acryloyl aminoacids) based thermosensitive hydrogels

Surfactant-Polymer interaction is a subject of considerable theoretical and practical interest. Addition of surfactants to polymers form complex structures, which influences the phenomena of conformation transition, volume phase transitions and rheological behaviors. This chapter deals with synthesis of gels based on poly(N-isopropylacrylamide) and poly(acryloyl aminoacids) and their interactions with an anionic surfactant namely, sodium dodecyl sulfate (SDS). Binding of SDS with copolymer gels enhanced the swelling ratios and LCSTs remarkably. This study led to an interesting observation of core-shell morphology in the swollen gels along with two unusual discontinuous volume phase transitions. These observations were explained on the basis of LCST of copolymer gels, electrostatic charge repulsion and restricted diffusion of surfactant into the gel. Such core-shell morphology in thermosensitive hydrogels can have potential applications in controlled drug delivery systems.¹⁴

Chapter 5: The influence of experimental conditions on the mesoscopic morphologies developed during the phase transitions of thermosensitive polymers

The experimental conditions of synthesis of an hydrogel play an important role in determining the morphology and optical properties of gel. For example, PNIPAm gel when synthesized below its LCST (32 °C) by the conventional route in an aqueous or non-aqueous solvent shows transparency to visible light below the volume phase transition temperature. However, upon heating above the LCST, the gel becomes opaque due to the formation of phase separated domains by spinodal decomposition mechanism. This chapter describes the synthesis of PNIPAm gels under different experimental conditions. These gels showed a wide range of mesoscopic structures depending on the experimental conditions. The mesoscopic structures in these morphologies were formed as a result of phase separation of the polymerizing mixture into polymer-rich and water-rich domains, which were simultaneously frozen into a permanent morphology due to gelation. It has been shown theoretically and experimentally that by controlling the gelation kinetics it was possible to freeze the morphology of a gel in the metastable or the unstable regions of the phase diagram.

Chapter 6: Conclusions and Directions for future work

This chapter summarizes the results and important conclusions of our study. An attempt is made to tailor-make thermosensitive hydrogels (with specific LCSTs) by synthesizing novel hydrophobic comonomers and copolymerising them with existing monomers. The role of hydrophobic and hydrogen bonding interactions on the volume phase transitions has been investigated. The influence of surfactant on the swelling behavior and on morphological and rheological properties of thermosensitive polymers has been studied. The important applications of these polymers in various fields are mentioned. This chapter also presents some suggestions towards the design, synthesis and applications of thermosensitive polymers based on the results obtained from our study.

References:

1. A. S. Hoffman, *Macromol. Symp.*, **98**, 645 (1995).
2. P. S. Russo, (Eds.), *Reversible Polymeric gels and Related Systems*, ACS Symp. Ser., **350**, Amer. Chem. Soc., Washington D.C. (1987).
3. R. A. Mashelkar, *J. Indian Inst. Sci.*, **73**, 193 (1993).
4. M. Heskins, J. E. Guillet, *Macromol. Sci. Chem.*, **2**, 1441 (1969).
5. L. C. Dong, A. S. Hoffman, *J. Controlled Release*, **11**, 255 (1990).
6. A. S. Hoffman, *J. Controlled Release*, **6**, 297 (1987).
7. H. G. Schild, *Prog. Poly. Sci.*, **17**, 163 (1992).
8. M. J. Snowden, M. J. Murray, B. Z. Chowdary, *Chemistry and Industry*, **15**, 531 (1996).
9. R. Dagani, *Chem. Eng. News*, **75**, 26 (1997).
10. K. Otake, H. Inomata, M. Konno, S. Saito, *J. Chem. Phys.*, **91**, 1345 (1989).
11. M. Marchetti, S. Prager, E. L. Cussler, *Macromolecules*, **23**, 3445 (1990).
12. M. M. Prange, H. H. Hooper, J. M. Prausnitz, *AIChE. J.*, **35**, 803 (1989).
13. A. K. Lele, M. V. Badiger, M. M. Hirve, R. A. Mashelkar, *Chem. Eng. Sci.*, **50**, 3535 (1995).
14. T. Kato, K. Fujimoto, H. Kawaguchi, *Polym. Gels Networks*, **2**, 307 (1994).

Chapter 1

Literature survey

1.1 Introduction

Recently, phase transitions in polymers, particularly in polymeric gels have attracted a great deal of attention because of their scientific interest and technological significance.¹ Polymeric gels are three dimensional networks and in the presence of solvent (especially water) are known to exist in two distinct phases, swollen and collapsed. The discontinuous, reversible volume transition occurs between the swollen and the collapsed phases in response to various external stimuli such as temperature, pH, solvent composition, ionic composition, electric field etc. Therefore, they are often termed in the literature as stimuli-sensitive or stimuli responsive gels.² The knowledge on physical and chemical fundamentals of gel phase transition will play a vital role as guiding principles for a wide variety of technological applications of gels. The exciting aspect of these stimuli-sensitive hydrogels is that their stimuli responses are smartly and intelligently manifested in changes in shape, phase, optics, mechanics, surface energies, permeation rates, recognition etc. Therefore, these hydrogels have shown promising applications in gel based actuators, valves, molecular sensors, controlled-release systems for drugs and other substances, artificial muscles for robotic devices, optical shutters and molecular separation systems.^{3,4} In view of the emerging practical applications in various fields as far-flung as in medicine and in robotics, these hydrogels have been considered as the materials of 21st century.

The phase transition is a manifestation of the competition between two forces acting on the polymer chain. Affinity between the polymer segments tends to shrink the polymer, while the entropic interactions due to thermal motion of the individual segments tends to expand it. In general, at higher temperature, the entropic interactions dominate the segmental affinity, and the polymer is expanded. At lower temperature the segmental affinity is dominant, and the polymer collapses and the phases separate. The temperature at which a polymer solution separates into two or more phases is known as the phase separation temperature (T_{ps}). Polymer solutions exhibit a great variety of temperature induced phase transitions.

TH-1284

1.2 Stimuli-responsive polymers

The term "stimuli-responsive polymers" refers to soluble, surface coated or crosslinked polymeric systems, which exhibit relatively large and sharp property changes in response to a small physical or chemical stimuli. There are many external stimuli, which have been applied and the different responses to these stimuli are listed in Table 1.1

There are many possible molecular mechanisms, which can cause such sharp and discontinuous transitions in polymer systems, and they are listed in Table 1.2

1.3 Gels

A polymeric gel is a crosslinked polymer network swollen in a liquid medium. Softness, elasticity and the capacity to store fluid make the gel a unique material. Gels can be crosslinked chemically by covalent bonds or physically by hydrogen bonding, van der Waals forces or hydrophobic and ionic interactions. Gels are interesting objects, which have both liquid-like and solid-like properties. The liquid-like properties result from the fact that the major constituent of gels is usually liquid. For example, a jelly consists of approximately 97% water and 3% gelatin. On the other hand, a gel can retain its shape since it has shear modulus, which becomes apparent when the gel is deformed. The modulus is due to the crosslinking of polymer molecules in the form of network. These aspects of a gel represent the solid nature of gels. In addition to these liquid- and solid-like aspects, a gel can change its state drastically similar to the way a gas changes its volume more than a thousand folds.

Significant progress has been made in the technological applications of gels. Disposable diapers and sanitary napkins use gels as superabsorbents. Gel sheets have been developed to keep fish and meat fresh. Gels are used as a molecular sieve in gel permeation chromatography and in electrophoresis. They are widely used as implants in plastic surgery and for artificial soft contact lenses and other fields like sensors, switches, membranes for separation, adsorbents, transducers, dehydrants and matrices for drug delivery systems, etc.⁵

Table 1.1
Environmental stimuli and their possible reponses

Environmental stimuli	Responses
<ul style="list-style-type: none">• Temperature• pH• Ions• Solvents or salts• Electric fields• Magnetic fields• Electromagnetic radiation• Mechanical stress	<ul style="list-style-type: none">• Phase separation• Shape• Optical• Mechanical• Electrical• Surface energies• Reaction rates• Permeability• Recognition

Table 1.2

Molecular mechanisms of sharp phase transition:

-
- Ionization or neutralization
 - Ion-exchange
 - Ion-ion repulsion or attraction
 - Release or formation of hydrophobically bound water
 - Coil-globule transition
 - Onset or inhibition of chain mobility
 - Crystallization or melting
 - Isomerization between hydrophilic and hydrophobic forms
 - Counter-ion movement in an electric field
 - Electron transfer redox reactions
-

1.4 Hydrogels

Hydrogels are coherent systems rich in water. Essentially, hydrogels are a type of gels in which polymer network is hydrophilic and the liquid component is aqueous in nature. The fundamental building block of a hydrogel is water-soluble monomers. The nature of the crosslinker, polymer network, tacticity and crystallinity can significantly influence the mechanical behavior of these hydrogels. The most characteristic property of hydrogel is that it swells in the presence of water and shrink in the absence of water. The extent of swelling is determined by the nature of polymer chains and crosslinking density. The equilibrium water content depends on swelling pressure of the network. The swelling pressure is the resultant of the difference in water activity inside and outside the polymer and is analogous to the osmotic pressure. Thus, the dried hydrogel (or xerogel) becomes much smaller in size than the hydrogel swollen in water. During swelling and shrinking process, hydrogel can preserve its overall shape.

Hydrogels are of special interest in biomedical and biotechnological fields because of their following properties: i) softness, ii) permeability to small molecules, iii) resemblance to tissues, iv) hydrophilicity or high water content, v) biocompatibility.

1.5 Classification of hydrogels

There are two types of hydrogels,

- (a) Naturally occurring hydrogels
- (b) Synthetic hydrogels

1.5.1 Naturally occurring hydrogels are polysaccharides, carrageenan, gum arabic, agarose, cuprophan, dextrans, collagens etc.⁶ They are mainly used in pulp and paper production, artificial silk and cellulosic membrane production. The limitations of naturally occurring hydrogels are their poor mechanical properties, low temperature tolerance and poor resistance to microbial attack.

1.5.2 Synthetic hydrogels on the other hand have better mechanical properties, good temperature tolerance and resistance to microbial attack. Some of these hydrogels are "conventional" in that they do not exhibit significant sensitivity to environmental changes

such as temperature and pH, while others show varying degrees of responses to such stimuli.⁷⁻⁹

1.5.3 Conventional Hydrogels

Conventional hydrogels have mostly been synthesized from hydroxyethyl methacrylate (HEMA), polyethyleneglycol methacrylate (PEGMA) and the methoxy-terminated derivative (MPGEMA) of an acrylamide (AAm), N-vinyl pyrrolidone (PVP) and polyethylene oxide (PEO). These gels have been most often prepared either as unsupported membranes or beads, or as graft copolymer coatings on more hydrophobic supports. Because such hydrogels are similar to body tissues in their high water contents and are biocompatible, they are used in contact lenses and burn wound dressings.¹⁰ Animal implant studies also suggested that they should be tissue-compatible in vivo in humans.¹¹

1.6 Stimuli-responsive Hydrogels

1.6.1 pH-sensitive Hydrogels

pH-sensitive hydrogels usually contain pendant acidic or basic groups such as carboxylic acids and primary amines or strong acid and bases, such as sulfonic acids and quaternary ammonium salts, which change ionization in response to changes in pH, thus changing the properties of hydrogel.¹² Among the first ionic hydrogels investigated were gels based on acrylic acid and methacrylic acid.^{13,14} Table 1.3 lists some of the monomers used in the preparation of pH-sensitive hydrogels.¹²

It was observed that the equilibrium degree of swelling of these gels responded to changes in pH. When the pH of the swelling solution was increased the gels showed an increase in swelling. The relation between the degree of ionization, α and pH is given by Henderson- Hasselbach equation,¹⁵

$$\text{pH} = \text{pK}_a - n_0 \log(1-\alpha)/\alpha \quad (1.1)$$

Table 1.3
Monomers used in pH-sensitive hydrogels

Type	Monomer	pH-sensitive group
Acidic	Acrylic acid	-COOH
	Methacrylic acid	-COOH
	Sodium styrenesulfonate	-SO ₃ Na ⁺
	Sulfoxymethacrylate	-SO ₃ H
Basic	Aminoethyl methacrylate	-NH ₂
	N, N-dimethylaminoethyl methacrylate	-N(CH ₃) ₂
	N, N-diethylaminoethyl methacrylate	-N(CH ₂ CH ₃) ₂
	Vinylpyridine	pyridine ring
	Vinylbenyl trimethylammonium chloride	-N(CH ₃) ₃ ⁺ , Cl ⁻

where, pK_a is the apparent ionization coefficient and n_0 is a parameter related to the intramolecular interactions in the gels. The equilibrium degree of swelling of pH-sensitive hydrogels is mainly influenced by the charge on the ionic monomer, pK_a of the ionizable group, degree of ionization, concentration of the ionizable monomer in the network and pH, ionic strength and composition of the swelling solution. Furthermore, factors such as crosslinking density and hydrophilicity/hydrophobicity of the polymer also influence the degree of swelling. An acidic hydrogel will be ionized at high pH but unionized at low pH, thus, the equilibrium degree of swelling will increase at high pH. On the other hand, a cationic or basic hydrogel has the opposite pH-dependence of swelling.

pH-sensitive swelling can be exploited in the development of drug delivery systems, which would release the drug in response to the pH of surrounding solution or where pH fluctuations occurs due to pathologic situations or other stimuli. The response of these hydrogels to pH change is very fast and reversible. These could be used for on-off type of drug delivery systems. For oral drug delivery, pH-sensitive hydrogels are useful because of the pH variation throughout the gastro-intestinal tract. The system developed by Siegel and coworkers¹⁶, based on a basic poly(methyl methacrylate-co-N,N-diethylaminoethyl methacrylate) hydrogel, which swells at low pH, can be used in the oral drug delivery of foul fasting drugs. At the neutral pH of mouth, the gel has a low degree of swelling and drug will not be released. As pH decreases in the acidic conditions of the stomach, the degree of swelling increases and drug will be released.

Several research groups developed devices, which release insulin in response to glucose levels.¹⁷⁻¹⁹ Ishihara *et al.*¹⁸ developed a glucose-sensitive membrane system composed of a basic polyamine hydrogels. As the glucose concentration increases, It will diffuse into membrane. It will be converted to gluconic acid by the action of glucose oxidase enzyme and the pH will decrease, resulting in the ionization of basic groups in the gel which will increase the degree of swelling. Insulin loaded in the gel will be then released. The release of insulin could be controlled in response to the changes in glucose concentration.

1.6.2 Light-sensitive hydrogels

Photoresponsive gels have been developed by incorporating photosensitive molecules such as bis (4-dimethyl-aminophenyl)-4'-vinyl-methane-leucocyanide into poly(N-isopropylacrylamide) [PNIPAm] gels.²⁰ When these gels were exposed to UV radiation, they showed a discontinuous volume phase transition. The driving force for the gel expansion was an osmotic pressure differential between the gel inside and the outer solution, which was produced as a result of the photodissociation of the leucocyanide groups, attached to the gel network. A visible light sensitive gel based on N-isopropylacrylamide and a chromophore, tri-sodium salt of copper chlorophyllin showed a discontinuous phase transition on illumination.²¹ They further developed a gel system with optical switch function that undergoes a local shrinking transition upon illumination with visible light that was stable, even after the light source was removed.²²

Similarly hydrogels containing azo linkages in the side chains exhibited a photosensitive behavior.^{23,24} The azobenzene moiety exhibited reversible isomerization from the trans to cis form.

1.6.3 Electric-field sensitive hydrogels

An electric field induced volume phase transitions in gels have been reported by many researchers in the literature.²⁵⁻²⁷ Kurauchi *et al.*²⁸ reported the electric-field sensitive hydrogels, based on poly(acrylic acid)-co-poly(acrylamide) and poly(vinyl alcohol)-co-poly(acrylic acid). These gels swollen in aqueous electrolyte solution showed three types of deformation under the influence of a d.c. electric field; shrinking, swelling and bending. The type of deformation depends on the fraction of sodium acrylate present in the gel, the shape and position of the gel between positive and negative electrodes. The deflection of gel occurs due to the drift of ions under the influence of an electric field. Using this electric field induced deformation, Kurauchi *et al.*²⁹ constructed a prototype of a robot's hand having soft fingers and an artificial fish having a soft tail.

1.6.4 Magnetic field-sensitive hydrogels

Magnetic field-sensitive hydrogels have been developed in which the magnetic and high elastic properties are coupled. This magneto-controlled elastic gel, called a ferrogel is a chemically crosslinked polymer network swollen by ferrofluid.³⁰ Zrinyi *et al.*³¹ prepared a chemically crosslinked poly(vinyl alcohol) (PVA) hydrogel filled with magnetite (Fe_3O_4) particles. When this ferrogel was placed in a nonuniform magnetic field, depending on the field distribution in space, significant elongation, contraction and curvature can be induced in a gel within a second. The peculiar magnetoelastic properties may be used to create a wide range of motions and to control the shape change so that they are smooth and gentle, similar to that observed in muscles. Unlike metallic machine systems, devices made up of gel work without noise, heat evolution or harmful by-products. The magnetic field-sensitive gels have wide range of applications and can be used as switches sensors, micromachines, biomimetic energy-transducing devices, artificial muscles and controlled delivery systems.

1.6.5 Biochemically-sensitive hydrogels

Recently, various schemes have been developed where a gel can undergo volume phase transition in specific response to only one kind of molecule. The idea to undergo phase transition of polymer gels in response to specific type of molecule has been developed by several researchers in the field of controlled-release systems such as drug delivery systems.³²⁻³⁴ The specific release of insulin in response to glucose could also be designed in the form of a 'chemical valve'. Lee *et al.*³⁵ used a hydrogel with entrapped glucose oxidase. The oxidation of glucose to gluconic acid changes ionization of the gel and subsequently the degree of swelling. The pores of the gels were expanded and the insulin previously incorporated in gel was then released.

Tanaka and Kokufuta³⁶ developed the gel that undergoes a discontinuous volume transition at a specific temperature in response to a biochemical reaction by sensing changes in substrate and product composition within the gel phase. The gel consists of network of PNIPAm in which liver esterase is immobilized. The enzyme hydrolyzes ethyl

butyrate into ethanol and butyric acid. A change in substrate-product composition triggers the phase transition.

1.6.6 Thermosensitive hydrogels

Of the various stimuli mentioned above, temperature is one of the most significant and extensively studied stimuli, which affects the phase transitions. The type of polymers, which undergo phase transitions as a function of temperature, are called as "thermosensitive or thermoreversible polymers".

It is well known that in general the solubility of a polymer in a solvent increase with an increase in temperature. However, there is a certain class of polymers, which exhibit the thermodynamic lower critical solution temperature (LCST), show an inverse solubility behavior with an increase in temperature. The classical example is the solution of poly(N-isopropylacrylamide)³⁷ [PNIPAm] in water which shows an LCST in the range of 31-33 °C. Below LCST, the polymer is completely soluble in water while it becomes insoluble and phase-separates above its LCST. The earliest report of the LCST of poly(N-isopropylacrylamide) was in 1967 by Scarpa *et. al.*³⁸ With an LCST that approached the normal body temperature made PNIPAm an attractive system for studies related to pharmaceutical and biomedical applications.^{32,39}

Crosslinked hydrogels obtained from these thermosensitive polymers undergo a first order volume transition at the LCST. Thus, the gels are highly swollen below LCST and completely collapsed or shrunk above the LCST. Figure 1.1 gives a schematic representation of the phase transition in thermosensitive polymers. These volume transitions are attributed to the hydrophobic interactions and polymer-polymer/polymer-solvent H-bonding interactions. Some examples of temperature sensitive polymers are listed in Table 1.4

The thermosensitive swelling-collapse transition of these gels has opened up a multitude of innovative applications in the areas of controlled drug delivery,^{40,41} bioseparations,⁴² robotics,⁴³ bio-medical,⁴⁴ and even consumer products, as summarized recently by Dagani.⁴⁵ Commercially, these polymers can be used in various processes

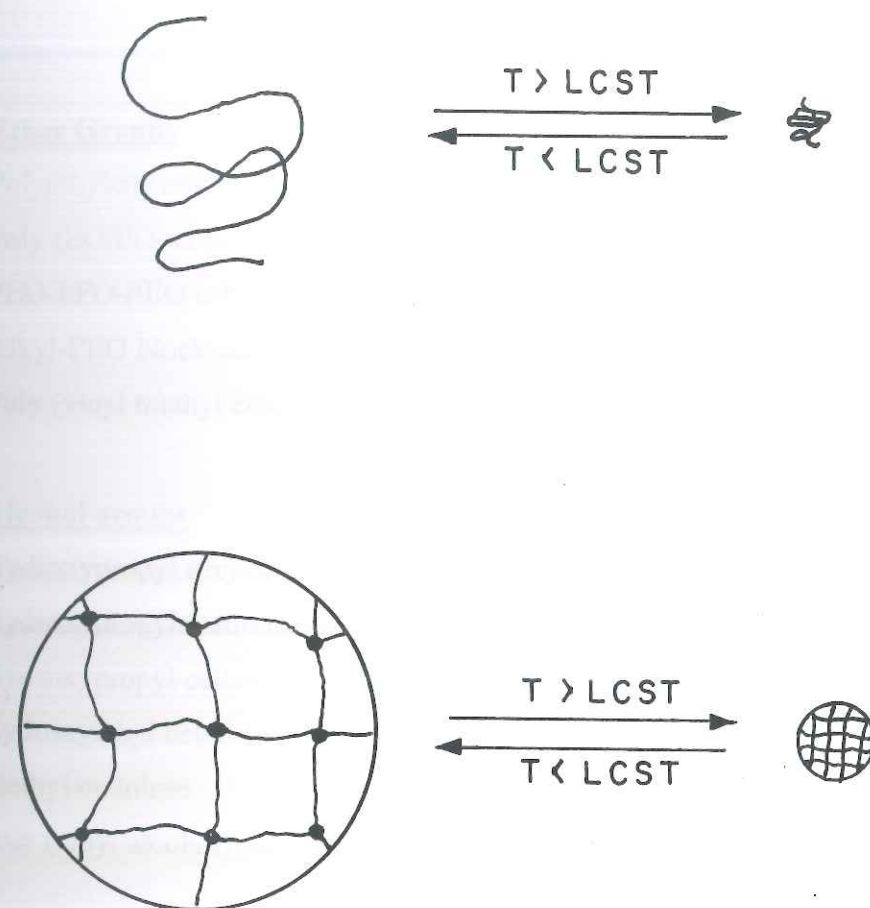


Figure 1.1: Schematic diagrams of phase transition of thermosensitive polymer system in solution and as hydrogel

Table 1.4

Some examples of polymers and surfactants which show LCST behavior in aqueous solutions

Ether Groups

Polyethylene oxide (PEO)
Poly (EO/PO) copolymers
PEO-PPO-PEO triblock surfactants
Alkyl-PEO block surfactants
Poly (vinyl methyl ether) [PVME]

Alcohol groups

Hydroxypropyl acrylate
Hydroxypropyl methylcellulose
Hydroxypropyl cellulose
Hydroxyethyl cellulose
Methyl cellulose
Poly (vinyl alcohol) and derivatives

Substituted Amide Groups

Poly (N-substituted acrylamides)
Poly (N-acryloyl pyrrolidine)
Poly (N-acryloyl piperidine)
Poly (acryloyl-L-amino acid esters)
Poly (ethyl oxazoline)

Others

Poly (methacrylic acid)

such as oil-dewatering, food protein separations, metal removal, chromatography, patch drug delivery, flavor release, waste dewatering etc.⁴⁶

1.7 Phase Transitions in Thermosensitive Polymers

The phase transition in thermosensitive polymers and gels is one of the most fascinating and important phenomena that allows us to explore the principles underlying the molecular interactions and recognition which exists in synthetic and biological polymers. The phase transition of thermosensitive polymers is classified in three categories. The most familiar case is in which the polymer is miscible in all proportions at high temperatures and separate into coexisting homogenous phases (polymer rich and polymer lean) as the temperature is lowered through critical point called as upper critical solution temperature (UCST). The classical example is the solution of polystyrene in cyclohexane.⁴⁷ On the other hand, many alkene polymers, when dissolved in aliphatic or aromatic solvents exhibit a lower critical solution temperature (LCST) that is they phase separate when temperature is increased.⁴⁸ While some systems for example, polyisobutylene in benzene show both UCST and LCST.⁴⁹ This system changes from a two phase to a one-phase system and subsequent changes from a one-phase system to a two phase system when temperature is increased or decreased.

Amongst these, LCST type transition in thermosensitive polymers is studied in the present thesis. Below the LCST, thermosensitive polymer is completely soluble in the solvent (typically in water) and above the LCST, the polymer becomes insoluble and phase separates into two liquid phases, a polymer lean phase and a polymer rich phase. The crosslinked hydrogels obtained from these thermosensitive polymers undergo a first order volume phase transitions at the LCST. These thermosensitive polymers have a balance of hydrophilic and hydrophobic groups. The main cause for thermally induced phase separation is breaking of polymer-water hydrogen bonding (i.e. release of hydrophobically bound water) and formation of polymer-polymer bonding at the critical temperature. The balance of hydrophilic and hydrophobic constituents of the polymer chain plays a major role in determining the LCSTs of these polymers. In general, the LCST is higher with high hydrophilic content and decreases with more hydrophobic content. Therefore, one can design these polymers with desired LCSTs by proper balance of hydrophilic/hydrophobic content. The phase transition in these polymers is attributed

to the fact that, in the solvated state, the polymer chains are extended and are surrounded by water molecules through H-bonding as well as structurally layered water molecules around the hydrophobic groups. However, upon increasing the temperature the H-bonding between polymer and water break and the inter and intra molecular hydrophobic associations dominate leading to the formation of a network like structure resulting in phase transition.

Such a transition is an entropy-driven process where, the release of structured bound water from hydrophobic groups along the polymer main chain is the major contributing thermodynamic force.

Important water-soluble, non-ionic polymers, which form thermosensitive polymers having a wide range of LCST's, are based on N-alkyl acrylamide homopolymers and copolymers. Equilibrium swelling ratios are reported for N-acrylamides gels in the presence of no additives, surfactants, inorganic salts, polar organic components and tetraalkyl ammonium bromides.⁵⁰ Thermal properties of N-alkylacrylamide^{51,52} are given in Table 1.5. Of these polymers, poly(N-isopropylacrylamide) [PNIPAm] having an LCST around 32 °C, has received the attention of most investigators.^{1-5,53}

In view of the increasing demand for thermosensitive polymers for various applications, there is a need to develop newer thermosensitive polymers. Therefore, this thesis focuses on the design and synthesis of new hydrophobic comonomers and consequent development of novel thermosensitive polymers by incorporating these new comonomers. The structural elucidation of these polymers has been carried out by various spectroscopic techniques. The influence of chemical structure and various additives on the transition properties of these polymers has been corroborated.

1.8 Experimental techniques for studying phase transitions in thermosensitive polymers

Phase transitions in aqueous PNIPAm solutions have been investigated in the literature by a wide variety of experimental techniques such as IR-spectroscopy, pH

Table 1.5
Thermal properties of aqueous poly(N-alkyl acrylamide) derivatives

Polymer	LCST (°C)	Heat of phase transition (cal/g)
Poly(N-ethylacrylamide)	72.0	0.1>
Poly(N-ethylmethacrylamide)	50.0	0.1>
Poly(N-n-propylacrylamide)	21.5	11.6
Poly(N-n-propylmethacrylamide)	28.0	12.9
Poly(N-isopropylacrylamide)	30.9	11.1
Poly(N-isopropylmethacrylamide)	44.0	12.0
Poly(N-cyclopropylacrylamide)	45.5	3.5
Poly(N-cyclopropylmethacrylamide)	59.0	4.2
Poly(N-methyl-N-ethylacrylamide)	56.0	5.0
Poly(N,N-diethylacrylamide)	32.0	6.3
Poly(N-methyl-N-isopropylacrylamide)	22.3	6.7
Poly(N-methyl-N-n-propylacrylamide)	19.8	8.3
Poly(N-acryloylpyrrolidine)	56.0	1.3
Poly(N-acryloylpiperidine)	5.5	10.0

measurements, NMR-spectroscopy, viscometry, light scattering, fluorescence, calorimetry, UV turbidimetry and visual observation of macroscopic phase separation. IR-spectroscopy provides molecular level information on possible inter- and intramolecular interactions between functional groups of polymer.^{38, 54} NMR is sensitive to the local structural differences of the polymer chains and has revealed the existence of a discontinuous transition in the relaxation times at the LCST.⁵⁵ Viscometry detects the hydrodynamic consequences of aggregation during the phase transitions.^{37, 56} Light scattering has the ability to monitor concentration fluctuations on a spatial scale of approximately 1000 Å and has been used to detect the collapse of a single PNIPAm chain at a temperature lower than that of the macroscopic phase separation.^{52, 57} An increased spatial resolution of the measurements has been reported for neutron and X-ray scattering and fluorescence techniques, although the latest requires the use of a probe either in free solution or covalently bound to PNIPAm in order to ascertain details of polymer solution behavior.⁵⁸ Solution calorimetry provides thermodynamic parameters that lend insight into the forces responsible for the phase separation.^{52, 59} In the case of hydrogels, the LCST is usually determined by the measurement of the swelling ratio as a function of temperature, or by DSC.

There are several methods for determining LCSTs of thermosensitive polymers, which are summarized in the following section.

1.8.1 Cloud Point Determination

In 1968, Heskins and Guillet³⁷ reported on the study of solution properties of PNIPAm, which is more frequently cited by other researchers. They determined the cloud point by visual observation of the temperature at which first turbidity appeared in a polymer solution immersed in a water bath as the temperature of the bath was raised at 3°C/hr. Measuring cloud point is the simplest and most convenient method of determining the LCST. Figure 1.2 illustrates a typical cloud point curve.

TH-1284

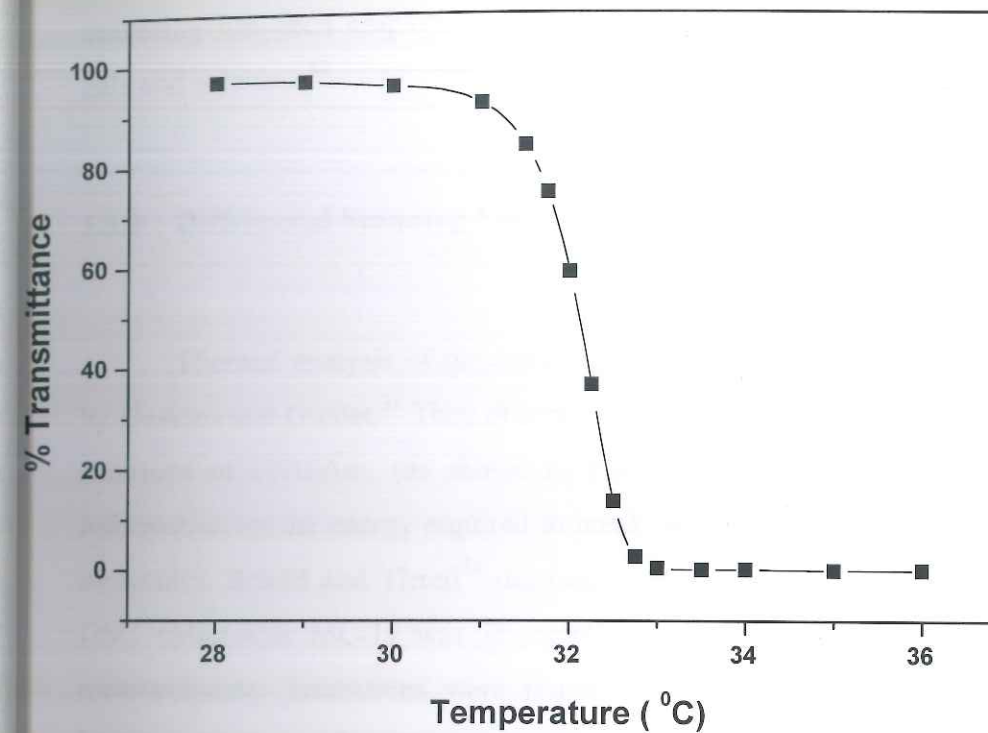


Figure 1.2: Phase transition temperature by cloud point determination

Various researchers have now improved upon these methods by using a standard UV-VIS spectrophotometer. Fixed wavelengths such as 500 nm⁵² or 600 nm⁶⁰ or computer-averaging turbidity from 400 to 800 nm⁵⁸ have been employed.

1.8.2 Light Scattering Study

Experiments using light as a probe offer information on the size, shape, and interactions of macromolecules. Heskins and Guillet³⁷ reported that the apparent molecular weight of a polymer increased 4.5 times on increasing the temperature from 25°C to 33°C, and suggested a simple aggregation phenomenon for the above observation. Kubota et al.⁵⁷ employed dynamic as well as static light scattering to dilute polymer solutions to detect the coil-to-globule transitions. Hirotsu and coworkers⁶¹ applied quasi-elastic light scattering (QELS) technique to study the coil-to-globule transition in

PNIPAm solutions. They observed a collapse of hydrodynamic radius of a polymer chain from 1000 Å to 600 Å upon heating through the LCST zone. Time resolved light scattering has been employed to study the gelation/polymerization kinetics of PNIPAm gels and solutions⁶².

1.8.3 Differential Scanning Calorimetry

Thermal analysis of the demixing transition of linear PNIPAm was first reported by Heskins and Guillet.³⁷ They observed an endotherm at an LCST upon heating aqueous solutions of PNIPAm. (as shown in Figure 1.3) The measured transition heats give information on the energy required to break hydrogen bonds between polymer and water molecules. Schild and Tirrell⁵⁹ demonstrated that the transition which was detected by DSC (MicroCal MC-1) was in excellent agreement with results from cloud point measurements. Transitions were found to be independent of heating rate. However, heating rates in the range of 0.2-0.5°C/min were used for consistent results. Characteristics of the endotherms such as height, width, peak position were also found to be independent of concentration for at least the range 0.4-4.0 mg/ml. However, there was a large difference in the shape and height of the endotherms in PNIPAm's having different molecular weight distributions.

Otake *et al.*⁶³ reported the enthalpy change related to the volume phase transition of PNIPAm gels and proposed a theory for the transition. Shibayama *et al.*⁶⁴ employed DSC to investigate the hydrophobic interaction of PNIPAm and found that about 750 cal/mol of NIPAm monomer units was required for dissociation of the hydrophobic interaction and about 13 water molecules were released from an NIPAm monomer unit.

1.8.4 Viscometry

Heskins and Guillet³⁷ reported viscometry study of PNIPAm in aqueous solutions. The intrinsic viscosity was seen to decrease with increasing temperature. Tam *et al.*⁶⁵ reported on the viscometric technique to study PNIPAm aqueous solutions during the

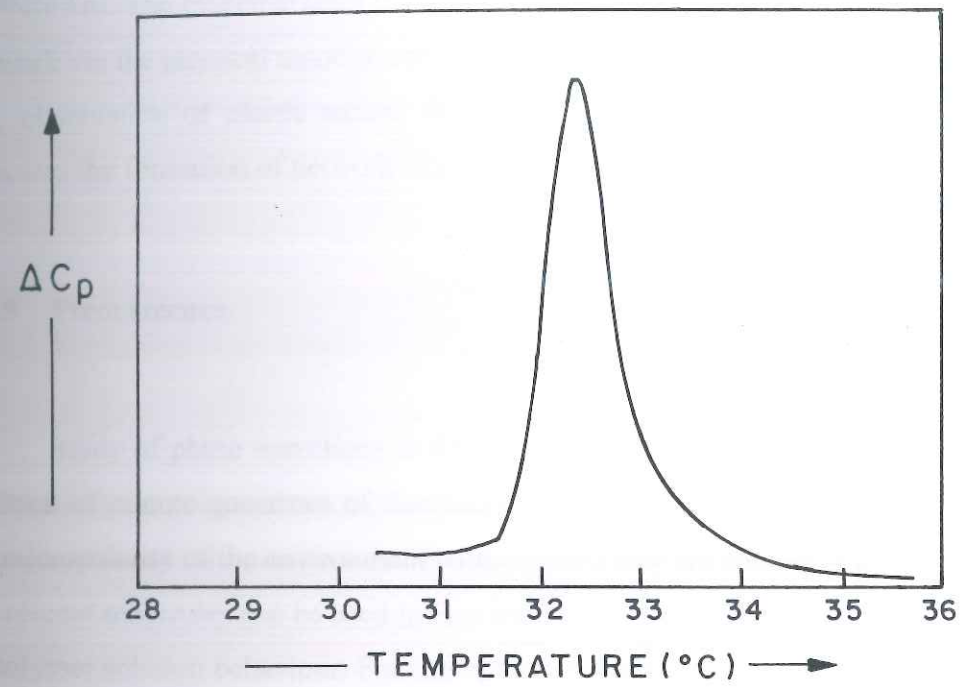


Figure 1.3: Phase transition temperature by DSC measurement

phase transition. The influence of temperature, shear rate, concentration and surfactants on the viscosity were studied and corroborated with the phase transition.

Dynamic viscoelasticity measurements were performed on the aqueous solutions of PNIPAm. The evidence from these measurements indicated the formation of reversible network via the physical associations of hydrophobic side groups in the polymer chains.⁶⁶ The observation of elastic nature, displaying spinnability and Weissenberg effect also indicates the formation of network like structure in the polymer.⁶⁷

1.8.5 Fluorescence

Study of phase transitions in thermosensitive polymers has been enhanced by the addition of minute quantities of fluorescent species whose emission spectra depends on the micropolarity of the environment within which they are solubilized. A wide variety of fluorescent molecules can be used in free solution or covalently bound to ascertain details of polymer solution behaviour. For example, they have been used to detect the LCST of a thermosensitive polymer through their preferential solubilization into a less polar polymer phase. The abrupt transitions in their emission spectra as they solubilized into the less polar, precipitated phase at the LCST would thus, serve as an indication of the transition.

Recently, two research groups have done detailed investigations on fluorescence studies with PNIPAm: Winnink and coworkers,^{58,68-70} and Schild and Tirrell.^{71,72} Both polymer-bound^{58,68,69} and free fluorescence probes^{71,72} have been employed in studying binary solutions of PNIPAm as well as solutions of hydrophobically modified PNIPAm^{58,68,69} and solutions of PNIPAm in the presence of additives.^{71,72}

1.8.6 NMR-spectroscopy

Variable temperature NMR spectroscopy has been used to determine the phase transition temperature of thermosensitive polymers.⁷³⁻⁷⁸ NMR spectroscopy has emerged

as an important tool to investigate the phase transition in polymers since it detects the LCST phenomenon at the molecular level.

Badiger *et al.*⁷⁷ have reported the determination of phase transition temperature of PNIPAm by ¹H-MASS (Magic angle Sample spinning) NMR spectroscopy using linewidth measurements of the resonance arising from the gel. They have recorded ¹H-MASS NMR spectra of D₂O swollen PNIPAm gel at different temperatures above and below LCST. With increase in temperature, the gel underwent volume phase transition resulting in a decrease in the molecular mobility of the polymer segments and intensities of all the proton lines diminished due to broadening of proton lines. The broadening of signals was more severe as the temperature crossed the LCST.

For the linear polymer, the increase in temperature leads to coil to globule transition as well as the interpolymer aggregation resulting in phase separation. Deshmukh *et al.*⁷⁸ have used solution mode NMR and plotted area under the signal as a function of temperature.

1.9 Theory

The volume phase transition was theoretically predicted first by Dusek and Patterson⁷⁹ in 1968 and then discovered experimentally. They suggested the possibility of a discontinuous change in the property of a gel when an external stress is imposed on it. Using the Flory-Huggins equation of state, they realized that with the presence of an external force, Maxwell's loop appears in the isobar of the gel. At the same time, Ptitsyn⁸⁰ showed that a polyelectrolyte chain could undergo coil-to-globule transition if the polymer-solvent interaction or the degree of ionization is changed. A similar phenomenon was theoretically studied by Lifshitz *et al.*⁸¹ and deGennes.⁸² The phase transition in gel is a macroscopic manifestation of a coil-globule transition. In 1977, the critical phenomena in gels were discovered when the light intensity scattered from the acrylamide gel in acetone-water mixture was being measured as a function of temperature by Tanaka.⁸³

The first order volume phase transition in a thermosensitive, nonionic polymeric gel such as PNIPAm, occurs near the LCST. Various theoretical developments have been proposed to model volume transitions in PNIPAm gels. The first attempt was made by Tanaka *et al.*⁸⁴ who used the Flory-Huggins lattice model to explain the LCST phenomenon in PNIPAm gel. They observed that the LCST could be predicted only through a negative entropic change with increasing temperature. This amounts to attractive molecular associations at the transition temperature. Otake *et al.*⁶³ attributed the cause of volume transition in PNIPAm gel solely to hydrophobic interactions. However, in their theory the hydrophobic interactions have been modeled empirically. Marchetti *et al.*^{85,86} used a compressible lattice theory and predicted the transitions by defining the interaction parameter on the basis of large differences in the cohesive energy densities of the components. Their theory however, does not consider any specific molecular interaction such as hydrogen bonding. Prange *et al.*⁸⁷ has developed a theory based on an incompressible lattice model to account for hydrogen bonding interactions in aqueous polymer solutions and gels. They propose that every segment of a molecule on the lattice can exhibit three types of contact sites: proton donating, proton accepting, and those, which interact through dispersion forces. Their theory also accounts for non-random distribution of molecules in a mixture due to hydrogen bonding interactions. However, the role of hydrogen bonding in effecting LCST is not clearly brought out in their theory. Panayioutou and Sanchez⁸⁸ have extended the lattice-fluid (LF) theory to account specifically for hydrogen-bonding interactions in mixtures. This theory also takes into consideration the compressibility of solutions and equation-of-state properties of individual components. The hydrogen-bonding contribution to the free energy is calculated by counting the hydrogen-bond arrangements and their energies in a given system. This theory, hereafter called the Lattice-Fluid-Hydrogen-Bond (LFHB) model, has been shown to successfully predict hydrogen bonding in water and in polymer solutions of supercritical solvents.

Recently Lele *et al.*⁸⁹ have proposed an extended LFHB theory to model the swelling behavior of a gels such as poly(ethylene oxide) and PNIPAm which interacts with a solvent through hydrogen bonding. The (LFHB) model can quantitatively predict the temperature driven volume transition of crosslinked PNIPAm gel in water.

The total free energy of the system is given as the sum of the free energies of mixing and the elastic free energy of an affine network. The free energy of mixing in the LFHB model can be calculated from the mixing rules and the hydrogen bonding fractions. The details of the free energy of mixing terms are described in Lele *et al.*⁸⁹

The elastic free energy ΔG_{el} is given by the theory of rubber elasticity as

$$\Delta G = \frac{3}{2} \left(\frac{v_e}{V_0} \right) \left\{ \left(\frac{V}{V_0} \right)^{2/3} - 1 - \frac{1}{3} \ln \left(\frac{V}{V_0} \right) \right\} \quad (1.2)$$

where, v_e is the moles of elastically active chains in the gel, V is the volume of the gel, and V_0 is the volume at synthesis at a given temperature and pressure.

From the free energy of mixing and the elastic free energy, the chemical potential of the solvent can be calculated as

$$\begin{aligned} \frac{\mu_1}{RT} = & \ln(\phi_1 / \omega_1) + \left(1 - \frac{r_1}{r_2} \right) \phi_2 + r_1 \tilde{\rho} \phi_2^2 X_{12} + r_1 \left\{ -\frac{\tilde{\rho}}{\tilde{T}_1} + \frac{\tilde{R}_1 \tilde{v}}{\tilde{T}_1} + (\tilde{v} - 1) \ln(1 - \tilde{\rho}) + \frac{1}{r_1} \ln \tilde{\rho} \right\} + \\ & r_1 \sum_i^m \sum_j^n v_{ij} - \sum_i^m d_i^1 \ln \frac{v_d^i}{v_{io}} - \sum_j^n a_j^1 \ln \frac{v_a^j}{v_{oj}} - \sum_j^n a_j^1 \ln \frac{v_a^j}{v_{oj}} \\ & + \left\{ r_1 \left(\frac{v_e}{V_0} \right) v_i^* \tilde{v} \left[\left(\frac{V_0}{V} \right)^{2/3} - \frac{1}{2} \left(\frac{V_0}{V} \right) \right] \right\} \end{aligned} \quad (1.3)$$

where, subscripts 1 and 2 represent the components solvent (1) and polymer (2), respectively. ϕ is the volume fraction, r_i is the number of lattice sites occupied by a molecule of component i , v_i^* is the characteristic mer volume of component i and ε_i^* is the characteristic mer-mer interaction energy for component i . A pure component i is thus characterized by three parameters r_i , v_i^* and ε_i^* . ζ_{12} is the binary interaction parameter between components 1 and 2.

The binary interaction parameter between the polymer (PNIPAm) and solvent (water) can be considered as simulating the 'hydrophobicity' of the polymer since the hydrophilic part of the interactions are considered separately in the hydrogen bonding terms in the mean-field framework of the LFHB theory

where,

$$X_{12} = \frac{\varepsilon_1^* + \varepsilon_2^* - 2\zeta_{12}(\varepsilon_1^* \varepsilon_2^*)^{1/2}}{RT} \quad (1.4)$$

and $\tilde{\rho}$ is the reduced density of the mixture which is related to the reduced pressure $\tilde{P} = P/P^*$ and reduced temperature $\tilde{T} = T/T^*$ by the equation of state

$$\tilde{\rho}^2 + \tilde{P} + \tilde{T} \left\{ \ln(1 - \tilde{\rho}) + \tilde{\rho} \left[1 - \left(\frac{1}{r} - \sum_i^m \sum_j^n v_{ij} \right) \right] \right\} = 0 \quad (1.5)$$

In the first line of eq (1.3), the first two terms are the combinatorial entropy contribution, the third term is energetic (effective hydrophobic) contribution and the fourth term in brackets represents the effect of the pure component properties. The terms in the second line represent the hydrogen bonding contribution and those in the third line represent the elastic energy contribution.

The swelling capacity of the gel at equilibrium, $q=1/\phi_2$, can be calculated by solving,

$$\mu_1^G = \mu_1^O \quad (1.6)$$

where, the superscripts G and O indicate the gel and the pure solvent phases and the chemical potentials are given by equation (1.3).

This theory successfully predicts continuous deswelling of PEO gels. Also it predicts a first order volume transition for PNIPAm gel. Thus, in the PNIPAm gel-water system, a sharp rearrangement of the number of interpolymer hydrogen bonds and polymer-water hydrogen bonds at the transition temperature, in addition to an increasing hydrophobicity of the polymer with temperature, together results in a first-order volume transition of the gel. The theory clearly indicates the governing role of hydrogen bonding and hydrophobic interactions in these volume transitions. This is shown for the first time that it has implications in designing novel thermosensitive hydrogels.

1.10 Effect of solvent on Phase transition of thermosensitive polymer

PNIPAm is soluble in many organic solvents such as acetone, methyl ethyl ketone, chloroform, ethyl alcohol, methyl alcohol, and tetrahydrofuran, which are capable of hydrogen bonding. But in all these cases, PNIPAm does not show any LCST behaviour. Schild and Tirrell⁹⁰ and Winnik and coworkers⁹¹ reported cononsolvency of PNIPAm in water and methanol mixtures. Both groups also cite an analogous observation of a "conosolvent" effect with gel swelling. Theoretically the free energy of methanol-water interaction for gels should be negative, whereas experimentally the binary value is always positive. Therefore, Winnik and coworkers conclude that the addition of PNIPAm enhances the attractive interaction for water and methanol.

According to Ptitsyn *et al.*⁹², the temperature at which a polymer undergoes phase transition is mainly determined by the polymer-solvent interaction parameter. Hirotsu⁹³ investigated a quantitative connection between the polymer-solvent interaction parameter and occurrence of a volume phase transition in polymer gels. PNIPAm gels when immersed in methanol, ethanol and n-propanol were swollen but their swelling ratios were independent of temperature. On the contrary, a gel in water shows a clear discontinuous volume transition around 33°C. Both Hirotsu and Tanaka⁹⁴ reported that the methanol-water solvent causes PNIPAm gels to go through a re-entrant transition. When the solvent composition is varied systematically, the gel undergoes two transitions: a discontinuous collapse followed by a discontinuous swelling. The reentrant transition defines a closed-loop instability phase boundary having both upper and lower critical points. In the case of ethanol-water mixtures, there appear two closed-loop phase boundaries, whose physico-chemical bases are not yet clear.

Hirotsu⁹³ calculated the values of χ parameters between PNIPAm and alcohols. Addition of a small amount of alcohol to PNIPAm/water system alters the transition behavior of PNIPAm gel significantly.

Tanaka *et al.*⁹⁵ reported for the first time the reentrant phase transition of PNIPAm in water-DMSO solvent mixture. Upon increasing the volume fraction of DMSO at constant temperature below LCST, the gel first collapsed and then reswollen at higher DMSO contents. The authors claimed that the phenomenon was a consequence of the free energy of contact between polymer segments not being a monotonic function of DMSO content. The attraction of two solvents for one another dominates at the middle of the phase diagram, promoting a greater number of polymer-polymer contacts, and hence collapses.

1.11 Effect of additives on the phase transition of thermosensitive polymers

Eliassaf⁶⁷ reported that the hydrogen-bond breaking agents LiCl and urea causes the precipitation of PNIPAm from aqueous dilute solution at 30°C. Schild and Tirrell⁵⁹ examined the effects of a number of salts on the LCST of aqueous PNIPAm. They observed that the well-known Hofmeister series seems to hold in terms of effectiveness of a series of salts in depressing the LCST. Saito and coworkers⁹⁶ observed that the phase transition temperature of NIPAm gels in inorganic salts depends more on anions rather than cations, and the change in transition temperature was linearly correlated with the viscosity B coefficient of anions. On the other hand, the transition temperature in organic salts like tetraalkylammonium bromides strongly depended on the alkyl chain length, and might be explained from the hydration structure and an adsorption of the salts to the polymer segments.

Park *et al.*⁹⁷ demonstrated that sodium chloride induced an abrupt volume transition in the nonionic PNIPAm gel, while the LCST of the gel was lowered by increasing the sodium chloride concentration. Kawasaki *et al.*⁹⁸ reported that the volume phase transition of the PNIPAm gel has significant effect on the distribution of the salts (LiCl, KCl, NaCl, CsCl, KNO₃, KSCN, K₂SO₄, CH₃COOLi, CH₃COONa, CH₃COOK, CH₃COOCs). Below the transition temperature, the salts were almost equally partitioned between the swollen gel phase and external salt solution and above the transition temperature, they were excluded from completely collapsed gel, and the exclusion tendency of the salts depends on the kinds of salts. Yang *et al.*⁹⁹ measured cloud point

temperatures of PNIPAm/water solutions with NaCl, NaBr, NaI. All these salts reduced the cloud point temperatures to different extents in the following order: NaCl>NaBr>NaI. The higher the concentration of added salts was, the more cloud point temperature dropped.

Kim and coworkers¹⁰⁰ studied the effect of low molecular weight monosaccharide, glucose and a disaccharide, maltose in the presence and absence of salts on the LCST of thermosensitive polymers, Pluronic, PNIPAm, and copolymers of PNIPAm with ionizable groups. The LCSTs of the polymers were significantly influenced by the polymer concentration. The addition of saccharides into aqueous polymer solutions decreased the LCSTs of polymers. As the polymer concentration increased, the saccharide effects became more pronounced. A monosaccharide, glucose was more effective than a disaccharide, maltose in lowering the LCST.

1.12 Fundamental Interactions for Volume Phase Transition in gels

Four fundamental interactions namely, hydrogen bonding; hydrophobic interactions; van der Waals interactions and electrostatic interactions govern the phase transition in gels.¹⁰¹ Gel phase transition is a result of the competitive balance between the repulsive force that acts to expand the polymer network and an attractive force that acts to shrink the network. The most effective repulsive force is the electrostatic interaction between the polymer charges of the same kind, which can be imposed upon a gel by introducing ionization into the network. The osmotic pressure by counter ions adds to the expanding pressure. Ilmain *et al.*¹⁰² presented a general scheme of gel volume phase transitions induced by these four intermolecular forces as illustrated in Figure 1.4

1.12.1 van der Waals interactions

A partially hydrolyzed acrylamide gel undergoes phase transition in acetone water mixtures.¹⁰³ The major interactions between polymer-polymer chains arise mainly due to

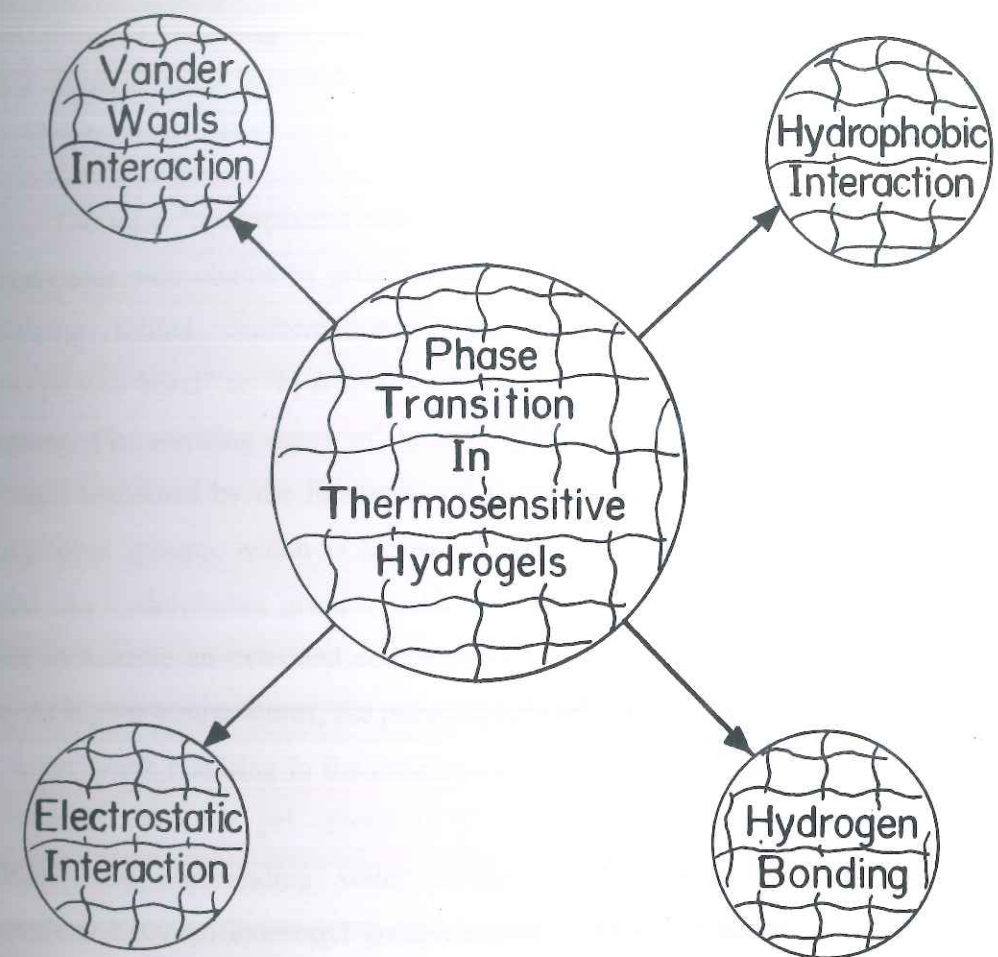


Figure 1.4: Schematic representation of four fundamental molecular interactions causing phase transition in thermosensitive hydrogel

the van der Waals interaction. Acetone, a nonpolar poor solvent, had to be added to water in order to increase the attractive interaction between polymers in the networks.

1.12.2 Hydrophobic interactions

The term "hydrophobic bond" was originally developed to describe the grouping of non-polar side chains in proteins and has been found to be an important factor in stabilizing folded conformations. Although no bond actually exists, the term "hydrophobic bond" or "hydrophobic associations" has received wide acceptance in the literature. The swelling curve of the hydrophobic polymer gels in the aqueous medium has been explained by the formation of an ice-like structure of water molecules around hydrophobic groups, which is familiar in proteins. The formation of ice-like structure around the hydrophobic groups makes it thermodynamically possible for the polymer chains to assume an extended conformation. Thus the gels expand to form the swollen state. At higher temperatures, the polymer network shrinks and H-bonds between polymer and water break resulting in the dominance of hydrophobic interactions. For example, in the case of PNIPAm gel, above LCST the H-bonds between the amide groups of PNIPAm and surrounding water molecules are destroyed, and the hydrophobic interactions between isopropyl groups increase. Although bond energy of hydrophobic interaction is of the same order or even smaller than that of hydrogen bonding, the hydrophobic interaction play very important role in the stabilization of the configuration of polymers.

The strength of the hydrophobic interaction is proportional to the number of water molecules, which form the hydrophobic hydration and increases with temperature. Therefore, the gel whose hydrophobic group has a larger surface (contact) area undergoes a discontinuous volume transition in water at lower temperatures. Inomata *et al.*¹⁰⁴ have shown that n-propylacrylamide (NPAm) gel has a lower LCST than NIPAm and cyclopropylacrylamide (CPAm) gels. The authors propose that the larger "contact area" of the n-propyl group as compared to isopropyl and cyclopropyl groups enables the structuring of hydrated water molecules to a greater extent, which results in lowering of the LCST. Even a "pin-point variation" of methyl to ethyl groups in L-alanine ester side

chains in hydrogels containing methacryloyl backbone makes the drastic volume phase transition.¹⁰⁵

1.12.3 Hydrogen bonding Interactions

Hydrogen bond is an electrostatic attraction between hydrogen atom and electronegative atom like oxygen, nitrogen. Compared to the ordinary covalent and ionic bonds, hydrogen bonds are weak bonds with bond energies in the range of 3-10 kcal/mol. However, they play very important role in determining the shapes and reactivities of the important biomolecules. For example, a protein molecule is held in helical form by hydrogen bonds.

By slightly ionizing the gel, Ilmain *et al.*¹⁰² induced a volume transition in a poly(acrylamide)/poly(acrylic acid) interpenetrating network (IPN). They claimed that this volume transition was driven independently by hydrogen bonding.

1.12.4 Electrostatic Interactions

Electrostatic interaction is the interaction between oppositely charged ions and a long-range order interaction. The electrostatic interaction is inversely proportional to the dielectric constant of the medium. Therefore, this interaction becomes more important in a hydrophobic environment, which is readily found in biopolymers. In case of synthetic polymers, either positive or negative charges can be introduced on the polymer chains by copolymerization or partial ionization, which give rise to a strong repulsive interaction. Since a free movement of the charges is not allowed because the charges are fixed on the polymer chains so as to keep the electroneutrality. As a result, Donnan potential is created between the inside and outside of the gel, resulting in an increase in the osmotic pressure.

Polyampholytes are the polymers with positively and negatively charged monomers. In neutral pH, both cations and anions are ionized and attract each other.

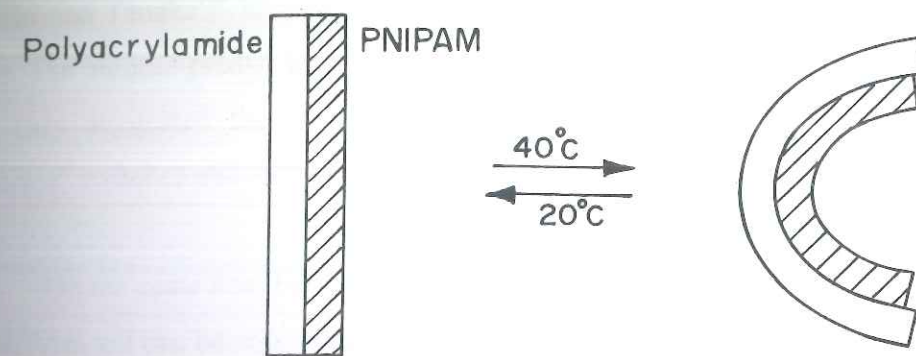
Myoga and Katayama¹⁰⁶ studied such a gel and observed that at a neutral pH the gel shrinks and is swollen at both lower and higher pH. In a neutral pH medium, both cations and anions are ionized and they attract each other, thus shrinking the gel. Otherwise one of the ionizable groups is neutralized, while the other remains ionized, and the gel swells. The volume change was gradual and continuous.

1.13 Applications of Thermosensitive polymers

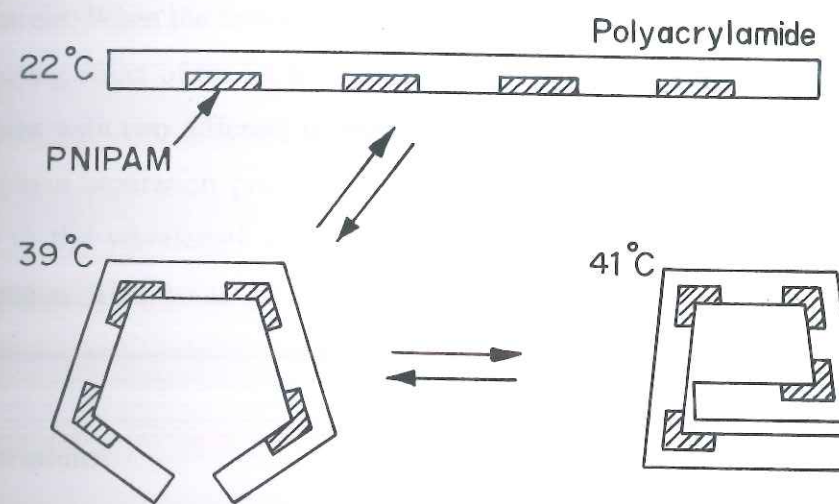
1.13.1 Switches and actuators

The potential for creating 'intelligent' materials has spurred on research into thermosensitive polymers. Hu and coworkers¹⁰⁷ recently designed partially interpenetrating networks (a mixture of two different polymers whose chains are entangled) made up of PNIPAm and poly(acrylamide) (PAAm). In the network, shrinking of one polymer and swelling of other simultaneously causes the gel to bend as shown Figure 1.5(a). The number of 'bending' points determines the shapes attainable in the gel. A 'bi-gel' strip will bend into a circle in response to an increase in temperature or to a change in the solvent quality. The shape of the 'shape memory gel' in Figure 1.5(b) can be straight, pentagonal or quadrangular depending on the temperature. Similarly, a gel 'hand' (as shown in Figure 1.5c) is designed to grasp or release an object by temperature adjustments as shown in figure. The difference in the thermal expansion coefficients between the two polymers is much larger than that between two metals, therefore bi-gels are much more sensitive to their environments than bi-metals. These materials could find applications in robotics.

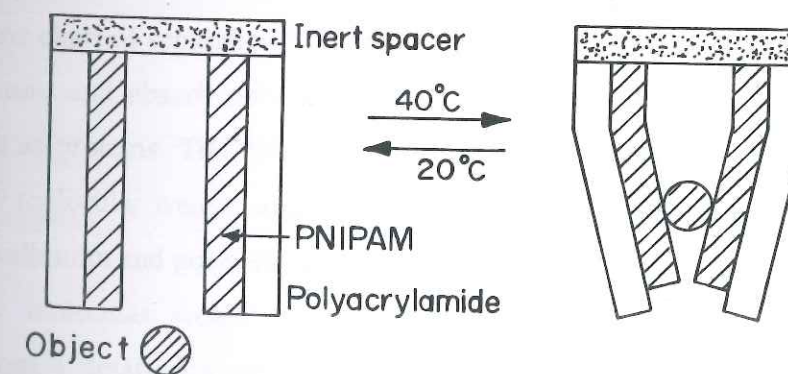
Mattiasson *et al.*¹⁰⁸ synthesized a thermosensitive reversible hydrogel with shape memory by polymerizing N-acryloxysuccinimide with N-isopropylacrylamide and styrene. Depending on the composition and temperature, the polymer undergoes phase transition to form either a compact polymer precipitate or a physically crosslinked gel. The physically crosslinked gel formed collapses with a further increase in temperature to result in shrunken, shape-remembered gel formation.



(a)



(b)



(c)

Figure 1.5: Intelligent polymeric bi-layers

Suzuki and Tanaka¹⁰⁹ have designed a gel based on PNIPAm that is sensitive to visible light. The authors predict that the response time of 1 μm -diameter gel will be about 5ms, and they suggested that such systems could be used as photo-responsive artificial 'muscles', switches and memory devices.

On the same line, Hu *et al.*¹¹⁰ found that the transmission of a visible laser beam in a PNIPAm gel can be controlled by adjusting the power of an infra-red beam, without the need to incorporate photo-sensitive molecules into the gel network. The laser beam and the IR beam are aligned along the same optical axis. Below the transition temperature the gel is transparent. When the temperature is raised above the transition temperature by the localized heating effect of the IR beam, the gel becomes opaque in the irradiated region. Micro-domains with two different network concentrations (dilute and dense regions) are formed (a phase separation process). When the sizes of the micro-domains become comparable to the wavelength of the visible light, the light is scattered and the gel becomes opaque. This could be used for making glass opaque in a 'self-regulating' greenhouse.

1.13.2 Separations

Thermosensitive polymers have been extensively used in the separation and recovery of numerous substances from aqueous solution. Cussler *et al.*¹¹¹⁻¹¹⁴ have reported the potential use of thermo-responsive materials in separation technology. Figure 1.6 shows a flow chart of separation using temperature sensitive gels. These gels are size selective in nature and absorb only low molecular weight substances excluding large molecules such as proteins. The PNIPAm or poly(N,N-diethylacrylamide) gel can swell and absorb low molecular weight solutes like urea and poly(ethylene glycol) (MW 400), but excludes ovalbumin and poly(ethylene glycol) (MW 18,500).¹¹¹ This system was used to absorb low molecular weight carbohydrates, minerals, and other small soluble components from a defatted soyabean extract.¹¹⁴ The PNIPAm gel could be used to absorb or release (deliver) a variety of biologically and industrially important substances such as vitamin B₁₂, myoglobin,¹¹⁵ or indomethacin.⁴⁰ Poly(vinyl methyl ether) hydrogels were used for the separation of organic substances, and in particular to recover non-ionic surfactants from waste water.¹¹⁶

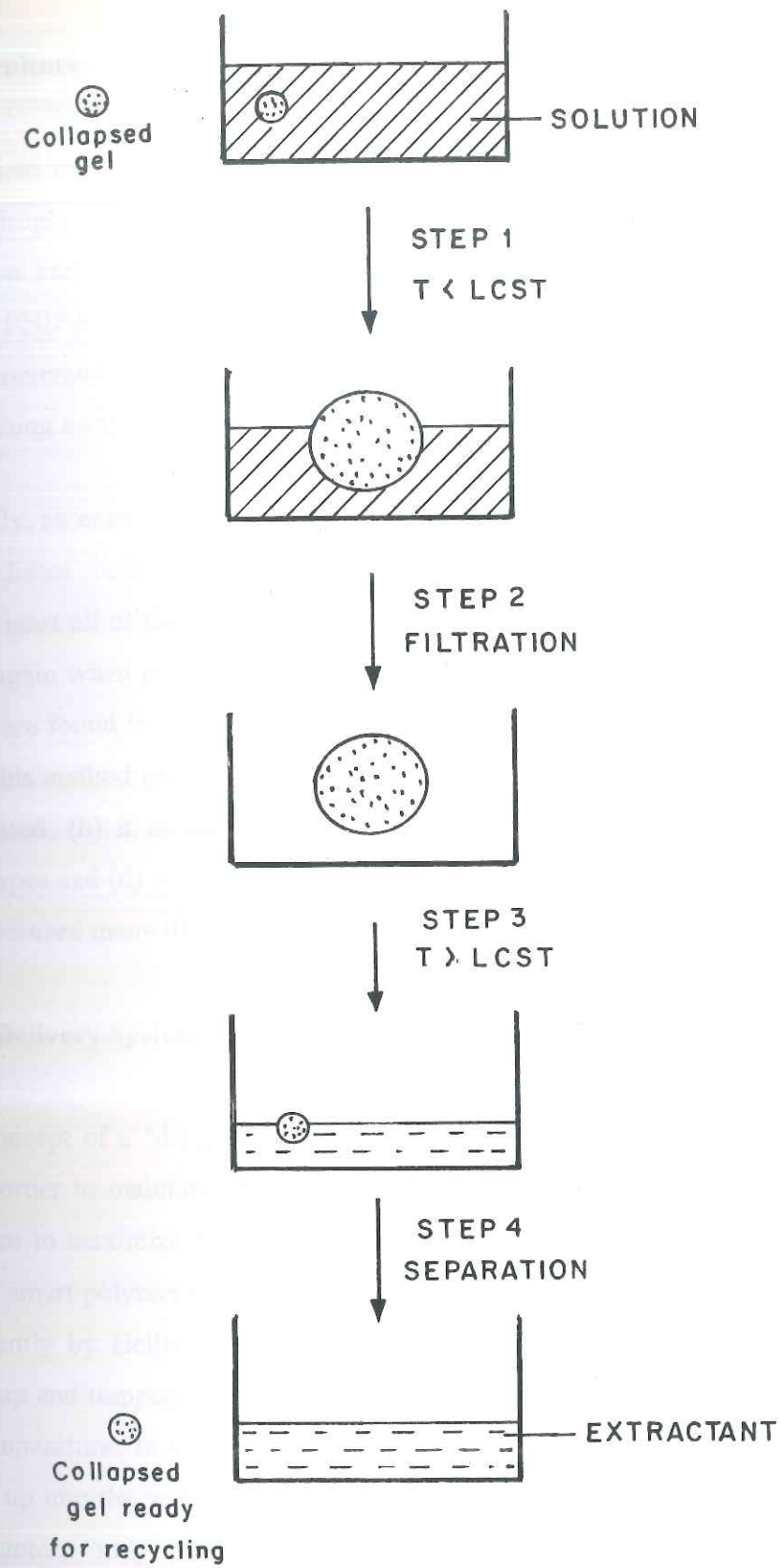


Figure 1.6: Separation process based on thermosensitive hydrogels

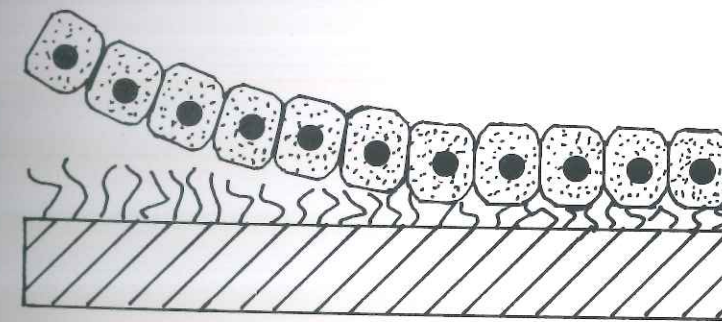
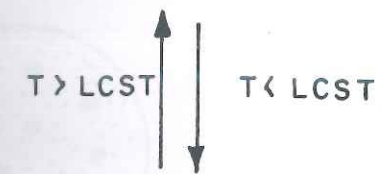
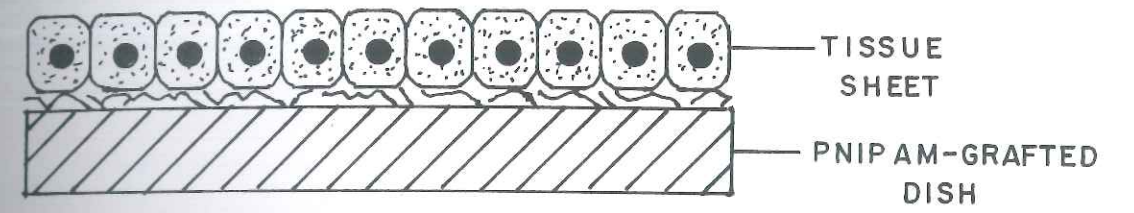
1.13.3 Tissue culture

In the field of cell and tissue culture, Yamada and co-workers have applied the hydrophilic-hydrophobic switching ability of PNIPAm to cell cultures.¹¹⁷ These researchers have grafted the cells onto PNIPAm and, above 32 °C, the hydrophobic nature of the PNIPAm aids cell adherence. Below this transition temperature, cell attachment is prevented because the PNIPAm becomes hydrophilic and binds to water in preference, pushing away the cells. (Figure 1.7)

Normally, an enzyme like trypsin would be used to detach the cultured cells from their culture dishes before they are used for further culturing. On lowering the temperature, almost all of the cells could be detached and recovered by this method, and 73% adhered again when plated onto new dishes. By contrast, only 14% of the trypsin-treated cells were found to adhere because of damage to the cells by the enzyme during detachment. This method offers a number of advantages: (a) the risk of contamination is almost eliminated, (b) it is simple and inexpensive, (c) it is not limited to enzyme-resistant cell types and (d) since the process is completely reversible, the polymer-grafted dishes can be re-used many times.

1.13.4 Drug Delivery System

The concept of a "drug delivery system (DDS)" has been developed in the past few years in order to maintain effective drug concentration in the blood over a longer period and also to maximize the efficiency and minimize the side effects of drugs. The application of smart polymer systems for drug delivery has been of increasing interest, as reviewed recently by Heller.¹¹⁸ Using temperature-sensitive polymers, drug molecules can be taken up and trapped within a network of hydrogels and released in response to a change in temperature. In the case of PNIPAm, for example, water-soluble drugs are readily taken up into the water-swollen network at room temperature. When the delivery system encounters body temperature (37°C), the network contracts, expelling the interstitial water together with the drug. (Figure 1.8) These systems could have potential applications in oral, insert or transdermal drug carriers.¹¹⁹



RECOVERY OF TISSUE SHEET

Figure 1.7: Tissue recovery by low temperature treatment

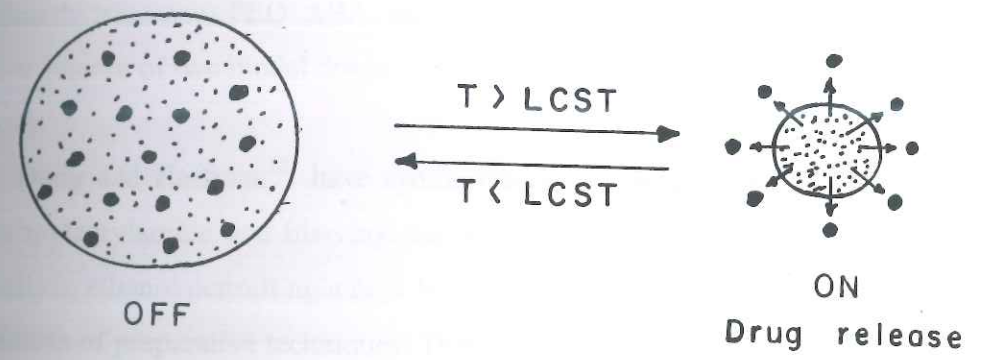


Figure 1.8: On-off switching mechanism of drug release

Hoffman and coworkers^{115,120} have developed a system that delivers vitamin B₁₂, myoglobin or methylene blue. Release kinetic studies showed a two-stage process, an initial rapid release, which is followed by a much slower diffusion of a biomolecule. This is attributed to the formation of a thick skin due to the phase transition at the interface of the gel with aqueous solution.

Okano *et al.*^{34,119} developed poly(PNIPAm-co-BMA) membranes which control the permeation of glucose and insulin. They used an IPN made up of PNIPAm and poly(tetramethylene ether glycol),³⁴ and another consisting of PNIPAm and PEO-poly(dimethylsiloxane)-PEO ABA triblock copolymers,¹¹⁹ as delivery devices for the pulsative release of two model drugs, indomethacin and ketoprofen.

Dong and Hoffman¹²¹ have synthesized a new heterogeneous PNIPAm gel from N-isopropylacrylamide and bis-vinyl-terminated polydimethylsiloxane (VTPDMS). The gel swells in ethanol permitting a high loading of either hydrophilic or hydrophobic drugs by variation of preparative techniques. They also introduced acrylic acid as a comonomer in this system which gives pH-sensitivity in addition to thermal response. *In vitro* study shows that the release of a drug, indomethacin occurs at a much higher rate at pH 7.4 than at pH 1.4. The ultimate goal is an *in vivo* system that protects the ingested drug from being delivered in the stomach, so that it instead reaches the intestine.

Chung *et al.*¹²² employed polymeric micelles comprised of AB block copolymers of PNIPAm with either PBMA [Poly(butyl methacrylate)] or PS (polystyrene). These block copolymers formed a core-shell micellar structure. The hydrophobic drug, adriamycin, (ADR), was loaded into the inner core of the polymeric micelles. The polymer showed reversible intermicellar dispersion/aggregation in response to temperature cycles through an outer polymer shell LCST.

1.13.5 Immunoassays and enzyme reactions

Immunoassays are widely used for detecting and measuring drugs, vitamins, hormones, proteins, metabolites, microorganisms in biological fluids, industrial process streams, and for the environmental monitoring of waterways. Using the LCST behaviour of PNIPAm, Hoffman and his coworkers have developed a novel polymer-based

immunoassay system.¹²³ They co-polymerized NIPAm with N-acryloxysuccinimide, the latter providing the reactive groups needed to attach the antibody, immunoglobulin (Ig). Polymer solutions were subsequently mixed with an antigen and a second antibody, which was conjugated to a fluorophore label. Thus a sandwich-type immune complex was then precipitated by raising the temperature above the LCST of the polymer. (Figure 1.9) Reaction kinetics was reported to be very favourable with little non-specific binding. This method also has been extended to mouse Ig and competitive immunoassays have been carried out well.

Recently, Stayton and co-workers¹²⁴ have linked PNIPAm near to the active center of streptavidin. This protein (the quaternary structure of which is a tetramer) binds the ligand, biotin with a very high association constant ($K_a=1015\text{mol/dm}^3$).

In addition to immunoassays, functional PNIPAm chains have been coupled with enzymes such as trypsin or cyclodextrin glycosyltransferase.¹²⁵ Such copolymers act as supports for enzymes in homogeneous biocatalysts. Kitano and coworkers¹²⁶ have prepared polyallylamine-graft-PNIPAM microgels wherein, the activity of an enzyme (trypsin), incorporated in the core of the particles, was regulated by the permeability of the PNIPAm shell.

Recently, Kato *et al.*¹²⁷, using the same principle, produced an 'ultra-fine redox reactor'. A hydrophobic core of styrene-co-2-ethylhexylmethacrylate-co-methylenebisacrylamide was surrounded by a thermosensitive PNIPAm shell. The hydrophobic molecule, ubiquinone, was trapped in the core matrix. Oxidation and reduction of ubiquinone by potassium ferricyanide and ascorbic acid, respectively, were controlled by their permeation through the PNIPAm 'shell', which was, in turn, controlled by temperature adjustment.

1.13.6 Enhanced oil recovery

Oil is an important source of energy and is also used as an important raw material in the chemical industries. Worldwide oil reserves are being depleted rapidly. Hence, there is an increasing demand for different oil recovery techniques to recover oil as much as possible from the existing sources. Different kinds of water-soluble polymers have

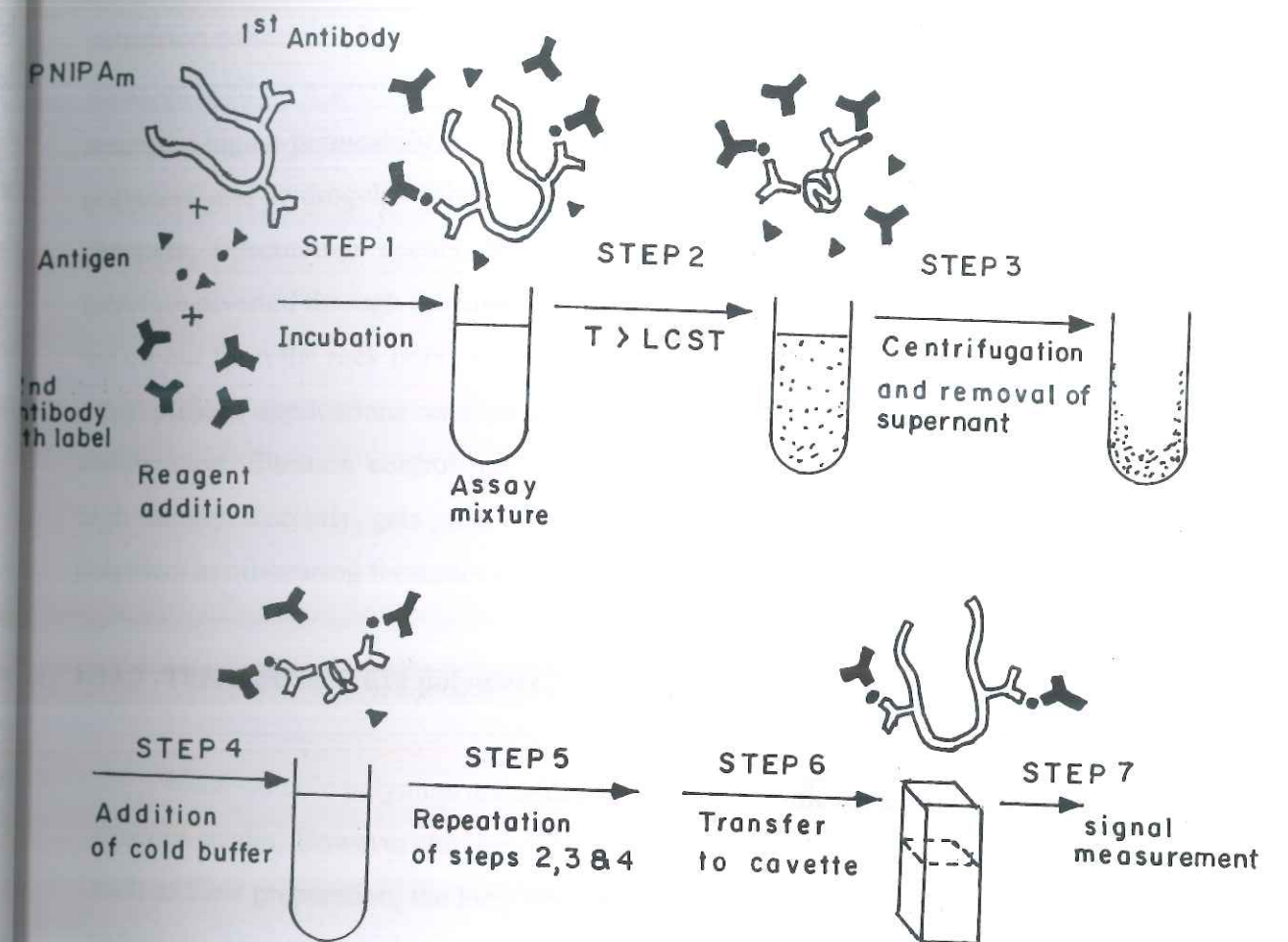


Figure 1.9: Thermally induced immunoassay scheme for thermosensitive hydrogels

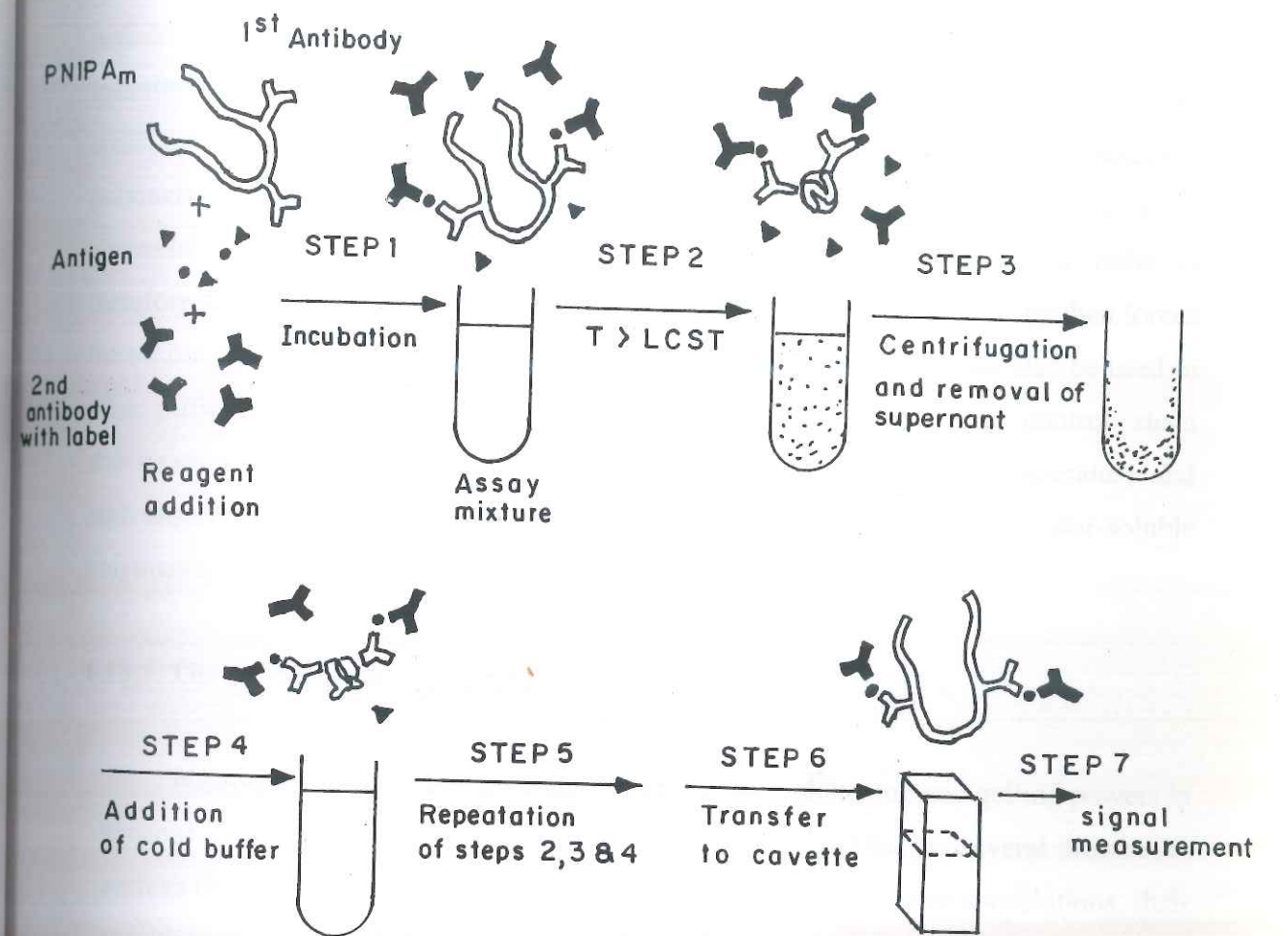


Figure 1.9: Thermally induced immunoassay scheme for thermosensitive hydrogels

been used in various oilfield applications including number of enhanced oil recovery (EOR) processes. Polymer-augmented water flooding is a more efficient alternative to just water flooding. Water-soluble polymers, which increase the viscosity of water and thereby reduce its mobility, are used in this process.^{128,129} During the water flooding of petroleum reservoirs, the injection fluid tends to take the most permeable route from an injection well to a production well. In order to mobilize oil present in less permeable areas, the higher permeability channels are blocked by injection of a temperature sensitive polymers and hydrogels. When it encounters the high temperatures of the reservoir channels, flocculation occurs, thus blocking high permeability areas, and water is therefore diverted through the lower permeability channels. This diverted flow then forces the oil out from the rock pores to the producing well. These polymers can also be used in other oilfield applications such as drilling mud additives for fluid loss control, shale stabilization, filtration control, etc. under extreme conditions of high temperature and high salinity. Recently, gels produced by an *in situ* crosslinking reaction of water-soluble polymers in oil-bearing formations have become popular in the EOR.¹³⁰

1.13.7 Thermoassociative polymers

Water-soluble polymers are widely used for their thickening and gelling powers in aqueous media. However the use of these polymers was limited by several drawbacks such as their preparation, the long time required to obtain homogeneous solutions, their sensitivity to mechanical degradation under high shear and the low flexibility for the operator to modulate the rheological properties of the solutions.

These drawbacks can be avoided by using thermoassociating polymers.^{131,132} A small amount of hydrophobic 'block' inserted into hydrophilic backbone gives rise to self-aggregation in solution. These hydrophobically modified polymers (HMP) finds various applications in pharmaceuticals, cosmetics, paints, enhanced oil recovery.^{3,128} These polymers have the ability to produce highly viscous aqueous solution above a threshold polymer concentration. The nature and concentration of added salt, pH, and temperature also influence the viscosity significantly. This viscosity enhancement is due to their hydrophobic parts which form inter molecular aggregates in aqueous solution.^{70,133} A thermally induced associative polymer was developed by grafting LCST side-chains onto water-soluble backbone. Hourdet *et al.*¹³⁴ developed a system

prepared from PEO-modified PAA (PAA-g-PEO) which provides an enhancement of viscosity upon heating.

At constant HMP concentration, the viscosity first increases on addition of surfactant molecules, passes a maximum and finally decreases. At high surfactant concentration, the mixed aggregates contain mainly surfactant molecules and only few alkyl groups belonging essentially to the same HMP chains.^{135,136} The interactions between PNIPAm and poly(sodium acrylate) hydrophobically modified with octadecyl groups, HMPA, in aqueous solution were studied by Bokias *et al.*¹³⁷ They observed the elevation of the phase separation temperature of PNIPAm in the PNIPAM/HMPA mixtures.

1.13 Concluding remarks:

The introductory chapter reviews the various aspects of hydrogels pertaining to the fundamental causes of phase transitions, the concept of LCST, molecular interactions, and applications in different fields. The major emphasis, however, is given to thermosensitive polymers, which is the subject of this thesis. A wide variety of experimental methodologies, which are used to study phase transition of thermosensitive polymers, are also discussed in this chapter.

A large number of theoretical models have been proposed in the literature to explain the first order volume transition in non-ionic thermosensitive gels. A brief account of this work is given in this chapter.

Thermosensitive polymers provide great opportunities for many diverse and novel applications in medical and biotechnology. In view of the increasing demand for thermosensitive polymers for various applications, there is a great scope to develop newer thermosensitive polymers. The present work, therefore, focuses on the design and synthesis of new hydrophobic comonomers and consequent development of novel thermosensitive polymers by incorporating these new comonomers. The structural elucidation of these polymers has been carried out by various spectroscopic techniques. The influence of chemical structure and various additives on the transition properties of these polymers has been corroborated.

1.15 References

1. A. S. Hoffman, *Macromol. Symp.*, **98**, 645 (1995).
2. K. Dušek (Ed.), *Responsive Gels: Volume Transition I and II*, Springer-Verlag, Berlin, Heidelberg, *Adv. Polym. Sci.*, Vol. 109-110 (1993).
3. P. S. Russo (Ed.), "Reversible Polymeric Gels and Related Systems", ACS Symp. Series 350, Amer. Chem. Soc., Washington D. C. (1987).
4. J. D. Andrade (Ed.), "Hydrogels for Medical and Related Applications", ACS Symp. Series 31, Amer. Chem. Soc., Washington D. C. (1987).
5. R. S. Harland, R. K. Prud'homme (Eds.), "Polyelectrolyte Gels: Properties, Preparation and Applications", ACS Symp. Series 480, Amer. Chem. Soc., Washington D. C. (1992).
6. B. D. Ratner, A. S. Hoffman, in "Hydrogels for Medical and Related Applications", J. D. Andrade (Ed.), ACS Symp. Series 31, Amer. Chem. Soc., Washington D. C. (1987).
7. A. S. Hoffman, in "Polymer Gels", D. DeRossi, K. Kajiwara, Y. Osada, A. Yamauchi (Eds.), Plenum Press, New York, p-289 (1991).
8. T. Tanaka, *Sci. Am.* **244**, 124 (1981).
9. T. Tanaka, *Phys. Rev. Lett.*, **40**, 820 (1978).
10. N. A. Peppas, R. W. Kormseyer (Eds.), "Hydrogels in Medicine and Pharmacology", CRC Press, Boca raton, Fl., (1987).
11. W. R. Gombetz, A. S. Hoffman, in "Hydrogels in Medicine and Pharmacy", Vol. 1, N. A. Peppas (Ed.), CRC Press, Boca raton, Fl., p-95 (1986).
12. H. Brondsted, J. Kopecek, in "Polyelectrolyte Gels: Properties, Preparation and Applications", R. S. Harland, R. K. Prud'homme (Eds.), ACS Symp. Series 480, Amer. Chem. Soc., Washington, D. C., p-285 (1992).
13. J. Kopecek, J. Vacik, D. Lim, *J. Polym. Sci.*, **9**, 2801 (1971).
14. A. Katchalsky, I. Michaeli, *J. Polym. Sci.*, **15**, 69 (1955).
15. A. Katchalsky, *J. Polym. Sci.*, **2**, 432 (1947).
16. R. A. Siegal, B. A. Firestone, *Macromolecules*, **21**, 3254 (1988).
17. K. Ishihara, M. Kobayashi, N. Ishimaru, I. Shinohara, *Polym. J.*, **8**, 625 (1984).

18. K. Ishihara, K. Matsui, *Polym. Sci.*, **24**, 413 (1986).
19. G. Albin, T. A. Horbett, B. D. Ratner, in "Pulsed and Self-regulated Drug Delivery", J. Kost, (Ed.), CRC Press, Boca raton, Fl., p-159 (1990).
20. M. Irie, D. Kungwatchakun, *Macromolecules*, **19**, 2476 (1986).
21. A. Suzuki, T. Tanaka, *Nature*, **346**, 345 (1990).
22. A. Suzuki, T. Ishii, Y. Maruyama, *J. Appl. Phys.*, **80**, 131 (1996).
23. K. Ishihara, A. Okazaki, N. Negishi, I. Shinohara, T. Okano, K. Katoka, Y. Sakurai, *J. Appl. Polym. Sci.*, **27**, 239 (1982).
24. K. Ishihara, N. Hamada, S. Kato, I. Shinohara, *J. Polym. Sci. Polym. Chem. Ed.*, **22**, 881 (1984).
25. Y. Osada, *Advances in Polymer Science*, Springer-Verlag, Berlin, **82**, 1 (1987).
26. Y. Osada, H. Okuzaki, H. Hori, *Nature*, **355**, 242 (1992).
27. T. Tanaka, I. Nishio, S-T Sun, S. Ueno-Nishio, *Science*, **218**, 467 (1982).
28. T. Shiga, T. Kurauchi, *Polymer Preprints, Jap.*, **36**, 2894 (1987).
29. T. Kurauchi, T. Shiga, Y. Hirose, A. Okada, in "Polymer Gels", D. DeRossi, K. Kajiwara, Y. Osada, A. Yamauchi (Eds.), Plenum Press, New York, p-237 (1991).
30. R. E. Rosenweig, *Ferrohydrodynamic*, Cambridge University Press (1985).
31. M. Zrinyi, L. Barsi, A. Buki, *Polym. Gels Networks*, **5**, 415 (1998).
32. A. S. Hoffman, *J. Controlled Release*, **6**, 297 (1987).
33. R. A. Siegel, B. A. Firestone, *J. Controlled Release*, **11**, 181 (1990).
34. T. Okana, Y. H. Bae, H. Jacobs, S. W. Kim, *J. Controlled Release*, **11**, 255 (1990).
35. Y. M. Lee, J. K. Shim, *Polymer*, **38**, 1227 (1997).
36. E. Kokufuta, T. Tanaka, *Macromolecules*, **24**, 1605 (1991).
37. H. Heskins, J. E. Guillet, *J. Macromol. Sci. Chem.*, **2**, 1441 (1969).
38. J. S. Scarpa, D. D. Mueller, I. M. Klotz, *J. Am. Chem. Soc.*, **89**, 6024 (1967).
39. L. C. Dong, A. S. Hoffamn, *J. Controlled Release*, **4**, 223 (1986).
40. Y. H. Bae, T. Okano, E. Hsu, S. W. Kim, *Makromol. Chem. Rapid. Commun.*, **8**, 481 (1987).
41. M. G. Kulkarni, S. S. Patil, V. Premnath, R. A. Mashelkar, *Proc. Roy. Soc. London, A* **439**, 397 (1992).
42. E. L. Cussler, M. R. Stokar, J. E. Varberg, *AIChE. J.*, **30**, 578 (1984).
43. M. J. Snowden, M. J. Murray, B. Z. Chowdary, *Chemistry and Industry*, **15**, 531 (1996).

44. B. Vernon, A. Gutowska, S. W. Kim, Y. H. Bae, *Macromol. Symp.*, **109**, 155 (1996).
45. R. Dagani, *Chem. Eng. News*, **75**, 26 (1997).
46. H. G. Schild, *Prog. Poly. Sci.* **17**, 163 (1992).
47. A. R. Schultz, P. J. Flory, *J. Am. Chem. Soc.*, **74**, 4760 (1952).
48. P. I. Freeman, J. S. Rowllison, *Polymer*, **1**, 20 (1960).
49. J. M. Bardin, D. Patterson, *Polymer*, **10**, 247 (1969).
50. S. Saito, M. Konno, H. Inomata, in "Responsive Gels: Volume Transition I, K. Dusek (Ed.), *Springer-Verlag, Berlin, Heidelberg, Adv. Polym. Sci.*, Vol. 109 p-207 (1993).
51. S. Ito, *Kobunshi Ronbunshu*, **46**, 437 (1989).
52. S. Fujishige, K. Kubota, I. Ando, *J. Phys. Chem.*, **93**, 3311 (1989).
53. D. DeRossi, K. Kajiwara, Y. Osada, A. Yamauchi (Eds.), "Polymer Gels", Plenum Press, New York, p-289 (1991).
54. W. D. Synder, I. M. Klotz, *J. Am. Chem. Soc.*, **97**, 4999 (1967).
55. H. Ohta, I. Ando, S. Fujishige, K. Kubota, *J. Polym. Sci. Part B Polym. Phys.*, **29**, 963 (1991).
56. K. Kubota, K. Hamano, N. Kuwahara, S. Fujishige, I. Ando, *Polym. J.*, **22**, 1051 (1990).
57. K. Kubota, S. Fujishige, I. Ando, *J. Phys. Chem.*, **94**, 5154 (1990).
58. F. M. Winnik, *Macromolecules*, **23**, 233 (1990).
59. H. G. Schild, D. A. Tirrell, *J. Phys. Chem.*, **94**, 4352 (1990).
60. J. H. Priest, S. L. Murray, J. R. Nelson, *Polym Prepr. (ACS, Div. Polym. Chem.)* **27**, 239 (1986).
61. I. Yamamoto, K. Iwasaki, S. Hirotsu, *J. Phys. Soc. Jpn.*, **58**, 210 (1989).
62. T. Norisuye, M. Shibayama, S. Nomura, *Polymer*, **39**, 2769 (1998).
63. K. Otake, H. Inomata, M. Konno, S. Saito, *J. Chem. Phys.*, **91**, 1345 (1989).
64. M. Shibayama, M. Morimoto, S. Nomura, *Macromolecules*, **27**, 5060 (1994).
65. K. C. Tam, X. Y. Wu, R. H. Pelton, *Polymer*, **33**, 436 (1992).
66. F. Zeng, X. Zheng, Z. Tong, *Polymer*, **39**, 1249 (1998).
67. J. Elaïssaf, *J. Appl. Polym. Sci.*, **22**, 873 (1978).
68. F. M. Winnik, *Macromolecules*, **23**, 1647 (1990).
69. F. M. Winnik, *Polymer*, **31**, 2125 (1990).
70. F. M. Winnik, H. Ringsdorf, J. Venzmer, *Macromolecules*, **24**, 1678 (1991).

71. H. G. Schild, D. A. Tirrell, *Polym Prepr. (ACS, Div. Polym. Chem.)*, **30**, 350 (1989).
72. H. G. Schild, D. A. Tirrell, *Langmuir*, **7**, 665 (1991).
73. P. R. Rajamohanam, S. Ganapathy, S. S. Ray, M. V. Badiger, R. A. Mashelkar, *Macromolecules*, **28**, 2533 (1995).
74. S. S. Ray, P. R. Rajamohanam, M. V. Badiger, I. Devotta, S. Ganapathy, R. A. Mashelkar, *Chem. Eng. Sci.*, **53**, 869 (1998).
75. S. Ganapathy, P. R. Rajamohanam, M. V. Badiger, A. B. Mandhare, R. A. Mashelkar, *Polymer*, **41**, 4543 (2000).
76. N. Tanaka, S. Matsukawa, H. Kurosu, I. Ando, *Polymer*, **39**, 4703 (1998).
77. M. V. Badiger, P. R. Rajamohanam, M. G. Kulkarni, S. Ganapathy, R. A. Mashelkar, *Macromolecules*, **24**, 106 (1991).
78. M. V. Deshmukh, A. A. Vaidya, M. G. Kulkarni, P. R. Rajamohanam, S. Ganapathy, *Polymer*, **41**, 7951 (2000).
79. K. Dušek, D. Patterson, *J. Polym. Sci. Part A2*, **6**, 1209 (1968).
80. O. B. Ptitsyn, Y. E. Eizner, *Biofizika*, **10**, 3 (1965).
81. I. M. Lifshitz, A. Y. Grosberg, A. R. Khokhlov, *Rev. Modern Phys.*, **50**, 683 (1978).
82. P. G. DeGennes, *Phys. Lett.*, **A38**, 339 (1972).
83. T. Tanaka, S. Ishiwata, C. Ishimoto, *Phys. Rev. Lett.*, **39**, 474 (1977).
84. T. Tanaka, *Phys. Rev. Lett.*, **40**, 820 (1978).
85. M. Marchetti, S. Parger, E. L. Cussler, *Macromolecules*, **23**, 1760 (1990).
86. M. Marchetti, S. Parger, E. L. Cussler, *Macromolecules*, **23**, 3445 (1990).
87. M. M. Prange, H. H. Hooper, J. M. Prausnitz, *AIChE. J.*, **35**, 803 (1989).
88. C. Panayiotou, I. C. Sanchez, *J. Chem. Phys.*, **95**, 10090 (1991).
89. A. K. Lele, M. V. Badiger, M. M. Hirve, R. A. Mashelkar, *Chem. Eng. Sci.*, **50**, 3535 (1995).
90. H. G. Schild, D. A. Tirrell, *Macromolecules*, **24**, 948 (1991).
91. F. M. Winnik, H. Ringsdorf, J. Venzmer, *Macromolecules*, **23**, 2415 (1990).
92. O. B. Ptitsyn, A. K. Aron, Y. Y. Eizner, *J. Polym. Sci.*, **C16**, 3509 (1968).
93. S. Hirotsu, *J. Phys. Soc. Jpn.*, **56**, 233 (1987).
94. T. Amiya, Y. Hirokawa, Y. Hirose, Y. Li, T. Tanaka, *J. Chem. Phys.*, **86**, 2375 (1987).

95. S. Katayama, Y. Hirokawa, T. Tanaka, *Macromolecules*, **17**, 2641 (1984).
96. H. Inomata, S. Goto, k. Otake, S. Saito, *Langmuir*, **8**, 687 (1992).
97. T. G. Park, A. S. Hoffman, *Macromolecules*, **26**, 5045 (1993).
98. H. Kawasaki, T. Mitou, S. Sasaki, H. Meada, *Langmuir*, **16**, 1444 (2000).
99. Y. Yang, F. Zeng, Z. Tong, X. Liu, S. Wu, *J. Polym. Sci.: Part B Polym. Phys.*, **39**, 901 (2001).
100. Y. H. Kim, I. C. Kwon, Y. H. Bae, S. W. Kim, *Macromolecules*, **28**, 939 (1995).
101. T. Tanaka in "Polyelectrolyte Gels: Properties, Preparation and Applications", R. S. Harland, R. K. Prud'homme, (Eds.), ACS Symp. Series 480, Amer. Chem. Soc., Washington, D. C., p-1 (1992).
102. F. Ilmain, T. Tanaka, E. Kokufuta, *Nature*, **349**, 400 (1991).
103. T. Tanaka, D.J. Fillmore, S-T. Sun, I. Nishio, G. Swislow, A. Shah, *Phys. Rev. Lett.*, **45**, 1636 (1980).
104. H. Inomata, S. Goto, S. Saito, *Macromolecules*, **23**, 4887 (1990).
105. R. Katakai, M. Yoshida, S. Hasegawa, Y. Lijima, *Macromolecules*, **29**, 1068 (1996).
106. A. Myoga, S. Katayama, *Polym. Prep. Japan*, **36**, 2852 (1987).
107. Z. Hu, X. Zhang, Y. Li, *Science*, **269**, 525 (1995).
108. B. K. Samra, I. Yu. Galaev, B. Mattiasson, *Angew. Chem., Int. Ed.*, **39**, 2364 (2000).
109. A. Suzuki, T. Tanaka, *Nature*, **346**, 345 (1990).
110. Z. Hu, Y. Li, *Polym. Gels Networks*, **3**, 267 (1995).
111. R. F. S. Freitas, E. L. Cussler, *Chem. Eng. Sci.* **42**, 97 (1987).
112. R. F. S. Freitas, E. L. Cussler, *Sep. Sci. Technol.* **22**, 911 (1987).
113. D. W. Johnson, E. L. Cussler, S. J. Trank, **US Pat. 4,863,613** (1989).
114. S. J. Trank, D. W. Johnson, E. L. Cussler, *Food Technol. (Chicago)*, **43**, 78 (1989).
115. A. S. Hoffman, A. Afrassiabi, L. C. Dong, *J. Controlled Release*, **4**, 213 (1986)
116. H. Ichijo, R. Kishi, O. Hirasa, Y. Takiguchi, *Polym. Gels Networks*, **2**, 315 (1994).
117. N. Yamada, T. Okano, H. Sakai, F. Karikusa, Y. Sawasaki, Y. Sakurai, *Makromol. Chem., Rapid Commun.*, **11**, 571 (1990).
118. J. Heller, *J. Controlled Release*, **8**, 111 (1988).
119. K. Mukae, Y. H. Bae, T. Okano, S. W. Kim, *Polym. J.*, **22**, 250 (1990).

120. A. Afrassiabi, A. S. Hoffman, L. A. Cadwell, *J. Membr. Sci.*, **33**, 1191 (1987).
121. L. C. Dong, A. S. Hoffman, *J. Controlled Release*, **13**, 21 (1990).
122. J. E. Chung, M. Yokoyama, T. Okano, *J. Controlled Release*, **65**, 93 (2000).
123. N. Monji, A. S. Hoffman, *Appl. Biochem. Biotechnol.*, **14**, 107 (1987).
124. P. S. Stayton, T. Shimoboji, C. Long, A. Chilkoti, G. Chen, J. M. Harris, A. S. Hoffman, *Nature*, **378**, 472 (1995).
125. K. D. Vorlop, K. Steinke, *Chem. Ing. Tech.* **60**, 790 (1988).
126. H. Kitano, C. Yan, K. Nakamura, *Makromol. Chem.*, **192**, 2915 (1991).
127. T. Kato, K. Fujimoto, H. Kawaguchi, *Polym. Gels Networks*, **2**, 307 (1994).
128. J. E. Glass, (Ed.), "Polymers in Aqueous Media: Performance through Association", *Advances in Chemistry Series 223*, ACS, Washington D.C. (1989).
129. M. J. Snowden, B. Z. Chowdhry, *Chemistry in Britain*, 943, Dec. (1995).
130. I. Ahmed, A. M. Araghi, *TRIP*, **2**, 92 (1994).
131. C. L. McCormick, T. Nonaka, C. B. Johnson, *Polymer*, **29**, 731 (1988).
132. P. L. Valint, J. Bock, *Macromolecules*, **21**, 175 (1988).
133. S. W. Shalaby, C. L. McCormick, G. B. Buttler, (Eds.) "Water Soluble Polymers: Synthesis, Solution Properties and Applications", *ACS Symp. Series 467*, Amer. Chem. Soc., Washington (1991).
134. D. Hourdet, F. L. Alloret, R. Audebert, *Polymer*, **35**, 2624 (1994).
135. I. Iliopoulos, U. Olsson, *J. Phys. Chem.*, **98**, 1500 (1994).
136. S. Biggs, J. Selb, F. Candau, *Langmuir*, **8**, 838 (1992).
137. G. Bokias, D. Hourdet, I. Iliopoulos, G. Staikos, R. Audebert, *Macromolecules*, **30**, 8293 (1997).

Chapter 2

Objectives & scope of work

2.1 Objectives and scope of work

Thermosensitive polymers, which exhibit the phenomenon of LCST, have been considered as a simple model to study the behavior of biopolymers, particularly proteins, in an aqueous system. There are four fundamental interactions, which play an essential role in determining the structures and specific functions of biopolymers. These are van der Waals, hydrophobic, hydrogen bonding and electrostatic interactions. These fundamental forces also govern the phase transition in gels. The scientific basis for LCST in thermosensitive polymers at a molecular level has not been properly understood so far. The LCST phenomenon in thermosensitive polymers is believed to arise from a balance of hydrophilicity and hydrophobicity of the polymers.¹⁻⁵ This balance could be obtained either from the side chains of repeat units of a homopolymer, random copolymers of different degrees of hydrophilicity, or from block copolymers of hydrophilic and hydrophobic blocks. Depending on the end application, the LCST can also be adjusted to a desired temperature by adding a third component (additive) such as salts,⁶⁻⁸ surfactants⁹ and nonelectrolytes.¹⁰ The various molecular interactions which results in LCST and their effects on the LCST is yet to be fully understood.

In order to meet the demands of a particular application, a polymer may be synthesized as discrete chains, as a microgel (nanoparticles), in gel form, as an interpenetrating polymer network, or it could be grafted onto a suitable matrix or substrate. The degree of swelling and the transition temperature can be modulated by adding co-solutes or co-solvents, by co-polymerization with monomers which are either more or less hydrophilic, by introducing ionic groups, or by varying the cross-linking density in the case of gels. Different properties are achieved depending on the nature of the copolymer: random as opposed to block copolymers. Copolymerization can also be used to create materials that are sensitive to other environmental stimuli such as pH, ionic strength, electric/magnetic fields and light instead of or in addition to temperature.¹¹

In view of the increasing demand for thermosensitive polymers in various applications as reviewed in previous chapter, there is a need to develop novel

polymers which will overcome difficulties associated with existing known polymers. The present investigation is undertaken with the following objectives:

1. To design and synthesize new thermosensitive polymers especially hydrogels having flexible hydrophobic groups and to study their volume phase transitions as a function of temperature. Novel hydrophobically modified monomers based on aminoacids with different alkyl chain lengths were synthesized and copolymerized with PNIPAm. A linear correlation between the transition temperature and the number of alkyl groups was found to exist in these gels. Such a correlation could be useful in designing gels with specific transition temperatures.
2. To synthesize thermosensitive copolymer gels based on biocompatible poly(ethylene oxide) and poly(*N*-isopropylacrylamide) by γ -radiation technique. Since these copolymer gels were synthesized by γ -radiation technique, they were free from impurities and can have potential biomedical applications.
3. To synthesize copolymer gels based on poly(*N*-isopropylacrylamide) and poly(acryloyl aminoacids) and their interactions with an anionic surfactant namely, sodium dodecyl sulfate (SDS). Such interactions in thermosensitive hydrogels will give an insight in developing novel drug delivery systems.
4. To synthesize of thermoassociating polymers based on copolymers of PNIPAm and *N*-benzylacrylamide and to study their rheological properties. The thermoassociative nature of the polymers influences the rheological properties significantly. Associations of such polymers in solutions cause shear thickening and form shear stable complexes, which have applications in drag reduction, enhanced oil recovery and coatings.
5. To investigate various experimental parameters on the mesoscopic morphologies developed during the phase transitions of thermosensitive polymers and also examine the coupling between the kinetics of phase separation and gelation.

2.2 References

1. L. Taylor, L. D. Cerankowski, *J. Polym. Sci.*, **13**, 2551 (1975).
2. H. Feil, Y. H. Bae, J. Feijen, S. W. Kim, *Macromolecules*, **26**, 2496 (1993).
3. P. S. Mumick, C. L. McCormick, *Polym. Eng. Sci.* **34**, 1419 (1994).
4. M. Shibayama, S. Mizutani, S. Nomura, *Macromolecules* **29**, 2019 (1996).
5. S. H. Cho, M. S. Jhon, S. H. Yuk, H. B. Lee, *J. Poly. Sci. Poly. Phys.* **35**, 595 (1997).
6. H. Inomata, S. Goto, K. Otake, S. Saito, *Langmuir*, **8**, 687 (1992).
7. S. Saito, *J. Polym. Sci., Polym. Chem. Ed.*, **7**, 1789 (1969).
8. T. G. Park, *Macromolecules*, **26**, 5045 (1993).
9. E. Kokufuta, Y. Zhang, T. Tanaka, A. Mamada, *Macromolecules*, **26**, 1053 (1993).
10. R. A. Horne, J. P. Almeida, A. F. Day, N. T. Yu, *J. Colloid Interface Sci.* **35**, 77 (1971).
11. P. S. Russo (Ed.), "Reversible Polymeric Gels and Related Systems", ACS Symp. Series 350, Amer. Chem. Soc., Washington D. C. (1987).

Introduction
1.1.1.1
1.1.1.2
1.1.1.3
1.1.1.4
1.1.1.5
1.1.1.6
1.1.1.7
1.1.1.8
1.1.1.9
1.1.1.10
1.1.1.11
1.1.1.12
1.1.1.13
1.1.1.14
1.1.1.15
1.1.1.16
1.1.1.17
1.1.1.18
1.1.1.19
1.1.1.20
1.1.1.21
1.1.1.22
1.1.1.23
1.1.1.24
1.1.1.25
1.1.1.26
1.1.1.27
1.1.1.28
1.1.1.29
1.1.1.30
1.1.1.31
1.1.1.32
1.1.1.33
1.1.1.34
1.1.1.35
1.1.1.36
1.1.1.37
1.1.1.38
1.1.1.39
1.1.1.40
1.1.1.41
1.1.1.42
1.1.1.43
1.1.1.44
1.1.1.45
1.1.1.46
1.1.1.47
1.1.1.48
1.1.1.49
1.1.1.50
1.1.1.51
1.1.1.52
1.1.1.53
1.1.1.54
1.1.1.55
1.1.1.56
1.1.1.57
1.1.1.58
1.1.1.59
1.1.1.60
1.1.1.61
1.1.1.62
1.1.1.63
1.1.1.64
1.1.1.65
1.1.1.66
1.1.1.67
1.1.1.68
1.1.1.69
1.1.1.70
1.1.1.71
1.1.1.72
1.1.1.73
1.1.1.74
1.1.1.75
1.1.1.76
1.1.1.77
1.1.1.78
1.1.1.79
1.1.1.80
1.1.1.81
1.1.1.82
1.1.1.83
1.1.1.84
1.1.1.85
1.1.1.86
1.1.1.87
1.1.1.88
1.1.1.89
1.1.1.90
1.1.1.91
1.1.1.92
1.1.1.93
1.1.1.94
1.1.1.95
1.1.1.96
1.1.1.97
1.1.1.98
1.1.1.99
1.1.1.100

Chapter 3

Molecular tailoring of thermosensitive hydrogels

3.0 Introduction

In order to develop a thermosensitive polymer for a specific end-application, its LCST has to be tailor made. This can be achieved by changing the ratios of two monomers concentration in the copolymerization and also by slightly varying the chemical structure of the hydrogel by introducing hydrophobic/hydrophilic groups in the chain. Hydrophobic and hydrogen bonding interactions play an important role in determining the transition temperature of the hydrogel. The degree of swelling and the transition temperature of an hydrogel can be modulated by adding co-solutes or co-solvents in the medium or by copolymerization with comonomers which are either more or less hydrophobic in nature. This chapter describes our strategies of changing the chemical structure of hydrogels and the results of our investigations are presented in two parts.

In the first part, we report on the synthesis of novel comonomers with increasing degrees of hydrophobicity by changing the alkyl chain length of monomers and copolymerization with PNIPAm. We also show that the hydrophobic content of the tailor-made copolymer gels has a significant effect on the phase transition temperature of the gels. Such gels can find novel applications in biotechnology, soft robotics, separation and sensors.

In the second part, we describe the copolymer gel synthesis by using γ -radiation technique. This technique is highly suitable for synthesizing hydrogels for biomedical applications since they are free from impurities.

Part A

Synthesis of hydrophobically modified thermosensitive hydrogels

3.1 Introduction

The ability of controlling volume transition temperatures has significance in synthesizing tailored gels for specific applications such as novel separation processes. The LCST-type volume transitions of non-ionic gels such as PNIPAm can not be predicted by the Flory theory of polymeric networks since it does not consider the specific energetic interactions such as hydrogen-bonding, which are predominantly present in hydrogels. The Lattice-Fluid-Hydrogen-Bond (LFHB)¹ theory clearly shows that the discontinuous volume transition of PNIPAm gel in water is caused by a large increase in the inter-polymer hydrogen bonds at the transition temperature and by the temperature dependent effective hydrophobicity of the polymer. Lele *et al.*² first time pointed out the role of both hydrogen bonding and hydrophobic interactions on the volume transition of gels and show how these interactions could be used to control the transition temperatures of gels.

In the study of copolymer gels, the effect of comonomers has been investigated by various groups. Mumick and McCormick³ reported that copolymerising NIPAm with acrylamide (AAm) resulted in higher transition temperatures than pure PNIPAm gel. Similarly, Shibayama *et al.*⁴ found that copolymerizing NIPAm with increasing quantities of acrylic acid (AAc) or dimethylacrylamide (DMAAm) gives gels with increasing LCSTs. They also found that the heat of demixing associated with the volume transition, which was experimentally measured by the area under the endothermic peak in DSC scans, decreased with the addition of AAc and DMAAm. Feil *et al.*⁵ found that copolymerization of hydrophilic comonomers such as AAm, AAc, and (diethylamino)ethyl methacrylate (DEAEMA) increased the LCST of poly(NIPAm-co-butyl methacrylate-co-X) terpolymer gels, while the copolymerization of hydrophobic butyl methacrylate with the terpolymer decreased the LCST of the gels.

The heat of volume transition, ΔH is considered to be associated with the breakage of hydration layers of water molecules surrounding the hydrophobic groups on

the polymer network. Feil *et al.*⁵ proposed that the presence of hydrophilic comonomers reduces the concentration of the hydrophobic groups and consequently the hydrating water layers, hence decreasing the ΔH . The opposite is true for the presence of hydrophobic comonomers in gels. Inomata *et al.*⁶ have shown that n-propyl acrylamide (NPAm) gel has a lower LCST, a higher ΔH and a larger magnitude of the transition than NIPAm and cyclopropyl acrylamide (CPAm) gels. The authors propose that the larger "contact area" of the n-propyl group as compared to isopropyl and cyclopropyl groups enables the structuring of hydrated water molecules to a greater extent, which results in lowering of LCST and increase of ΔH for NPAm gels.

It is clear from the foregoing that the balance of hydrophobic and hydrophilic groups in the copolymer gels plays a vital role in determining the LCST. However, it is not yet fully understood as to how various factors such as the hydrophobicity affect the LCST of copolymer gels. In this chapter, we will investigate the role of chemical structure of the hydrophobic comonomer on the volume phase transition and heat of demixing in PNIPAm gel. We show that, while our experimental results are in agreement with earlier theoretical predictions², they also provide new insights into the subtle effects of hydrophobic interactions on volume transitions.

We have synthesised three comonomers with increasing alkyl chain lengths using 4-amino butyric acid, 6-amino caproic acid and 11- ω , amino undecanoic acid. The above compounds were condensed with acryloyl chloride in the presence of alkali to get monomers, which were copolymerized with NIPAm to give novel hydrophobically modified copolymer gels. We observe a reduction in the LCST as well as a decrease in the heat of demixing of the copolymer gels by increasing the hydrophobic alkyl chain length in the comonomer or by increasing the content of the hydrophobic comonomer in the copolymer. A linear relation was observed between the length of the alkyl chain and the transition temperature. This result provides a deeper mechanistic insight into the nature of volume transition phenomenon in gels.⁷

3.1.1 Theory

We have described the extended LFHB model as applicable for the binary system of a copolymer gel and water in chapter 1.

The free energy of mixing is calculated from a mean field assumption in which the mers of the two components 1 and 2 are randomly placed in a lattice. For the mixture of n_1 molecules of component 1 and n_2 molecules of component 2 ($N = n_1 + n_2$) the mer length (r), the characteristic mer volume (v^*) and the characteristic mean field mer-mer interaction energy (ε^*) are given by

$$\frac{1}{r} = \frac{\phi_1}{r_1} + \frac{\phi_2}{r_2} \quad (3.1)$$

$$v^* = \phi_1 v_1^* + \phi_2 v_2^* \quad (3.2)$$

$$\varepsilon^* = \phi_1^2 \varepsilon_1^* + \phi_2^2 \varepsilon_2^* + 2\phi_1 \phi_2 \zeta_{12} (\varepsilon_1^* \varepsilon_2^*)^{0.5} \quad (3.3)$$

where, subscripts 1 and 2 represent the components water (1) and polymer (2), respectively. ϕ is the volume fraction, r_i is the number of lattice sites occupied by a molecule of component i , v_i^* is the characteristic mer volume of component i and ε_i^* is the characteristic mer-mer interaction energy for component i . A pure component i is thus characterized by three parameters r_i , v_i^* and ε_i^* . ζ_{12} is the binary interaction parameter between components 1 and 2.

The characteristic parameters of the pure copolymer are obtained from equations (3.1) to (3.3) by assuming that the copolymer can be considered as a random mixture of the two homopolymers A and B, which form the copolymer A-B, and that the binary interaction parameter between the two polymers ζ_{AB} is unity. In using equations (3.1) to (3.3) for the copolymer the subscripts 1 and 2 are replaced by A and B representing the two homopolymers. Thus the theory is essentially applicable only for a random copolymer A-B. The volume fractions of the mers of two homopolymers are calculated as

$$\phi_i = \frac{w_i / \rho_i^*}{\sum_i w_i / \rho_i^*} \quad (3.4)$$

where w_i is the weight of the component i ($i=A,B$) and ρ_i^* is its characteristic density.

In a mixture of the copolymer (component 2) and the water (component 1), the binary interaction parameter ζ_{12} is calculated as

$$\zeta_{12} = \zeta_{1A}\phi_A + \zeta_{1B}\phi_B \quad (3.5)$$

where, the binary interaction parameters between water and the two homopolymers A and B are in general given as

$$\zeta_{1i} = a_i T + b_i; \quad i = A, B \quad (3.6)$$

The binary interaction parameter between the copolymer and the water can be considered as simulating the 'hydrophobicity' of the copolymer since the hydrophilic part of the interactions are considered separately in the hydrogen bonding terms in the mean-field framework of the LFHB theory as summarized below.

Let there be i ($i=1,m$) types of proton donors and j ($j=1,n$) types of proton acceptors in the system of gel and solvent. The total number of donors and acceptors are given by

$$N_d^i = \sum_k d_i^k n_k \quad \text{and} \quad N_a^j = \sum_k a_j^k n_k \quad (3.7)$$

where d_i^k and a_j^k are the number of donors of type i and acceptors of type j in component k . If N_{ij} is the total number of hydrogen bonds formed between an i - j donor-acceptor pair, then the number of undonated protons of type i and unaccepted protons of type j are given by

$$N_{io} = N_d^i - \sum_j N_{ij} \quad \text{and} \quad N_{oj} = N_a^j - \sum_i N_{ij} \quad (3.8)$$

If E_{ij}^o , S_{ij}^o and V_{ij}^o are the changes in the energy, entropy and volume due to the formation of an i - j hydrogen bond, then the fraction of such i - j bonds formed are given by

$$v_{ij} = \left[v_d^i - \sum_k^n v_{ik} \right] \left[v_a^j - \sum_k^m v_{kj} \right] \exp(-G_{ij}^o / RT) \quad (3.9)$$

where,

$$v_{ij} = \frac{N_{ij}}{rN}; \quad v_d^i = \frac{N_d^i}{rN}; \quad v_a^j = \frac{N_a^j}{rN}; \quad G_{ij}^o = E_{ij}^o + PV_{ij}^o - TS_{ij}^o \quad (3.10)$$

The free energy of mixing in the LFHB model can be calculated from the mixing rules given by eq. (3.1)-(3.3) and the hydrogen bonding fractions given by eq. (3.9). The details of the free energy of mixing terms are described in Lele *et al.*¹

The model parameters for a binary mixture include six pure component parameters (three for each component), one binary interaction parameter (ζ_{12}), three hydrogen bonding parameters ($E_{ij}^o, S_{ij}^o, V_{ij}^o$) for each i - j type of H-bond, and the cross-link density (v_c/V_o). Parametric values are discussed in the Results and Discussions section.

The collapse of the gel at the transition temperature occurs by demixing of polymer and water molecules, which is accompanied by a heat of demixing. This heat of demixing per gram of dry polymer gel, which is observed as an endothermic peak in a DSC experiment, can be calculated from the LFHB model by using the following thermodynamic cycle:

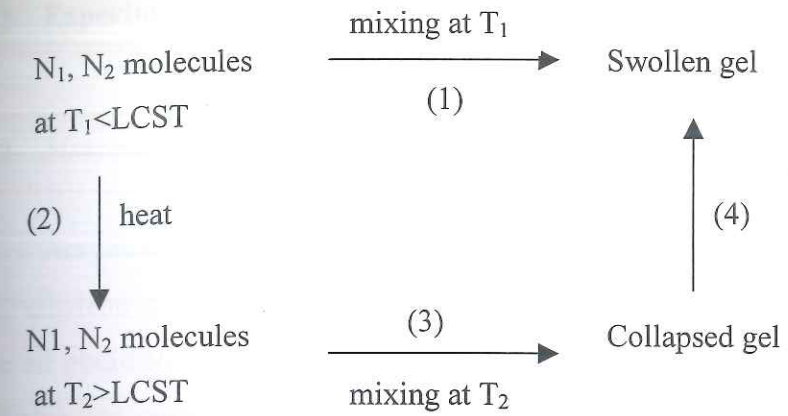


Figure 3.1: Sequence of swelling and collapse in the LFHB model

From the above cycle, the heats associated with steps 1 and 3 are responsible for the peak in the DSC endotherm. Therefore,

$$\Delta H_4 = -\Delta H_1 + \Delta H_3 \quad (6.11)$$

where, ΔH_1 and ΔH_3 are the enthalpies of mixing and can be calculated from the LFHB theory on a per gram dry polymer basis by the following equation.

$$\Delta H_{mix} = \frac{r}{x_2 MW_2} \left\{ -\tilde{\rho} \varepsilon^* + \sum \tilde{\rho}_k \phi_k \varepsilon_k^* + \sum_i^m \sum_j^n E_{ij}^o \left[v_{ij} - \sum_k v_{ij}^k \right] \right\} \quad (6.12)$$

where, MW_2 is the molecular weight of the polymer, $\tilde{\rho}_k$ is the reduced density of pure component k and v_{ij}^k is the number of hydrogen bonds between an i - j pair in pure component k .

In the following section, we show that the extended LFHB model can quantitatively predict the experimental swelling measurements of the copolymer gels, and also qualitatively show the experimentally observed trends in the heat of demixing of copolymer gels.

3.1.2 Experimental Section

3.1.3 Materials

Acrylic acid, 4-amino butyric acid, 6-amino caproic acid, 11, ω -amino undecanoic acid, ethylene glycol dimethacrylate (EGDMA) and methylene bis-acrylamide(Bis-A) were all obtained from Aldrich Chemical Company Inc. USA. *N*-isopropyl acrylamide (NIPAm) was purchased from PolySciences Inc. (Warrington, PA, USA) and was used without further purification. AR grade 1,4-dioxane was obtained from J.T.Baker Chemical Co., Philipsberg, NJ, USA. Thionyl chloride was procured from S.D.Fine Chemicals, Mumbai, India and purified by distillation. The initiator azo isobutyronitrile (AIBN) was purchased from SAS Chemical Co., Mumbai, India and was purified by recrystallisation in ethanol. The deionized distilled water was prepared in the laboratory using standard procedures.

3.1.4 Synthesis of Monomers

3.1.4.1 Acryloyl Chloride

Acryloyl chloride was synthesised by the reaction between acrylic acid and thionyl chloride. Thus, acrylic acid (20.5ml, 0.3M) along with dimethyl formamide (2ml) and hydroquinone (3g) was taken in a round bottomed flask. Freshly prepared thionyl chloride (23ml, 0.3M) was added dropwise over a period of 1-2 hrs. After complete addition of thionyl chloride, the reaction mixture was heated at 60 °C for 6hrs. with continuous stirring. The flask was then kept overnight at room temperature. Further, 3g of hydroquinone was added and pure acryloyl chloride was distilled out from the flask at 70-71°C under normal conditions.

¹H NMR (200MHz, CDCl₃) δ 6.1 (d, 1H), 6.3 (m, 1H), 6.5 (d, 1H).

The hydrophobic monomers were synthesised by the reaction between acryloyl chloride and corresponding aminoacids as per the reaction scheme shown in Figure 3.2. The hydrophobic comonomers are coded on the basis of length of the alkyl chain (X).

3.1.4.2 Acryloyl-4-amino butyric acid [X3]

In a 100ml beaker equipped with a pH electrode, 2.25g of 4-amino butyric acid (0.02M), 15ml distilled water, 0.8g sodium hydroxide were placed to give a clear solution. The solution was stirred with a magnetic needle at 5-10 °C (ice-water bath). To this solution, 1.7ml acryloyl chloride (0.02M) in 2ml of dichloromethane was added dropwise over a period of 1-2 hrs. After addition of half of the acid chloride, pH of the reaction mixture dropped to 7.5 and it was maintained between 7.5 and 7.8 by the addition of sodium hydroxide solution. Unreacted acryloyl chloride and dichloromethane was removed by extraction with ethyl acetate. The clear aqueous layer was acidified to pH 5.0-5.5 with dilute hydrochloric acid and extracted with ethyl acetate. The product in the ethyl acetate layer was dried with anhydrous sodium sulfate and concentrated in rotavapour. On cooling the concentrate, solid monomer was precipitated. It was further purified by redissolving in ethyl acetate and reprecipitating in petroleum ether. (white powder, yield-49%, m.p. 90.1°C).

IR (Nujol)

3278 cm^{-1} (-NH and -OH stretching), 2950 cm^{-1} and 2957 cm^{-1} (-CH stretching), 1701 cm^{-1} (-CO stretching of -COOH), 1643 cm^{-1} (-CO stretching of -CONH₂), 1540 cm^{-1} (-NH bending)

¹H NMR (D₂O, ppm)

δ2.3 (-CH₂COO), δ1.8 (-CH₂-), δ3.3 (-CH₂-N), δ4.8 (HOD), δ5.8 (CH₂=CH), δ6.2 (CH₂=CH)

3.1.4.3 Acryloyl-6-amino caproic acid [X5]

X5 was synthesized by the reaction between acryloyl chloride and 6-amino caproic acid using the same procedure used for the preparation of X3 mentioned above. Stoichiometric amounts of reactants were used for the reaction. (white powder, yield-55%, m.p 77.4 °C)

IR (Nujol)

3284 cm^{-1} (-NH and -OH stretching), 2978 cm^{-1} and 2852 cm^{-1} (-CH stretching), 1697 cm^{-1} (-CO stretching of -COOH), 1650 cm^{-1} (-CO stretching of -CONH₂), 1622 cm^{-1} (-C=C stretching), 1546 cm^{-1} (-NH bending)

¹H NMR (CDCl₃, ppm)

δ 2.3 (CH₂-COO), δ 1.7 (-CH₂)₂, δ 1.4 (-CH₂)₂-CH₂, δ 3.3 (-N-CH₂), δ 5.6 (-CH=CH), δ 6.2 (CH₂=CH).

3.1.4.4 *Acryloyl-11, ω-amino undecanoic acid [X10]*

X10 monomer was synthesised by the reaction between acryloyl chloride and 11-ω, amino undecanoic acid, using the same procedure with the stoichiometric amounts of reactants. The dissolution of 11-ω, amino undecanoic acid in aqueous alkali, however, was carried out at room temperature (28⁰C) instead of 5-10⁰C because of its precipitation at low temperature (white powder, yield-53%, mp 237⁰C).

IR (Nujol)

3304 cm^{-1} (-NH and -OH stretching), 2924 cm^{-1} and 2854 cm^{-1} (-CH stretching), 1693 cm^{-1} (-C=O stretching of -COOH), 1652 cm^{-1} (-C=O stretching of -CONH₂), 1623 cm^{-1} (-C=C stretching), 1540 cm^{-1} (-NH bending).

¹H NMR (CDCl₃, ppm)

δ 2.3 (CH₂-COO), δ 1.6 ((CH₂)₂-CH₂-COO), δ 1.3 ((-CH₂)₆), δ 3.3 (NH-CH₂), δ 5.7 (-CH=CH₂), δ 6.25 (CH₂=CH-).

3.1.5 *Synthesis of Copolymer Gels*

We synthesized the gels by copolymerizing X3, X5 and X10 monomers with *N*-isopropyl acrylamide as per the feed composition given in Table 3.1. The copolymerisation was carried out in 1,4 Dioxane using EGDMA as cross linker and AIBN as a free radical initiator. The reaction scheme is shown in Figure 3.2. The required amounts of monomers (with defined mole ratios), crosslinking agent and initiator were

Table 3.1
Feed compositions of copolymer gels

Sample Code	Mole Ratio=1/0.1 (moles)	Cross linker (moles)	Initiator (moles)	Solvent (ml)
X3-1	NIPAm/X3 (0.0177 / 0.00177)	EGDMA (1.5x 10 ⁻³)	AIBN (4.87x10 ⁻⁴)	1,4-Dioxane (20)
X5-1	NIPAm/X5 (0.0177 / 0.00177)	EGDMA (1.5x 10 ⁻³)	AIBN (4.87x10 ⁻⁴)	1,4-Dioxane (20)
X10-1	NIPAm/X10 (0.0177 / 0.00177)	EGDMA (1.5x 10 ⁻³)	AIBN (4.87x10 ⁻⁴)	1,4-Dioxane (20)
X5-3	NIPAm/X5 (0.0177 / 0.00531)	EGDMA (1.5x 10 ⁻³)	AIBN (4.87x10 ⁻⁴)	1,4-Dioxane (20)
X5-5	NIPAm/X5 (0.0177 / 0.0885)	EGDMA (1.5x 10 ⁻³)	AIBN (4.87x10 ⁻⁴)	1,4-Dioxane (20)
NIPAm	N-isopropyl acrylamide			
EGDMA	Ethylene glycol dimethacrylate			
AIBN	Azo-bis-isobutyronitrile			
X3	Acryloyl-4-amino butyric acid			
X5	Acryloyl-6-amino caproic acid			
X10	Acryloyl-11-ω-amino undecanoic acid			

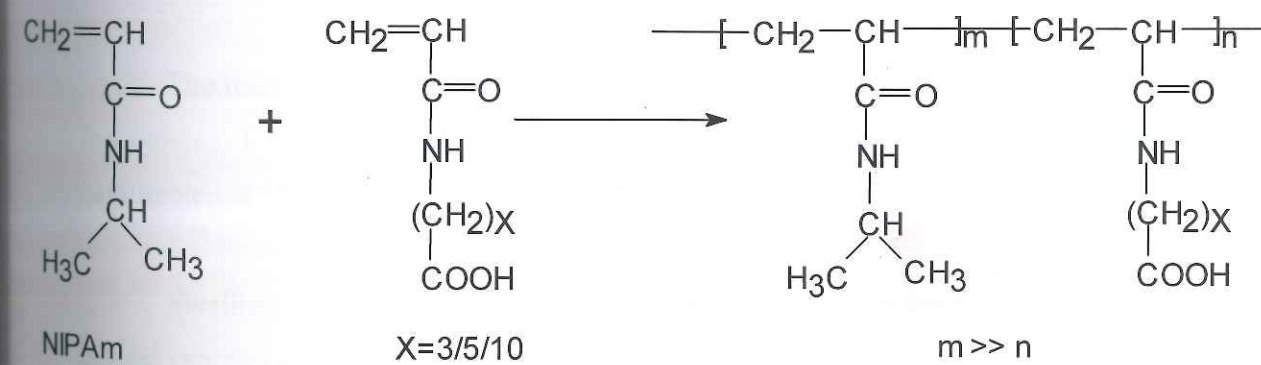
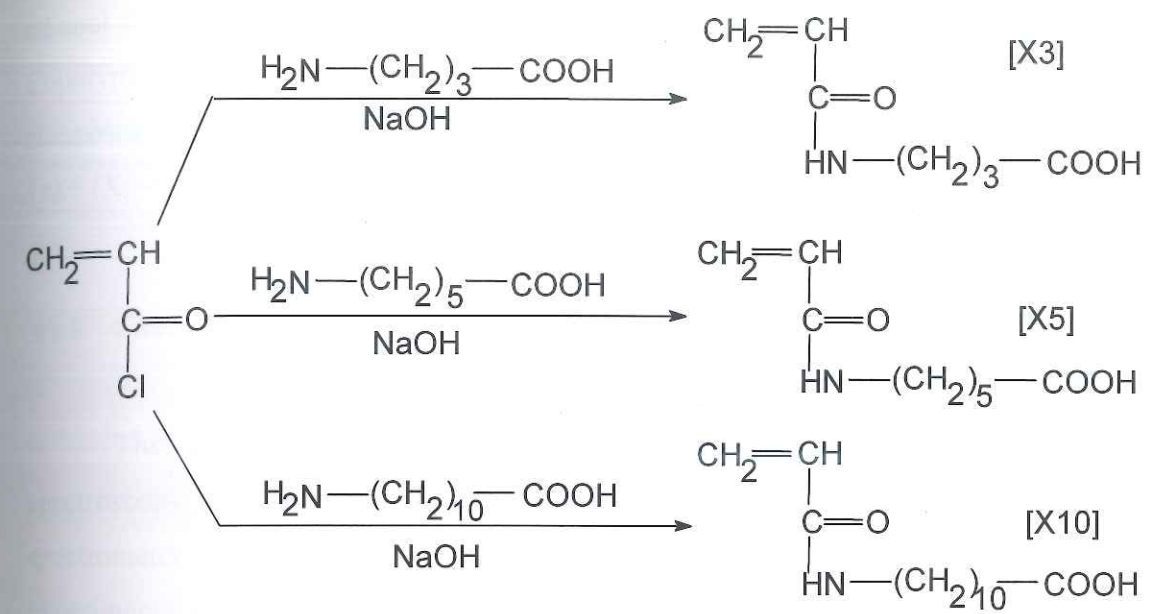


Figure 3.2: Reaction scheme for the synthesis of hydrophobic monomers and the copolymer gels.

taken in a beaker and dissolved in 1,4-dioxane with constant stirring and N₂ bubbling. The reaction mixture was poured into test tubes and sealed. The polymerisation was carried out 70 °C for 24 hrs. The gels obtained in a cylindrical form were washed with water and ethanol for one day and dried in oven at 40 °C till the constant weight was obtained. Copolymer gels of NIPAm and monomer X5 were prepared with three different compositions corresponding to NIPAm/X5 mol ratio of 1/0.1 (X5-1), 1/0.3 (X5-3) and 1/0.5 (X5-5).

3.1.6 Characterization of gels

The gels were characterized for their molecular structure by ¹³C MASS spectroscopy. All ¹³C-NMR spectra were obtained on a Bruker MSL-300 FT NMR spectrometer operating at a carbon frequency of 75.47 MHz. For the CP-MASS experiments, cross-polarization was established using matched Hartmann-Han conditions at 50kHz using an adamantane as standard. ¹³C CP-MASS spectra of each sample were taken at two different speeds to identify the center band and side bands. The spectra were recorded at a probe temperature of 25°C.

The thermal characterization of the gels was done using a DSC (Model 2920, TA Instruments, USA) at heating scan rate of 3°C/min. Thoroughly sealed samples were equilibrated at 5°C and then heating scan were recorded from 5°C to 50°C.

Swelling measurements were carried out by immersing 4mm x 5mm cylindrical dry gel samples in excess water, which was maintained at a controlled temperature within ±0.5°C. The gels were allowed to equilibrate for 72 hours during which constant weight was reached, after which they were quickly removed and weighed. The surface water was carefully wiped off before weighing. Swelling capacity was recorded gravimetrically as

$$q = \frac{\text{Weight of equilibrated gel}}{\text{Weight of dry gel}} \quad (3.13)$$

3.1.7 Results and Discussions:

3.1.7.1 Copolymer structure

We show in Figure 3.3 the ^{13}C spectra of X3-1, X5-1 and X10-1 copolymer gels and compare them with the spectra of two homopolymer gels PNIPAm and X10. In the PNIPAm homopolymer spectrum the $-\text{CH}_3$ peaks appears at 24.8 ppm, carbonyl of $-\text{CONH}$ appear at 174.7 ppm. The backbone $-\text{CH}$ and $-\text{CH}_2$ peaks resonate at the broad range of 40-50 ppm. The incorporation of hydrophobic monomer in the copolymer is confirmed by careful analysis of all the spectra. The ^{13}C spectrum of homopolymer of acryloyl-11, ω -aminoundecanoic acid shows a characteristic peak of hydrophobic side chain $-\text{CH}_2$ group at 29.6 ppm, which is totally absent in the ^{13}C spectrum of PNIPAm homopolymer. However, this peak is progressively distinct in copolymer gels X3-1, X5-1 and X10-1 as the chain length of $-\text{CH}_2$ increases. This clearly indicates the incorporation of hydrophobic comonomer in the copolymer gels. It is difficult to distinguish between the $-\text{CO}$ signals arising due to $-\text{CONH}_2$ and $-\text{COOH}$ of copolymer gels because of their very small chemical shift differences. The quantitative estimation of the copolymer composition is extremely difficult due to uncertainties in the integration of the ^{13}C signals of copolymer gels. Moreover, the mole ratios of hydrophobically modified monomer to NIPAm monomer used for copolymerisation is very low to get well resolved ^{13}C signals from comonomer structure.

We assume that since the concentration of comonomer in the gel is very small and the monomers are completely soluble in the solvent used for synthesis (1,4-Dioxane), the copolymers thus formed are random copolymers.

3.1.7.2 Swelling behavior and LCST

The effect of the presence of hydrophobic comonomers on the swelling of PNIPAm based gels is shown in Figure 3.4. PNIPAm homopolymer gel was found to undergo a non-discontinuous but a steep LCST-type deswelling as the temperature was raised between 27°C to 30°C.

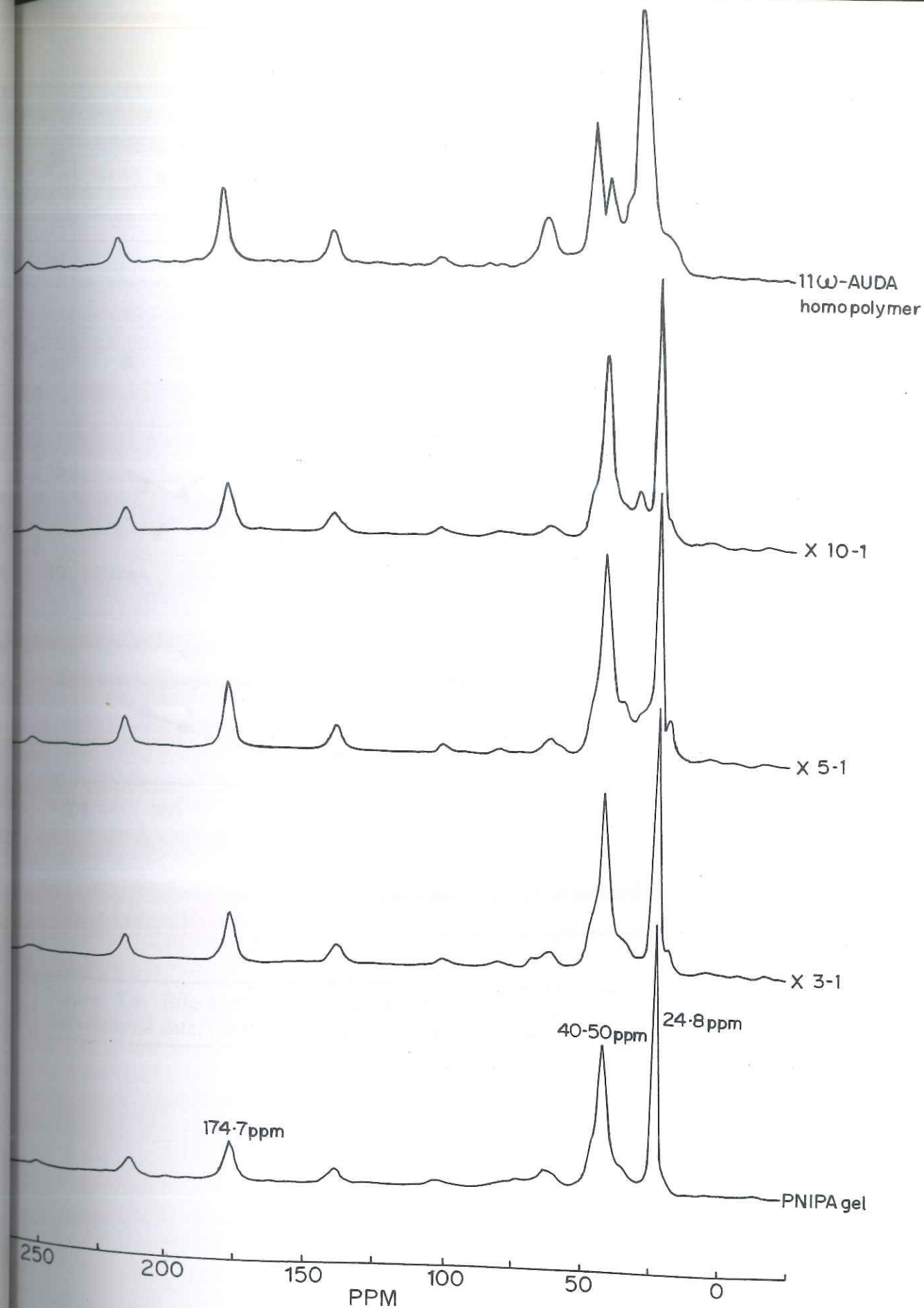


Figure 3.3: Comparison of ^{13}C NMR spectra of homopolymer and copolymer gels

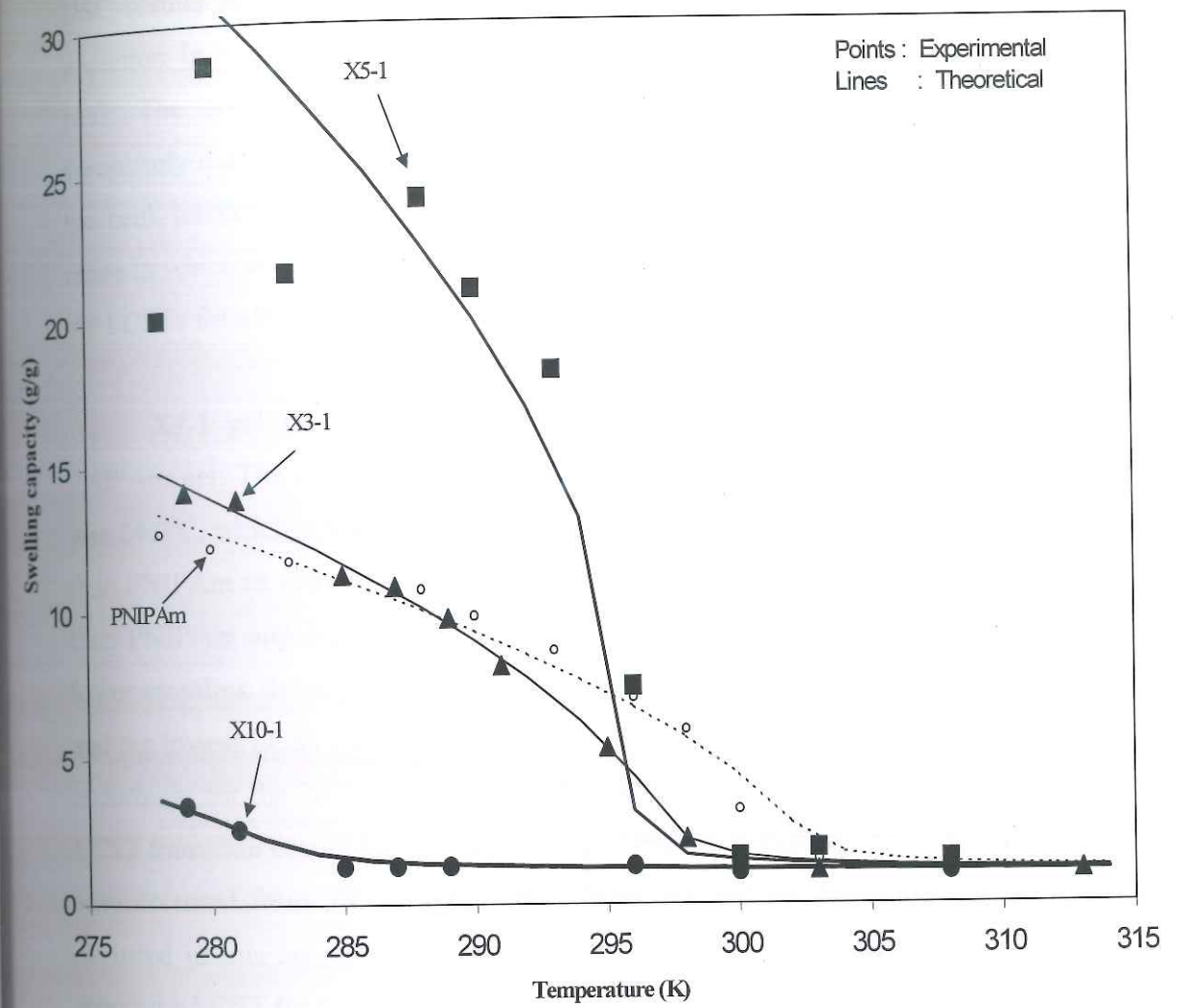


Figure 3.4: Effect of alkyl chain length on swelling behavior of copolymer gels. Experimental data: (○) PNIPAm; (▲) X3-1; (■) X5-1; (●) X10-1. Lines are theoretical fits.

The nature of the transition and the LCST of the gel was also confirmed from the DSC results shown in Figure 3.5. As seen from the DSC heating scans, the volume transition is accompanied with a heat of demixing, which appears as an endothermic peak. The broadness of the endotherm indicates that the volume transition is not completely discontinuous, which is in agreement with the swelling measurements. Also, the peak temperature of 28.5°C corresponds closely to the mid-way temperature of the range in which deswelling occurs. Therefore, we will report here the peak temperatures as the LCSTs for all gels.

X3-1 gel was found to have a lower equilibrium swelling capacity than the PNIPAm gel. The LCST of the gel as measured from swelling measurements and DSC was 24.9°C, which is lower than that of PNIPAm gel. X5-1 has a higher swelling capacity than PNIPAm as seen from Figure 3.4. However, the LCST of 21.3°C for X5-1 is lower than PNIPAm and X3-1 gels. The higher swelling capacity of X5-1 could be due to a lower crosslink density of the gel. X10-1 has the smallest equilibrium swelling capacity and the lowest LCST (10°C) of all the copolymer gels. It was not possible to observe the endotherm for the X10-1 gel in the DSC because of the low temperatures at which the LCST transition occurs for this gel. The equilibration to baseline from the initiation of the scan occurred from 5°C to about 10°C. Since the volume transition for the X10-1 gel occurred in this range, it was not possible to record its endotherm in DSC. Hence we report the LCST for this gel from the swelling measurements alone.

The effect of increase in the concentration of the hydrophobic comonomer X5 on the swelling ratio is shown in Figure 3.6. Copolymer gels X5-1, X5-3 and X5-5, which contain increasing concentrations of X5 show a decrease in LCSTs and reduced equilibrium swelling capacities. The corresponding DSC endotherms for these gels are shown in Figure 3.5. X5-3 shows an LCST of 13.5°C compared to 21.3°C for X5-1. The scan for X5-5 does not show any endotherm for the same reasons as for X10-1 described above.

It can be seen from the above results that the main effect of copolymerizing NIPAm with hydrophobic comonomers is to lower the LCST of the gel. The higher the concentration of the hydrophobic comonomer and the longer the hydrophobic alkyl chain length, the lower is the LCST of the gel. Thus, increasing concentration of X5

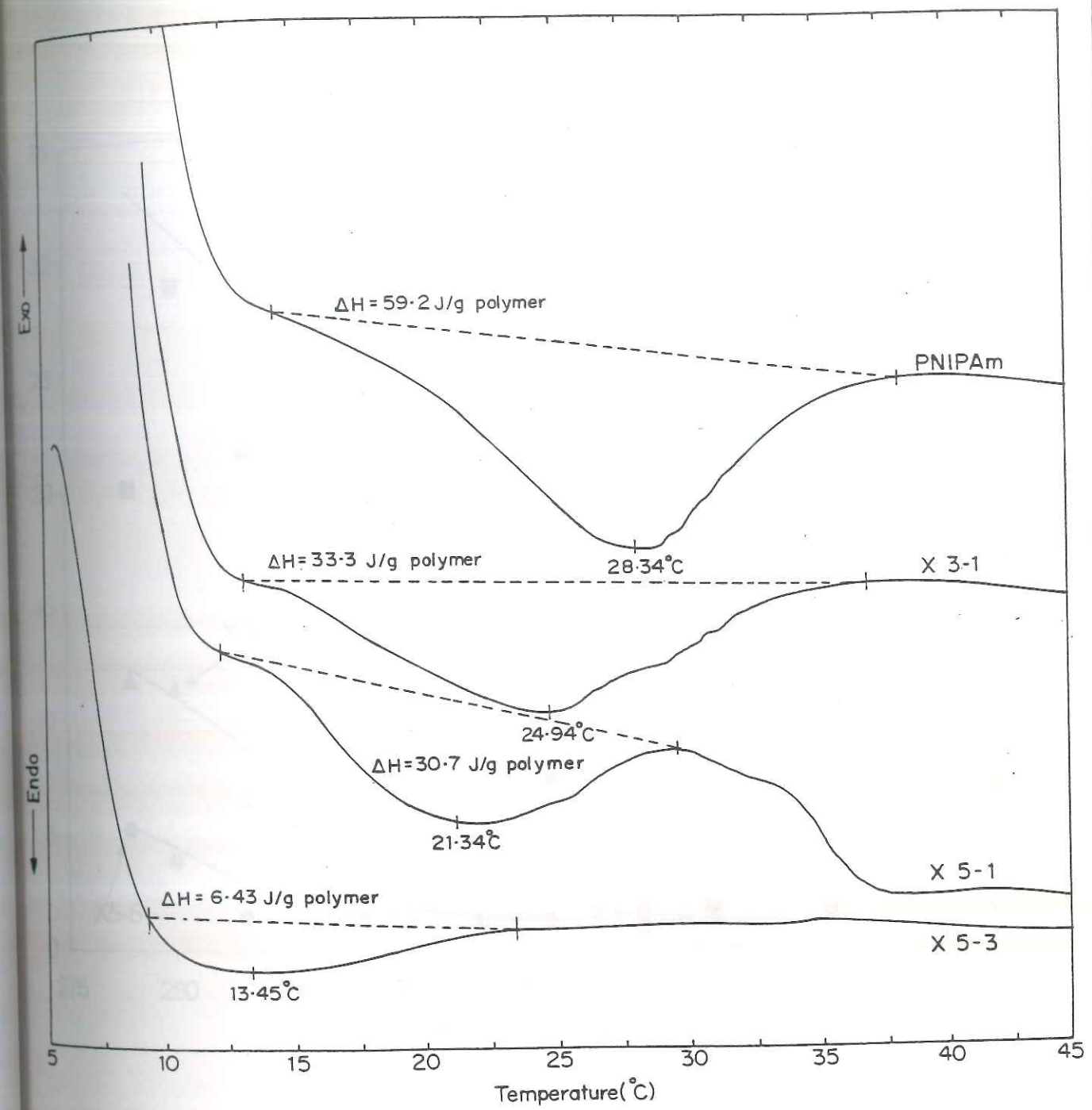


Figure 3.5: DSC heating scans of copolymer gels

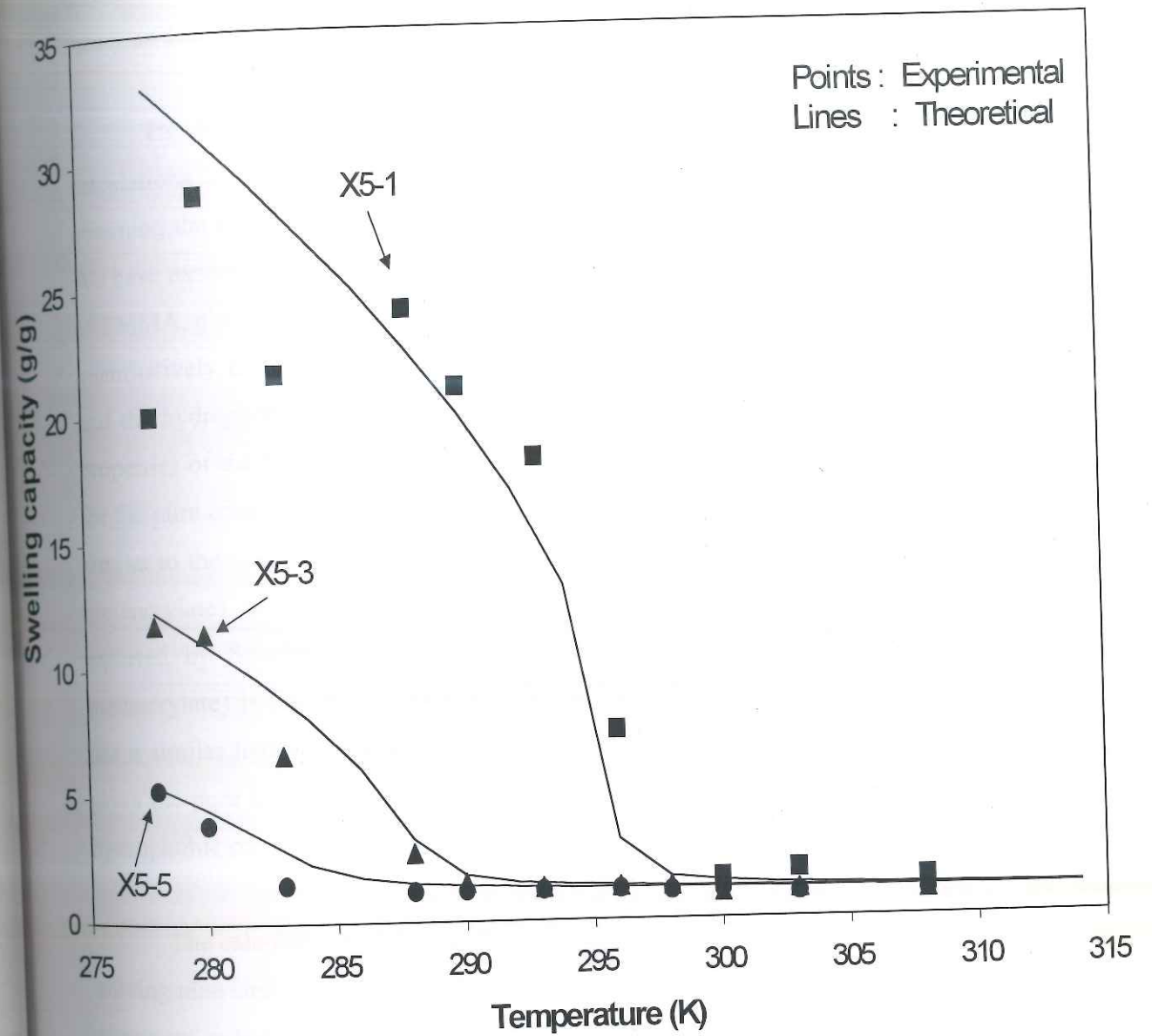


Figure 3.6: Effect of concentration of hydrophobic comonomer on swelling behavior of copolymer gels. Experimental data: (■) X5-1; (▲) X5-3; (●) X5-5. Lines are theoretical fits.

comonomer reduces the LCST significantly, and increasing the chain length of the hydrophobe from X3 to X5 to X10 also reduces the LCST of the gel. These effects can be understood more quantitatively by fitting the experimental data to the extended LFHB theory as described below.

The lines through the experimental data points in Figures 3.4 and 3.6 are the calculations of the extended LFHB theory. The various model parameters used for obtaining the theoretical fits are listed in Table 3.2 to Table 3.4 and are discussed below. We have assumed that the pure component parameters of PNIPAm are the same as those of PMMA, given by Sanchez and Lacombe.^{8,9} We have shown that these parameters can quantitatively fit the swelling behavior of PNIPAm gel.¹ For the copolymers of NIPAm and the hydrophobic comonomers, the extended LFHB model requires pure component properties of the homopolymer of the hydrophobic monomer. In the absence of any data for the pure component properties of these homopolymers, we have assumed, in a manner similar to the case of PNIPAm, the values for pure component properties of poly(*n*-butyl methacrylate) as being applicable for these homopolymers. These values have been reported by Sanchez and Lacombe.¹⁰ The rationale for the choice of poly(*n*-butyl methacrylate) is that it is more hydrophobic than poly(methyl methacrylate) and that it has a similar hydrophobic side chain as that for the comonomers in our case. Table 3.2 gives the pure component properties assumed for PNIPAm and the homopolymer of the hydrophobic comonomers.

The calculations of the hydrogen bonding terms in the chemical potential requires solving nine simultaneous equations represented by eq. (3.9) for three pairs of donors and acceptors, which are listed in Table 3.3. The number of donors and acceptors, and their hydrogen bonding energies, entropies and volume changes are also listed in Table 3.3. The hydrogen bonding parameters for PNIPAm-water system are the same as those reported by Lele *et al.*¹. The parameters corresponding to the hydrogen bonding between the terminal carboxyl (-COOH) group on the hydrophobic comonomer and the other donors and acceptors in the mixture are assumed to be such that the hydrogen bonds formed are slightly stronger than those for the amide groups.

Table 3.2
Molecular parameters

Component	P^* (MPa)	T^* (K)	ρ^* (kg/m ³)	MW (g/mol)
PNIPAM	503	699	1269	10,000
Homopolymers of hydrophobic monomers	431	627	1125	10,000
Water	475	578	853	18

Table 3.3
Hydrogen Bonding Parameters

H-bonding parameters	Donors → ↓ Acceptors	-NH $d_1^2 = 80$	-OH $d_2^1 = 2$	-COOH $d_3^2 = 8, 24, 40^*$
E_{ij}^0 (J/gmol)		-3.24×10^3	-16.0×10^3	-3.24×10^3
S_{ij}^0 (J/gmolK)	-C=O	-9.9	-25.8	-10.0
V_{ij}^0 (cm ³ /gmol)	$a_1^2 = 80$	-0.85	-0.85	-0.85
E_{ij}^0 (J/gmol)		-12.5×10^3	-16.595×10^3	-12.5×10^3
S_{ij}^0 (J/gmolK)	-OH	-17.8	-26.6	-17.8
V_{ij}^0 (cm ³ /gmol)	$a_2^1 = 2$	-0.85	-4.2	-0.85
E_{ij}^0 (J/gmol)		-12.5×10^3	-16.0×10^3	-12.5×10^3
S_{ij}^0 (J/gmolK)	-COOH	-7.8	-16.6	-7.8
V_{ij}^0 (cm ³ /gmol)	$a_3^2 = 8, 24, 40^*$	-0.85	-0.85	-0.85

* $a_3^2 = d_3^2 = 8$ for X3-1, X5-1 and X10-1

$a_3^2 = d_3^2 = 24$ for X5-3

$a_3^2 = d_3^2 = 40$ for X5-5

Table 3.4

Binary interaction parameters and crosslink density

Gel	Components	ζ	(v_e/v_0) (gmol/cm ³)
PNIPAM	NIPAm	1.5-1.56x10 ⁻³ T	90
X3-1	NIPAm	1.5-1.56x10 ⁻³ T	65
	X3	1.5-1.78x10 ⁻³ T	
X5-1	NIPAm	1.5-1.56x10 ⁻³ T	20
	X5	1.5-1.82x10 ⁻³ T	
X10-1	NIPAm	1.5-1.56x10 ⁻³ T	250
	X10	1.5-2.1x10 ⁻³ T	
X5-3	NIPAm	1.5-1.56x10 ⁻³ T	55
	X5	1.5-1.82x10 ⁻³ T	
X5-5	NIPAm	1.5-1.56x10 ⁻³ T	135
	X5	1.5-1.82x10 ⁻³ T	

The effective hydrophobicity of the copolymer gel is represented by the binary interaction parameter ζ_{12} given by eq. (3.5) and (3.6). The binary interaction parameters for homopolymer, PNIPAm (ζ_{1A}) and homopolymer of the comonomer (ζ_{1B}) which are required for fitting the experimental swelling data are listed in Table 3.4. A lower value of ζ indicates greater hydrophobicity. It is seen from the values of ζ that the effective hydrophobicity of all gels is temperature-dependent and that the value of ζ at any temperature decreases for increasing chain length of the hydrophobic group. Figure 3.7 shows a correlation between the experimental LCST, ζ and X for the copolymer gels. The almost linear correlation between the LCST and X suggests that the LCST is reduced by about 2°C for every additional $-\text{CH}_2$ group on the terminal side chain of the hydrophobe. The correlation between X and ζ at any given temperature is also almost linear. These correlations can be useful not only in quick “designing/tailoring” of gels, but could also provide insights into the mechanism of volume transition of gels. It is also important to note that in fitting the swelling behavior of X5-1, X5-3 and X5-5 gels, we have not changed the interaction parameter ζ_{1B} of the hydrophobic homopolymer. Since the value of ζ determines the transition temperature of the gels, the predicted lowering of the LCSTs with increasing composition of X5 validates our assumption of a “random” copolymer in the model and proves the strength of the model.

The values of crosslink density of the gels required for quantitatively fitting the experimental swelling data are reported in Table 3.4. It is seen that X3-1 and X5-1 required a lower value of crosslink density than PNIPAm gel, however, the X10-1 gel required a very high value of crosslink density. Similarly, the X5-3 and X5-5 gels, which contain increasing concentrations of X5 comonomer, required increasing values of the crosslink densities. Our synthesis procedure for copolymer gels does not provide any control over the crosslink density, hence it is possible that the copolymer gels X3-1 and X5-1 have lower crosslink densities than the PNIPAm gel. However, it is also possible that the effective crosslink density of the copolymer gels could increase as a result of additional ‘physical’ crosslinks such as hydrophobic interactions or chain entanglements of the long hydrophobic side groups of the comonomers. This effect will increase with an increase in the chain length of the side group and with increasing contents of the hydrophobe in the copolymer gels. This could be the reason for the higher crosslink density values for the X10-1, X5-3 and X5-5 gels.

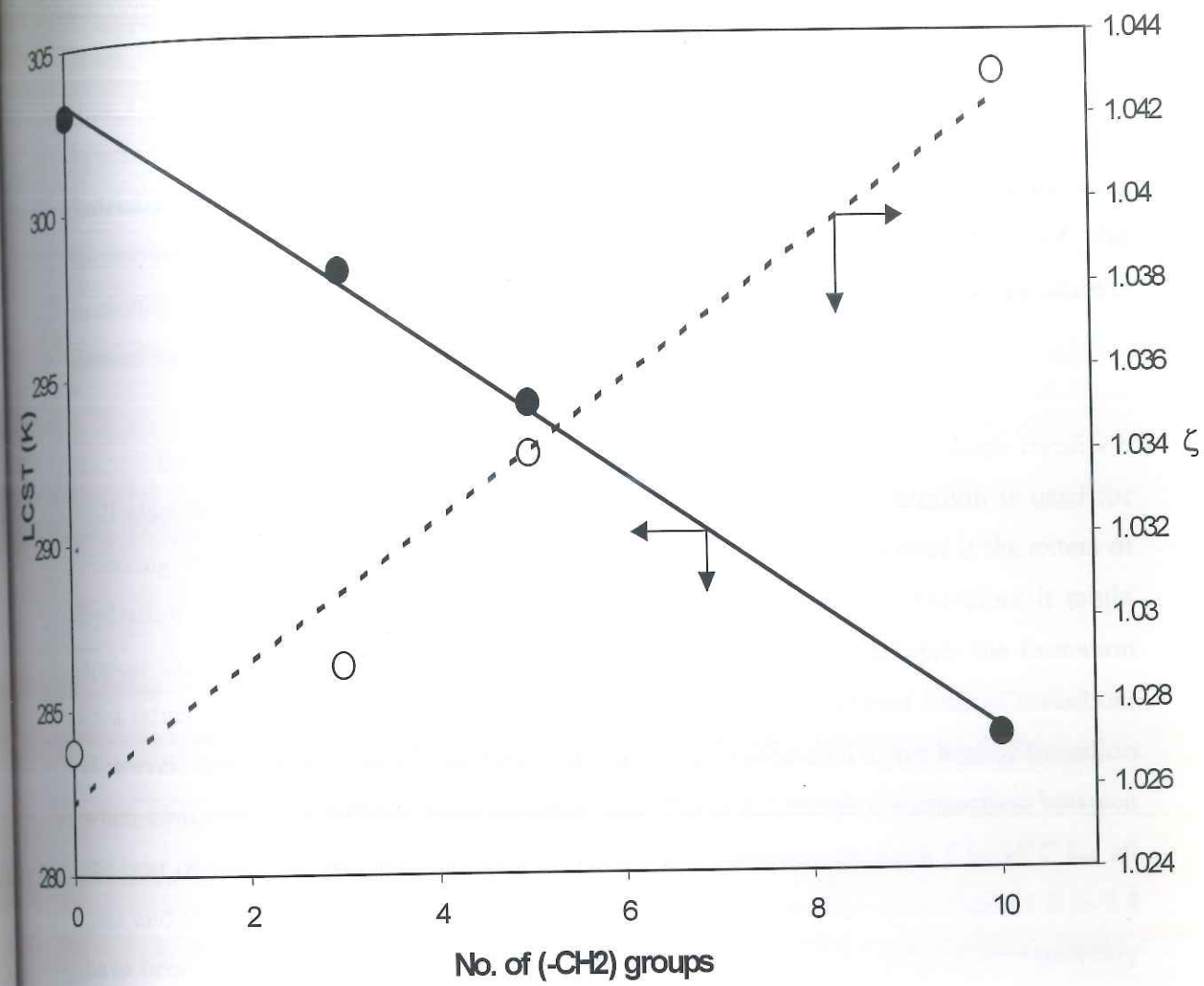


Figure 3.7: Correlation between LCSTs, ζ and length of alkyl group (X) of the comonomer.

The DSC heating scans in Figure 3.5 show the endothermic heat associated with the volume transitions of the gel. It is believed that this externally supplied heat is used to break the hydration layers around the hydrophobic groups. The exposed hydrophobes then associate causing the gel to collapse. The temperature at which the hydrophobic hydration breaks down would decrease with an increase in the hydrophobicity of the gel. Indeed in our copolymer gels, we find a decrease in the transition temperature with increasing hydrophobic nature (increasing X) and content (composition of the comonomer). The LFHB model also shows that a decrease in the transition temperature is caused by an increase in hydrophobicity (lower ζ) of the gel.

Besides the transition temperature, the heat associated with the volume transition will also depend on the hydrophobicity of the gel. If the heat of transition is used for breaking the hydration layers around the hydrophobic groups, then greater is the extent of hydration, the larger will be the heat associated with the transition. Therefore it might appear that increasing the hydrophobic alkyl chain length would facilitate the formation of a larger hydration layer and therefore would result in an increased heat of transition. However, our hydrophobically modified copolymer gels showed a lower heat of transition when compared to PNIPAm homopolymer gels. Table 3.5 shows a comparison between the heat of mixing calculated from eq. (3.12) for the transitions between 5 to 40°C for all gels and the endotherms of the DSC. All the model parameters given in Table 3.2 to 3.4 have been used for calculating the heat of mixing. The calculations thus become probably because of errors in the baseline fitting of heating scans and perhaps also because of the transient nature of the DSC experiment. However, it is important to note that the trends are in agreement, namely, the heat of demixing decreases with an increase in the hydrophobicity of the copolymer gels.

Table 3.5
Comparison between experimentally measured heat of demixing (DSC) and theoretical predictions from equation (3.12)

Length of hydrophobe (No. of -CH₂ groups, X)	Experimental (J/g dry polymer) (area under DSC endotherm)	Theoretical (J/g dry polymer) (equation 3.12)
0	59.2	53.90
3	33.3	50.04
5	30.7	48.30
10	-	29.94

Table 3.5
Comparison between experimentally measured heat of demixing (DSC) and theoretical predictions from equation (3.12)

Length of hydrophobe (No. of -CH₂ groups, X)	Experimental (J/g dry polymer) (area under DSC endotherm)	Theoretical (J/g dry polymer) (equation 3.12)
0	59.2	53.90
3	33.3	50.04
5	30.7	48.30
10	-	29.94

The above observations suggest that the water molecules are unable to structure around the hydrophobic groups in our copolymer gels. This can be probably attributed to the presence of the terminal hydrophilic carboxyl group, which hinders the formation of hydrophobic hydration around the $-CH_2$ groups of the alkyl chain. Thus, our comonomers increase the overall hydrophobicity of the copolymer gels compared to PNIPAm gel and thereby reduce the LCSTs. However, the comonomers do not allow structuring of water molecules around them and therefore do not increase the heat of demixing. The LFHB model also supports this rationale. Being an essentially mean-field theory, the model does not account specifically for structuring of water molecules around hydrophobic groups. Therefore it can not predict an increase in the heat of demixing caused by breaking down of hydration layers around the hydrophobes. On the contrary it predicts a decrease in the ΔH due to decreased polymer-water interactions caused by the increased hydrophobicity of the copolymer (as indicated by reduced ζ). The experimental results match with the predictions, thus indicating that water does not hydrate the hydrophobic groups in our copolymers.

This shows that the subtleties of chemical structure of hydrophobes play an important role in determining the extent of hydration.

3.1.8 Conclusions

We have synthesized hydrophobic vinyl monomers containing varying lengths of alkyl groups, X and copolymerized these monomers with N-isopropyl acrylamide monomer to give hydrophobically modified copolymer gels. These gels show lower volume phase transition temperatures than that of pure PNIPAm gel. The reduction in the transition temperature was found to increase with the length of the alkyl group in the hydrophobic comonomers and also with an increase in the content of the comonomers. A linear correlation between the transition temperature and the number of alkyl groups was found to exist in these gels. Such a correlation could be a useful in designing gels having a specific transition temperature.

We have also shown that the extended LFHB theory can quantitatively fit the swelling data of the copolymer gels. The temperature dependent binary interaction

parameter ζ , which simulates the effective hydrophobicity of the gels, was found to decrease with an increase in the alkyl chain length. The predictions of the transition temperatures of NIPAm-X5 gels containing increasing concentrations of the comonomer validates the assumption of a "random" copolymer in our model.

In apparent contradiction to previous work,^{5,6} our copolymer gels show that the heat associated with the volume transition decreases with an increase in the hydrophobic alkyl chain length. Our theoretical predictions of the heat of demixing are also in qualitative agreement with experimental observations. These results suggest that the hydrophobic groups used in our copolymer gels do not allow structuring of water around them, which is probably due to the presence of the strongly hydrophilic carboxyl terminal group. The lack of structured water reduces the heat of demixing, however, the increase in the overall hydrophobicity of the comonomer causes a reduction in LCSTs.

3.1.9 References

1. A. K. Lele, M. V. Badiger, M. M. Hirve, R. A. Mashelkar. *Chem. Eng. Sci.* **50**, 3535 (1995).
2. A. K. Lele, I. Devotta, R. A. Mashelkar, *J. Chem. Phys.* **106**, 4768 (1997).
3. P. S. Mumick, C. L. McCormick, *Polym. Eng. Sci.* **34**, 1419 (1994)
4. M. Shibayama, S. Mizutani, S. Nomura, *Macromolecules* **29**, 2019 (1996).
5. H. Feil, Y. H. Bae, J. Feijen, S. Wan Kim, *Macromolecules* **26**, 2496 (1993).
6. H. Inomata, S. Goto, S. Saito, *Macromolecules* **23**, 4887 (1990).
7. M.V.Badiger, A.K.Lele, V.S.Bhalerao, S.Varghese, R.A.Mashelkar *J. Chem. Phys.*, **109**, 1175 (1998).
8. I. C. Sanchez, R. H. Lacombe, *J. Phys. Chem.* **80**, 2352 (1976)
9. I. C. Sanchez, R. H. Lacombe, *Macromolecules* **11**, 1145 (1978).
10. I. C. Sanchez, R. H. Lacombe, *J. Polym. Sci. Polym. Lett. Ed.* **15**, 71 (1977)

Part B

Synthesis of thermosensitive gels by γ -radiation technique

3.2 Introduction

There is a renewed interest in the radiation induced polymerization and cross-linking in polymeric hydrogels. The advantages of radiation methods are that they are relatively simple and do not require addition of any extra materials for polymerization and cross-linking. Moreover, the degree of cross-linking, which strongly determines the extent of swelling in hydrogels can be controlled easily by varying the dose rates. Therefore, these methods are found to be very useful in preparing hydrogels for medical applications where, even a small contamination is undesirable. For example, fast responding thermosensitive gels based on poly(vinyl methyl ether) [PVME] have been prepared by γ -radiation and are used in controlled release applications.¹ Uenoyama and Hoffman² have grafted poly(*N*-isopropylacrylamide) [PNIPAm] onto silicone rubber substrate for model implants. Recently, Nagaoka *et al.*³ have reported for the first time the synthesis of PNIPAm hydrogel by γ -radiation technique. Radiation cross-linked poly(ethylene oxide) [PEO] gels have also been used as highly active phase transfer catalysts in alkylation reactions.⁴ Non-ionic flocculants, specifically for the applications in pulp manufacturing have been synthesized by γ -radiation of mixtures of poly(acrylamide) and poly(ethylene oxide).⁵

We report here on the synthesis of thermosensitive hydrogel based on the radiation induced copolymerisation of poly(*N*-isopropylacrylamide) and poly(ethylene oxide). Recently, Yoshioka *et al.*⁶ have reported on the synthesis of block-copolymers of PNIPAm-*co*-(*n*-butyl methacrylate) [BMA] and poly(ethylene glycols). However, these copolymers were prepared by the reaction between diamino-PEG and activated copolymer [PNIPAm-*co*-*N*-aryloxysuccinimide (NASI)-*co*-BMA] and not by using the γ -radiation technique. Moreover, these polymers were not truly covalently cross-linked gels but exhibited reversible cross-linking during sol-gel transition as a result of cooling and heating cycles. Gelation was believed to occur mainly due to the formation of thermosensitive cross-linkages between intermolecular poly(NIPAm-*co*-*n*-butyl methacrylate) blocks by hydrophobic interactions. Interestingly, the same authors also

showed the effect of sequence length of PNIPAm on the LCST of the block copolymer. For example, in their DSC study⁷ the block copolymer, PNIPAm-co-PEG showed an endothermic peak at 38 °C whereas, the random copolymer based on PNIPAm-co-PAM showed no endothermic peak.

Although, PNIPAm LCST hydrogels have been extensively studied and demonstrated to be the promising materials, their commercial exploitation has been limited due to the extremely high cost of NIPAm monomer. Therefore, combination of NIPAm monomer with other cheaper materials (such as PEO) while retaining the crucial properties of products such as thermoreversibility is a challenging task. Besides its cost, we have chosen poly(ethylene oxide) mainly due to its excellent biocompatibility and good aqueous swelling characteristics. Moreover, poly(ethylene oxide) gel although, falls under the class of thermosensitive hydrogels, it does not exhibit a well defined first order volume phase transition as a function of temperature. In this work, we have synthesized copolymers based on poly(ethylene oxide) and poly(N-isopropylacrylamide) by γ -radiation technique. These gels are easy to synthesize in any shape and size and are found to be having good mechanical strength even in the fully swollen state. We believe that our synthesis results in grafting of PNIPAm onto PEO chains. The structure and copolymer compositions have been quantitatively determined by ¹³C NMR spectroscopy. We show that the copolymers exhibit a discontinuous thermosensitive volume transition as studied by swelling ratio measurements.

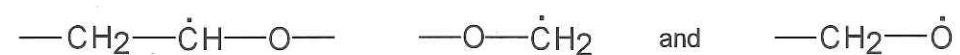
3.2.1 Mechanism of Radiation Polymerization and Cross-linking

Mechanism of radiation cross-linking in PEO and PNIPAm has been independently investigated by many research groups. When aqueous solutions of PEO are subjected to γ -ray irradiation, they yield cross-linked gels. This is possible however, only when certain minimum concentration and molecular weight of PEO is used for the γ -ray irradiation. The mechanism involves the radical formation on the polymer chain either by a direct action of the high-energy radiation on the polymer chain, or by indirect attack on the polymer chain by solvent derived radicals. Earlier, Charlesby and Kopp⁸ reported that, the cross-linking and subsequent gelation in PEO solutions due to γ -radiation arises mainly from the direct effect *i.e.* the energy absorbed directly by the polymer molecule is

solely responsible for the radical formation and cross-linking. Based on their ESR study, Ferloni *et al.*⁹ have indicated that, γ -ray radiation on the PEO chains leads to the localization of positive charges on the PEO oxygen atoms as shown below,



The positive polymer radicals then undergo α and β scissions resulting in three types of radicals

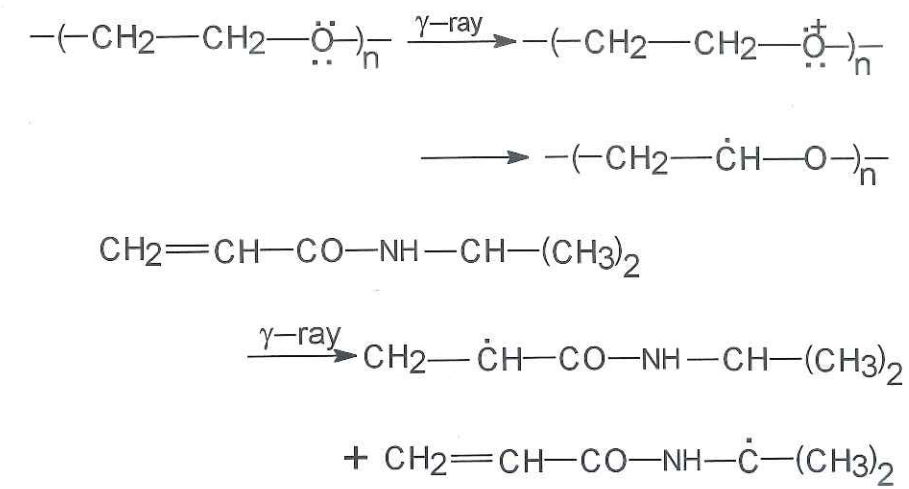


Finally, the combination of these radicals can lead to cross-linking in PEO structure. However, later reports indicated that the indirect effect definitely plays a dominant role in generating free radical and subsequent reaction.

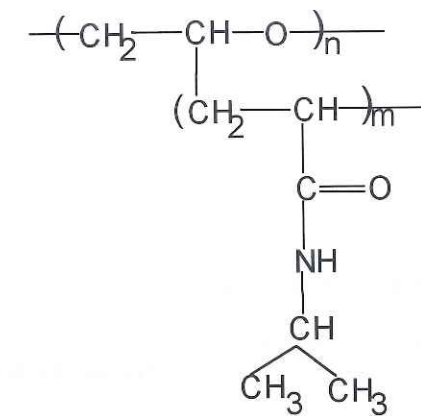
In the case of indirect effect, radiolysis of water can lead to H and OH radicals as intermediates, which can react with polymer to give polyradicals. Two such polyradicals combine together resulting in covalent bond formation leading to cross-linking. The fact that radiolysis of water indeed contributes significantly for generating polyradicals and which eventually gives cross-linked gels was further supported by other workers^{10,11}.

In a separate study, Nagaoka *et al.*³ have reported the radiation polymerization and cross-linking of *N*-isopropylacrylamide monomer. The formation of the monomer radical was reported via both the direct effect of radiation and also indirect effect based on the reaction of products of water radiolysis with the monomer. They have reported the formation of radical on the isopropyl group of the monomer along with the formation of carboxyl alkyl radical. However, the radical on the isopropyl group being more stable than the other is unlikely to take part in the polymerization and cross-linking reaction. Therefore, considering all the above discussions the possible mechanism of copolymerisation of NIPAm onto PEO can be proposed as follows,

(a) Formation of radicals on both PEO and NIPAm by direct and indirect effect as follows,



(b) The combination of above radicals gives rise to cross-linked copolymers of PEO and PNIPAm with the following structure,



3.2.2 Experimental Section

3.2.3 Materials

PEO (MW-6000 and 100,000) polymers and NIPAm monomer were obtained from Polysciences, Inc. USA and used as such. The purities of these materials have been checked by m.p. and ^1H NMR spectroscopy. Distilled ethanol and deionized water have been used for all the experiments.

3.2.4 Synthesis of PEO-co-PNIPAm gels

Aqueous solutions of PEO (1.5 wt%) were prepared in distilled water by gentle stirring of PEO powder and water. The dissolution took 10-15 hrs. to get homogeneous solutions. The concentration of NIPAm monomer was varied accordingly (Table 3.6) and dissolved in the PEO solution. The solutions were degassed by bubbling nitrogen gas continuously for 15 minutes. The solutions were sealed in glass tubes and samples were exposed to γ -radiation from a ^{60}Co source at a dose rate of 0.361 Mrad/hr at room temperature for 15 hrs. After the irradiation, the resulting gels were taken out and washed several times with distilled water and ethanol. The washed gels were dried in vacuum oven at 40-45 °C till the constant weight was obtained

Table 3.6: Feed compositions for the preparation of hydrogels

Samples	PEO (g)	NIPAm (g)	Water (g)
VE	0.6	-	40.0
VA-1	0.6	0.2	40.0
VA-2	0.6	0.4	40.0
VA-3	0.6	0.8	40.0
VA-4	0.6	1.0	40.0

3.2.5 Swelling Ratio Measurements

The dried cylindrical gels (with known weight) were placed in pure water taken in glass tube with standard joints. The tubes were kept at different temperatures in a temperature-controlled oven (with an accuracy of ± 0.2 °C) and samples were allowed to equilibrate for 4-5 days. Cryostat bath was used for the low temperature swelling measurements. After attaining equilibrium, the swollen gels were taken out and weighed accurately to the fourth decimal point. The swelling ratios were expressed as the ratio of swollen weight to the dry weight (W_s / W_d) of gel samples.

3.2.6 ^{13}C NMR Measurements

All the ^{13}C spectra were obtained on a Bruker MSL-300 FT-NMR spectrometer operating at 75.47 MHz for carbon using a conventional high-resolution 10mm probe. Dry samples were swollen in $\text{H}_2\text{O}/\text{D}_2\text{O}$ (90/10 vol%) mixture in 10 mm NMR tube till equilibration. The samples were directly taken for ^{13}C NMR measurements at room temperature (26 °C). The quantitative ^{13}C spectra were obtained using inverse gated decoupling mode with 36° flip angle and 2 sec. recycle delay. Ideally, determination of quantitative relative intensities requires obtaining nuclear Overhauser enhancement (nOe) suppressed spectra with a recycle time in excess of five times the relaxation time. Freeman *et al.*¹² reported a gated decoupling technique in which the nOe's were eliminated by cycling the decoupler on only during signal acquisition. This results in completely decoupled spectra without nOe. In our case, we have used only 36° flip angle and hence do not require the recycle delay of $5T_1$. Moreover, we have roughly estimated the T_1 's of the order of 300-400 milliseconds. Typically 15,000 accumulations were made to get highly resolved spectra for all the samples. Chemical shift positions were referred with respect to an external sample of dioxane in D_2O taken at 67.8ppm. Integrated areas were used for the estimation of copolymer composition.

3.2.7 Results and Discussion

3.2.7.1 Structure and Composition of Copolymers

We show in Figure 3.8, the completely decoupled ^{13}C a NMR spectrum of PEO and PNIPAm-co-PEO samples swollen in $\text{H}_2\text{O}/\text{D}_2\text{O}$ mixture at room temperature. The spectra were obtained using high resolution probe. It may be noted at this point that, the hydration levels achieved at the equilibrium swelling of the samples was sufficient to average the C-H dipolar interactions to a greater extent. Hence, a reasonably well resolved ^{13}C spectra could be obtained in the conventional high resolution mode with Broad-Band (BB) decoupling. More narrowing of ^{13}C peaks is certainly achievable by Magic Angle Sample Spinning (MASS) with dipolar decoupling. However, we find that the spectra obtained in the high resolution mode is good enough for the quantitative estimation of the copolymer composition.

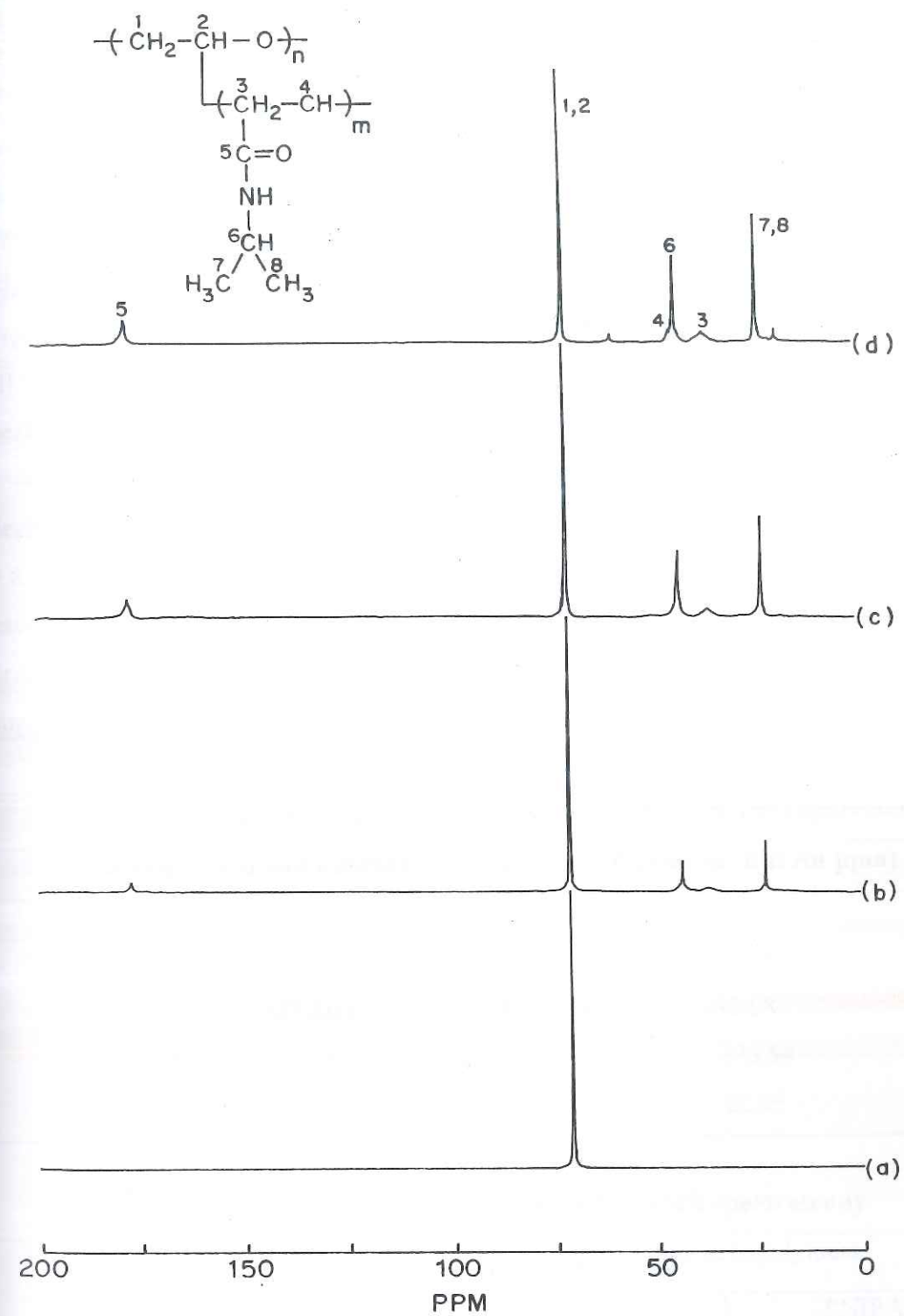


Figure 3.8: ^{13}C NMR spectra of PEO homopolymer gel VE (a) and copolymer gels VA-2 (b); VA-3 (c); VA-4 (d)

It can be seen from Figure 3.8(a) that, pure PEO sample shows single ^{13}C peak at 70.8ppm, which is the backbone $-\text{CH}_2$ carbon. However, upon copolymerization with PNIPAm, all the ^{13}C peaks of PNIPAm also appear in the spectra. The chemical shift assignments for all the carbons is made and summarized in Table 3.7. The possible structure of the copolymer along with carbon numbers is given in the inset of Figure 3.8. We have prepared PEO-*co*-PNIPAm copolymers with increasing amounts of PNIPAm. The feed composition of the monomers is given in Table 3.6. It can be readily seen from Figure 3.8 that, with increasing PNIPAm content in the copolymer gel, the intensities of all the ^{13}C peaks of PNIPAm progressively increase with respect to the intensity of PEO peak at 70.8 ppm. Significant improvement in the resolution was also observed. The copolymer compositions were determined by measuring the integral areas of all the peaks. The experimental copolymer composition obtained by ^{13}C NMR is given in Table 3.8. These values were compared with the feed composition. It can be seen that there is an excellent agreement with the values of the feed composition indicating that the reaction proceeds to completion. Moreover the yields of all the reaction products were quantitative suggesting the completion of the reaction.

Table 3.7: Chemical shift assignments for ^{13}C peaks in the copolymer

Type of Carbon and number	Chemical shift (in ppm)
1, 2 $-\text{CH}_2$ (PEO)	70.8
3, $-\text{CH}_2$ (PNIPAm)	36.08
4, 6 $-\text{CH}$ (PNIPAm)	43.08
5, $-\text{C}=\text{O}$ (PNIPAm)	176.54
7, 8 $-\text{CH}_3$ (PNIPAm)	22.85

Table 3.8: Copolymer composition by ^{13}C NMR spectroscopy

Sample	Mole ratios in copolymers	
	PEO	PNIPAm
VA-2	1.0 (1.0)	0.27 (0.26)
VA-3	1.0 (1.0)	0.54 (0.52)
VA-4	1.0 (1.0)	0.69 (0.65)

♦ molar feed ratios are given in the parenthesis

3.2.7.2 Swelling ratios of copolymer gels

We show in Figure 3.9, the temperature dependent swelling ratios of PEO homopolymer gel (VE) and compare them with the swelling ratios of PEO-co-PNIPAm copolymer gels (VA-2 and VA-4). The PEO gel shows a continuous decrease in swelling ratio as a function of increasing temperature with no sharp volume transition. There are no reports as yet on the well-defined LCST of PEO hydrogels. However, upon copolymerisation of PNIPAm and PEO, the resultant gels showed a discontinuous volume transition between 35 and 42 °C, releasing almost 70-80% of the absorbed water above the transition temperature. The transition temperatures of the copolymer gels were found to be changing with the composition of the gel. Figure 3.9 shows that the transition temperature is a non-monotonic function of the composition of the copolymer gel. It is also interesting to note that, the equilibrium swelling ratios of PEO-co-PNIPAm copolymer gels at any temperature are found to be lower than the swelling ratios of PEO gel. This could be due to the fact that, copolymerisation of PNIPAm with PEO increases the hydrophobic content of the polymer resulting in the lower swelling ratios of copolymer gels. While the hydrophobicity of the copolymer comes from the pendent isopropyl groups of the PNIPAm, the PEO chains in the structure mainly contribute the hydrophilicity. It is also expected that, copolymerisation of NIPAm monomer with PEO undergoes randomly and can lead to an additional inter, intra-molecular cross-linking in the copolymer structure. This additional cross-linking can also decrease swelling capacity of gels significantly.

3.2.7.3 Effect of Molecular Weight of PEO on the swelling ratios of copolymer gels

We have copolymerized NIPAm with PEO of molecular weights of 6000 and 100,000. Figure 3.10 show the swelling of these gels as a function of temperature. The gel prepared from 6000 molecular weight PEO shows a discontinuous volume transition and a higher swelling capacity at temperature below the transition temperature. On the contrary, the gel prepared from 100,000 molecular weight PEO exhibit rather a continuous decrease in swelling capacity as a function of temperature and also show a lower swelling capacity at temperatures below the transition point.

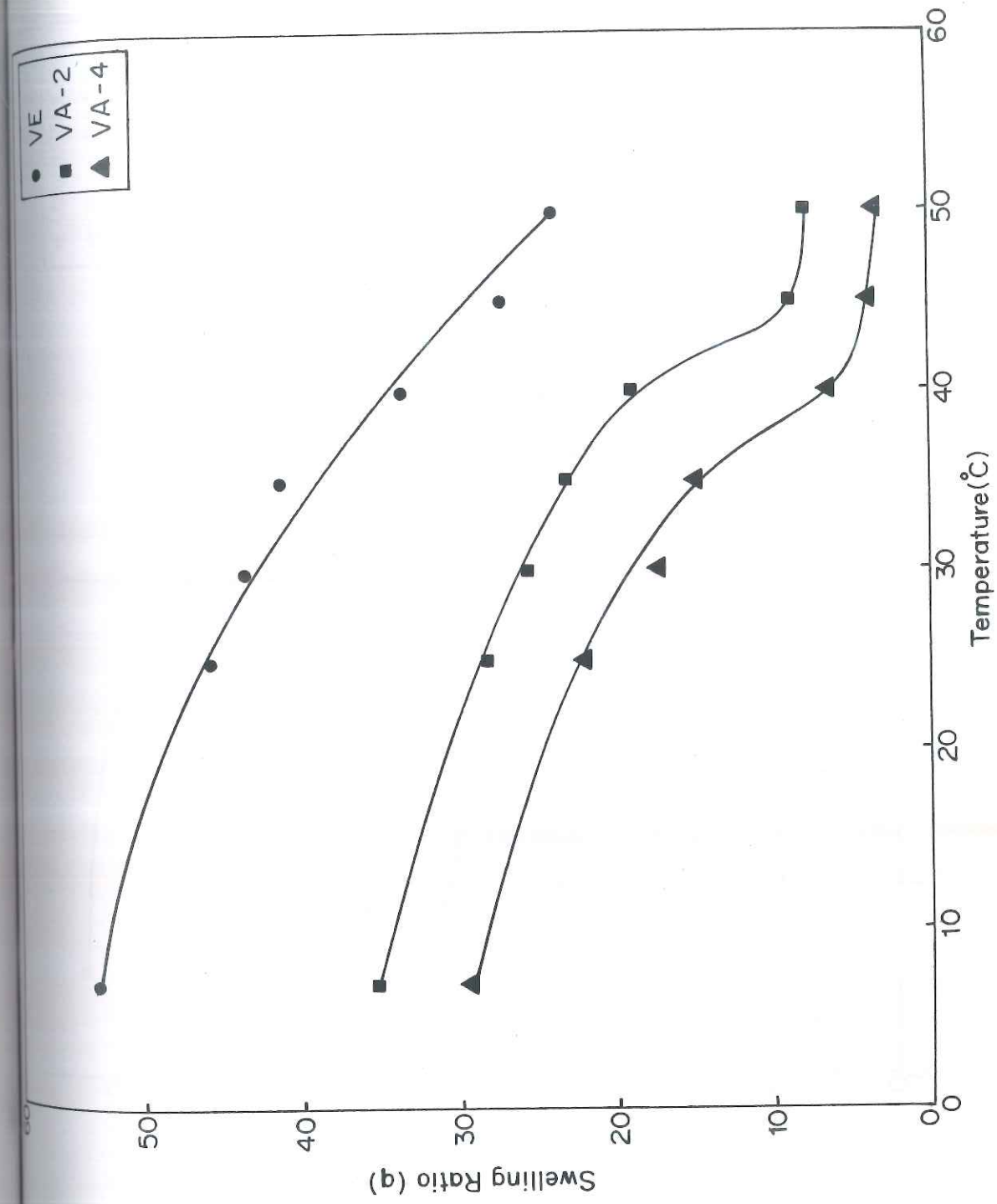


Figure 3.9: Swelling ratios as a function of temperature

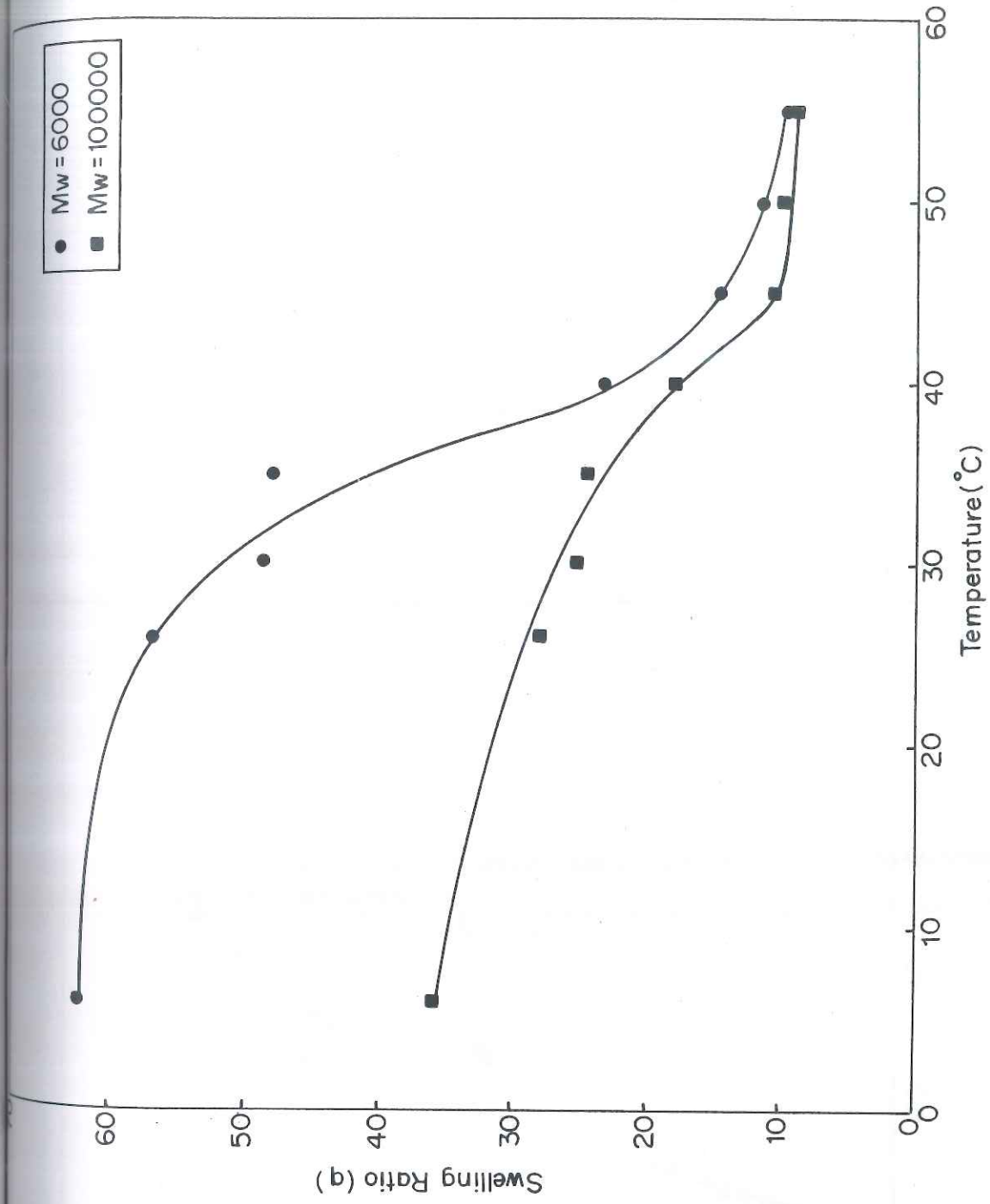


Figure 3.10: Temperature dependent swelling ratios of copolymer gels prepared from PEO of different molecular weights

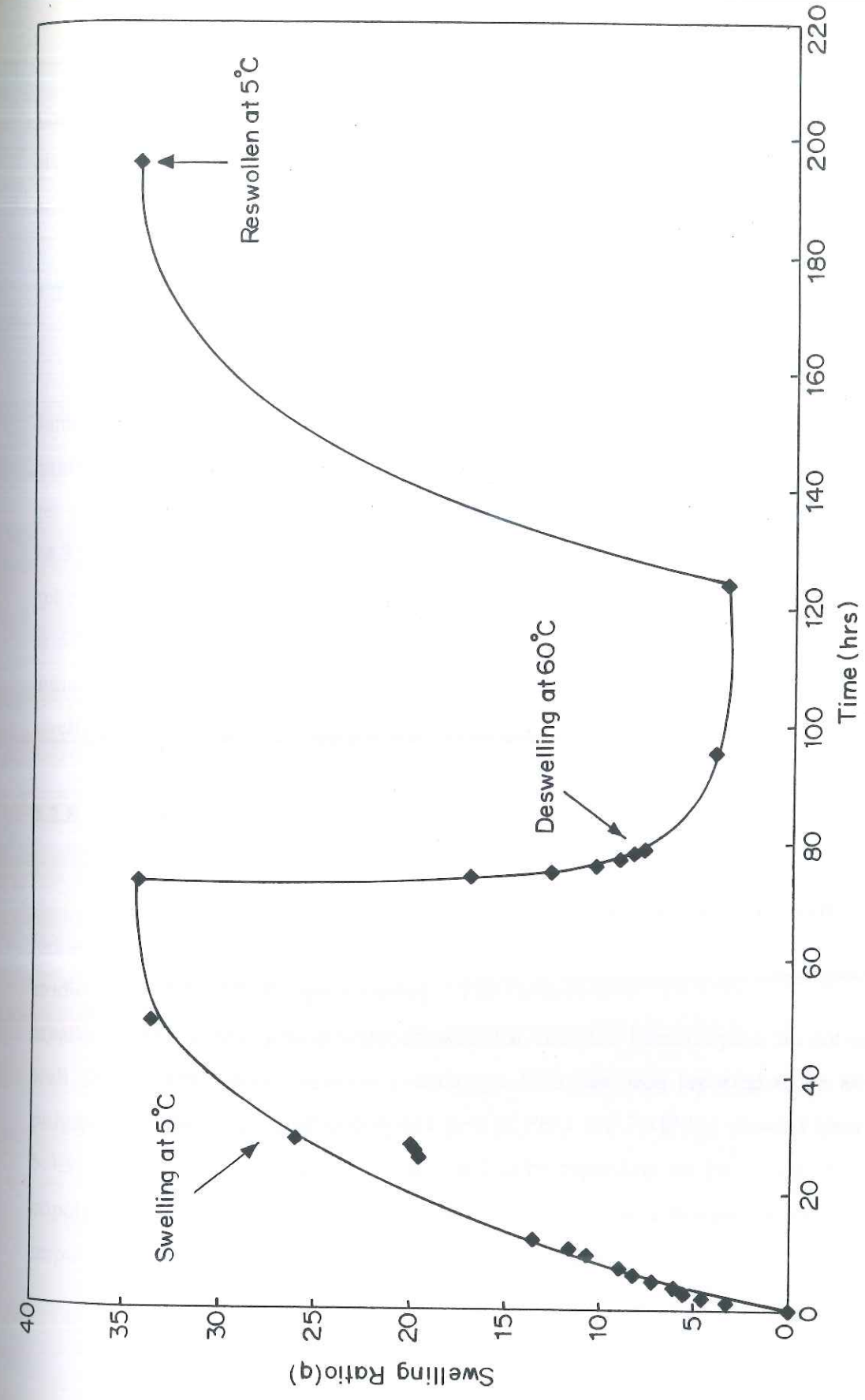


Figure 3.11: Kinetics of swelling-deswelling of PEO-PNIPAm copolymer gel

This behavior could be attributed to the fact that higher molecular weight PEO indeed gives a high degree of cross-linking during γ -radiation resulting in lower swelling ratios of the copolymer gels. This is in agreement with the earlier report by Deng *et al.*⁵.

3.2.7.1 Thermoreversibility of copolymer gel

We have also studied the thermoreversibility of the copolymer gel, which is demonstrated in Figure 3.11. A disk-shaped gel of 0.7cm diameter in dry state was immersed in water at 5 °C until equilibrium swelling was attained. The diameter of the gel was increased to 2.5cms in 75hrs. indicating the equilibrium swelling ratio (q) of 34.3. The gel was then transferred to a water bath maintained at 60°C for deswelling. The gel collapsed in 6hrs. showing the swelling ratio of 6.2. However, upon reswelling the gel at 5 °C the equilibrium swelling was reached to an earlier value of 34.4. This clearly indicates the thermoreversible nature of the gel. Figure 3.11 shows the reversible swelling-deswelling kinetics of the copolymer gel.

3.2.8 Conclusions

We have synthesized thermosensitive PEO-PNIPAm copolymer gels using γ -radiation technique. The structure and composition of the copolymer gels have been studied by ¹³C NMR spectroscopy. The temperature dependent swelling ratio measurements of these gels in water showed that, the PEO homopolymer do not exhibit a well defined first order transition eventhough PEO has been reported to be an LCST polymer. On the other hand copolymer gels of PEO and PNIPAm showed clear LCST behavior. The LCSTs of the gels were found to be dependent on the composition of the copolymers. Since these gels are synthesized by γ -radiation technique they are free from impurities and can have potential biomedical applications.

3.2.9 References

1. X. Huang, H. Unno, T. Akehata, O. Hirasa, *J. Chem. Eng. Japan*, **20**, 123 (1987).
2. S. Uenoyama, A. S. Hoffman, *Radiat. Phys. Chem.*, **32**, 665 (1988).
3. N. Nagaoka, A. Safranj, M. Yoshida, H. Omichi, H. Kubota, R. Katakai, *Macromolecules*, **26**, 7386 (1993).
4. T. Tsanov, R. Stamenova, C. Tsevtanov, *Polym. J.*, **25**, 853 (1993).
5. Y. Deng, R. Pelton, H. Xiao, A. Hamielec, *J. Appl. Polym. Sci.*, **54**, 805 (1994).
6. H. Yoshioka, M. Mikami, Y. Mori, *J. Macrom. Sci-Pure. Appl. Chem.*, **A31(1)**, 113 (1994).
7. H. Yoshioka, M. Mikami, Y. Mori, *J. Macrom. Sci-Pure. Appl. Chem.*, **A31(1)**, 109 (1994).
8. A. Charlesby, P. M. Kopp, *Proc. Roy. Soc(London), Ser A.*, **291**, 129 (1966).
9. P. Ferloni, A. Magistris, G. Chiodelli, A. Faucitano, A. Buttafava, *Radiat. Phys. Chem.*, **37(4)**, 613 (1991).
10. P. A. King, J. A. Ward, *J. Polym. Sci.*, **A(1)**, **8**, 253 (1970).
11. L. Mikova, R. Stamenova, C. Tsvetanov, V. Nedkov, *J. Polym. Sci. B, Polym. Phys.*, **27**, 621 (1989).
12. R. Freeman, H. D. W. Hill, R. Kaptein, *J. Magn. Reson.*, **7**, 327 (1972).

Chapter 4
*Effect of surfactants on the phase
transition of poly(acryloyl aminoacids)
based thermosensitive hydrogels*

4.1 Introduction

Aspects of interaction of non-ionic, water soluble polymers with surfactant, a subject of considerable theoretical and practical interest has been reviewed by Goddard.¹ Addition of surfactants to polymers forms complex structures, which influences the phenomena of conformation transition,² phase separation,³ volume phase transition⁴ and rheological behavior.^{5,6} Extensive studies have been done on the effect of various surfactant systems on the transition phenomena of a thermosensitive polymer, poly(N-isopropylacrylamide).⁷ This polymer is used as a model system for understanding the folding and unfolding of biopolymers, which is otherwise difficult to study in real systems due to the complexity of biological macromolecules.

In such thermosensitive polymers, it is known that the binding of surfactant molecules to the polymer causes an elevation of LCST as a result of the electrostatic repulsion between the charges of polymer bound micelles, which prevents the polymer chain collapse and aggregation.⁸ Although, there are large number of reports on PNIPAm gel-surfactant systems, the exact mechanism of surfactant binding to PNIPAm gel is still unclear. The concentration at which such a surfactant binding takes place has been referred to as the Critical Aggregation Concentration (CAC). The CAC of sodium dodecyl sulfate (SDS) in PNIPAm solution was determined to be 0.79mM by Schild and Tirrell using the fluorescence probe method.³ However, the same may not be true for the PNIPAm gel system since the mechanism of surfactant binding to PNIPAm gel is still unclear. As the surfactant concentration increases, all the possible sites within the gel network, to which the surfactants may bind, are occupied, thereby giving rise to a saturation value for LCST. Large number of experimental techniques has been employed to study the interaction between surfactants and polymers. In most cases, the binding of surfactants to polymer was found to start at a concentration of surfactant less than the Critical Micellar Concentration (CMC) of surfactant.

The interaction between a surfactant and a polymer will depend strongly on the structural parameters, such as the charge on the surfactant and the length of its tail. Schild and Tirrell³ have reported that surfactants with small chain lengths in sodium alkyl sulfate (number of -CH₂ groups in the alkyl chain, $n < 4$) depresses the LCST and surfactants with intermediate chain lengths ($n = 5-10$) also depresses the LCST at low surfactant

concentrations but cause an increase in LCST at concentrations above the CAC. On the contrary, the surfactant, sodium dodecyl sulfate, SDS with $n = 12$, elevates LCST even at low concentrations of SDS and forms aggregates in PNIPAm solutions at a concentration that is ten folds lower than the CMC of SDS.

In this chapter, we report on the synthesis of homopolymer and copolymer gels of poly(N-isopropyl acrylamide) and poly(acryloyl aminoacids).⁹ The characterization of these new copolymer gels was made by swelling ratio measurements and NMR spectroscopy. A major thrust was on the study of interaction of anionic surfactant namely, SDS with these copolymer gels. While we were studying the swelling behavior of these copolymer gels in SDS solutions, we observed some hitherto unreported core-shell morphology in the swollen gels along with two discontinuous volume transitions. Such morphologies have a potential application in drug delivery systems. We provide a mechanistic interpretation of these new observations on the basis of electrostatic charge repulsion and restricted diffusion of surfactant into the gel.

4.2 Experimental Section

4.3 Materials

Acrylic acid, N-isopropylacrylamide (NIPAm) and ethylene glycol dimethacrylate (EGDMA) were obtained from Aldrich Chemicals and used without further purification. AR-grade 1,4-dioxane, thionyl chloride, L-phenylalanine were procured from S. D. Finechem Ltd. Thionyl chloride was purified by distillation. Sodium dodecyl sulfate (SDS) was provided by Sisco Research Laboratories and was recrystallized from a methanol solution. The initiator azobisisobutyronitrile (AIBN) was purchased from SAS Chemicals and was purified by recrystallisation in ethanol.

4.4 Synthesis of Monomers

4.4.1 Acryloyl chloride

The exact procedure and characterization was described in chapter 3 (3.1.4.1).

4.4.2 *N-Acryloyl-L-phenylalanine [APA]*

The hydrophobic comonomer was synthesized by the reaction between acryloyl chloride and L-phenylalanine. To a well-stirred aqueous solution (100 ml) containing L-phenylalanine (16.52 g, 0.1 mol) and sodium hydroxide (6 g, 0.15 mol), an acryloyl chloride (10.08 ml, 0.1 mol) with dichloromethane (10 ml) was added dropwise over a period of 1 hr. at 5-7 °C in ice-water mixture. During the addition of reagents, the pH was maintained between 7.5-7.8. The reaction mixture was further stirred for a period of 1 hr while increasing the temperature to room temperature. Then it was acidified to pH 5-5.2 with concentrated hydrochloric acid and extracted with ethyl acetate, dried over anhydrous sodium sulfate and concentrated on rotavapor. On cooling the concentrate, a solid monomer was precipitated out. It was further purified by redissolving in ethyl acetate and precipitating in petroleum ether to obtain 15.35 g (Yield 70 %) of *N*-acryloyl-L-Phenylalanine (APA), mp 120-121 °C.

IR (KBr),

3340 cm^{-1} (N—H), 2940 cm^{-1} and 2845 cm^{-1} (C—H), 1710 cm^{-1} (C=O, acid), 1650 cm^{-1} (C=O, amide), 1600 cm^{-1} (C=C), 1530 cm^{-1} , 1456 cm^{-1} , 1377 cm^{-1} , 989 cm^{-1} , 812 cm^{-1} , 696 cm^{-1} .

^1H NMR (200MHz, DMSO- d_6).

δ 2.89 (m, 1H), 3.07 (m, 1H), 4.49 (m, 1H), 5.58 (d, 1H), 6.06 (m, 1H), 6.22 (m, 1H), 7.23 (m, 5H), 8.42 (d, 1H).

4.4.3 *N-benzylacrylamide [NBAm]*

To an ice-cold mixture of benzylamine (5.5ml), triethylamine (7.0ml) in benzene (50ml), a solution of acryloyl chloride (4.1ml) in benzene (6.0ml) was added dropwise while maintaining the temperature between 0-5 °C during the addition. After complete addition, the reaction mixture was stirred for 3 hrs at room temperature and filtered to remove the salt. With several benzene washings, the filtrate and washings were collected together and concentrated on rotavapour. The concentrate was precipitated in hexane with white solid coming out after keeping it in freezer overnight. (Yield 75% mp. 63-65 °C)

IR (KBr),

3274 cm^{-1} (N—H), 3033 cm^{-1} and 3064 cm^{-1} (C—H), 1660 cm^{-1} (C=O, amide), 1625 cm^{-1} (C=C), 1600 cm^{-1} , 1540 cm^{-1} , 1496 cm^{-1} , 1400 cm^{-1} , 985 cm^{-1} , 732 cm^{-1} , 698 cm^{-1} .

^1H NMR (200MHz, CDCl_3)

δ 4.4 (d, 2H), 5.6 (d, 1H), 6.1 (m, 1H), 6.3 (d, 1H), 7.3 (m, 5H).

4.4.4 *N-Acryloyl-6-amino caproic acid [A6ACA]*

The exact procedure and characterization was described in chapter 3 (3.1.4.3).

4.5 Synthesis of polymers

We have synthesized homopolymer gels of PNIPAm and copolymer gels of poly (*N*-isopropylacrylamide)-co-poly(*N*-acryloyl L-phenyl alanine) [PNIPAm-co-PAPA], PNIPAm-co-poly(acryloyl 6-aminocaproic acid) [PNIPAm-co-PA6ACA] and PNIPAm-co-(*N*-benzylacrylamide) [PNIPAm-co-PNBAm]. The feed compositions and the chemical structures of these gels are given in Table 4.1 and Figure 4.1 respectively. The polymerization was carried out in 1,4-dioxane using AIBN as a free radical initiator and EGDMA as a cross-linker. The monomer in required amount (with defined mole ratios, Table 4.1), initiator and cross-linker were dissolved in 1,4-dioxane with constant stirring and nitrogen bubbling. The monomer solutions were poured into test tubes and sealed. The polymerization was carried out at 60 °C for 24 h. The degree of crosslinking in both homopolymer and copolymer gels was in the range of 10-12% on the basis of weight of the monomer.

The cross-linked gels were washed with distilled water for a week and dried in oven at 40 °C till the constant weight was obtained.

4.6 Swelling ratio measurements

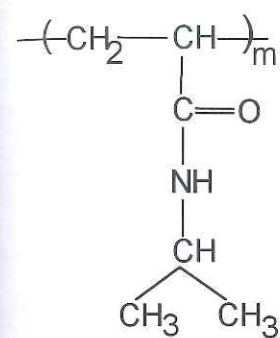
Swelling measurements were carried out by immersing dry gel samples in water or aqueous SDS solutions of different concentrations. The gels were allowed to equilibrate for 72 hrs. till a constant weight was reached. The surface water was carefully wiped off before weighing and the swelling ratio (q) was recorded gravimetrically as,

Table 4.1

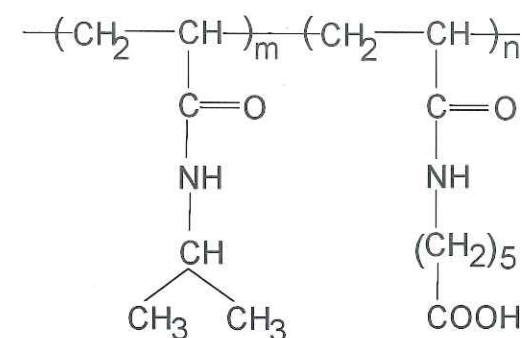
Feed Composition of homopolymer and copolymer gels

Sample code	Mole ratio	NIPAm (mmoles)	Comonomers (mmoles)
PNIPAm	100:0	8.8	0.0
PNIPAm-co-PAPA	95:5	9.5	0.5
PNIPAm-co-PAPA	80:20	6.0	0.15
PNIPAm-co-PNBAm	80:20	6.66	1.66
PNIPAm-co-PA6ACA	80:20	6.66	1.66

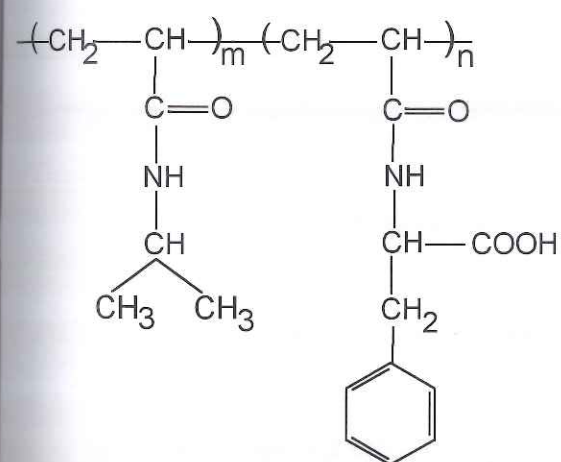
- NIPAm : *N*-isopropylacrylamide
- APA, NBAm, A6ACA : Comonomers
- AIBN : Azo-bis-isobutyronitrile, initiator, 0.01 mole/mole of monomers
- EGDMA : Ethylene glycol dimethacrylate, crosslinker, 0.1 mole/mole of monomers
- Solvent : 1,4-dioxane, 10 ml
- Polymerization temperature : 60°C for 24



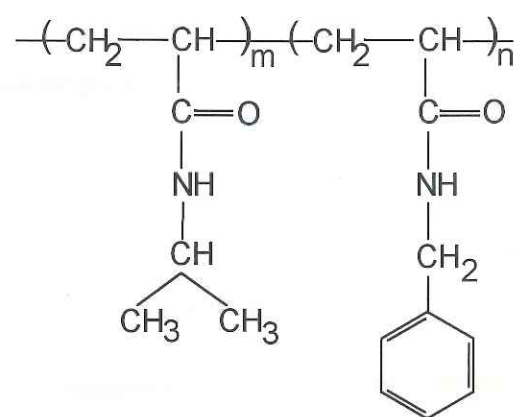
[PNIPAm]



[PNIPAm-co-PA6ACA]



[PNIPAm-co-PAPA]



[PNIPAm-co-NBAm]

Figure 4.1: Chemical structures of gels

$$q = \frac{\text{wt. of equilibrated gel}}{\text{wt. of dry gel}}$$

4.7 ¹³C NMR Measurements

The compositions of the copolymer gels [PNIPAM-co-PAPA] were determined by ¹³C Cross-Polarization-Magic Angle Sample Spinning (CP-MASS) nuclear magnetic resonance spectroscopy. All the ¹³C-NMR spectra were obtained on a Bruker DRX-500 FT-NMR spectrometer operating at a carbon frequency of 125.75MHz. For the CP-MASS experiments, the cross-polarization was established using Hartman-Hahn match conditions at 50 kHz. using adamantane as a standard. Contact time (CT) of 1 ms and recycle delay of 3 secs were used in the CP-MASS experiments. The MASS was maintained at 8 kHz and the number of scans collected were 8500. Center bands and side bands were identified by recording spectra of each sample at two different spinning speeds. The spectra were recorded at a probe temperature of 20 °C.

4.8 Results and Discussion

4.8.1 Composition of copolymer gels by solid-state ¹³C NMR spectroscopy

The assignments of ¹³C peaks in the chemical structure are discussed below. We show in Figure 4.2 the ¹³C spectra of PNIPAm (homopolymer) and PNIPAM-co-PAPA (copolymer) gels taken in the dry state. It can be seen that, CH₃ peaks appear at 23 ppm, and carbonyl of -CONH appear at 174.5ppm. The backbone -CH and -CH₂ peaks resonate at the broad range of 40-50 ppm. It is difficult to distinguish between the -CO signals arising due to -CONH₂ and -COOH groups of copolymer gels because of their small chemical shift differences.

The quantitative determination of the copolymer compositions was done by measuring the integral intensities of ¹³C peaks in the spectra of copolymer gels. Especially, the ¹³C signals arising from the aromatic ring in the copolymer gels has been focussed. The experimental copolymer composition obtained by ¹³C NMR spectroscopy was compared with the feed composition (see Table 4.2). It can be seen that there is a good agreement between the two, which suggests that the reaction proceed to completion with quantitative yields of the products.

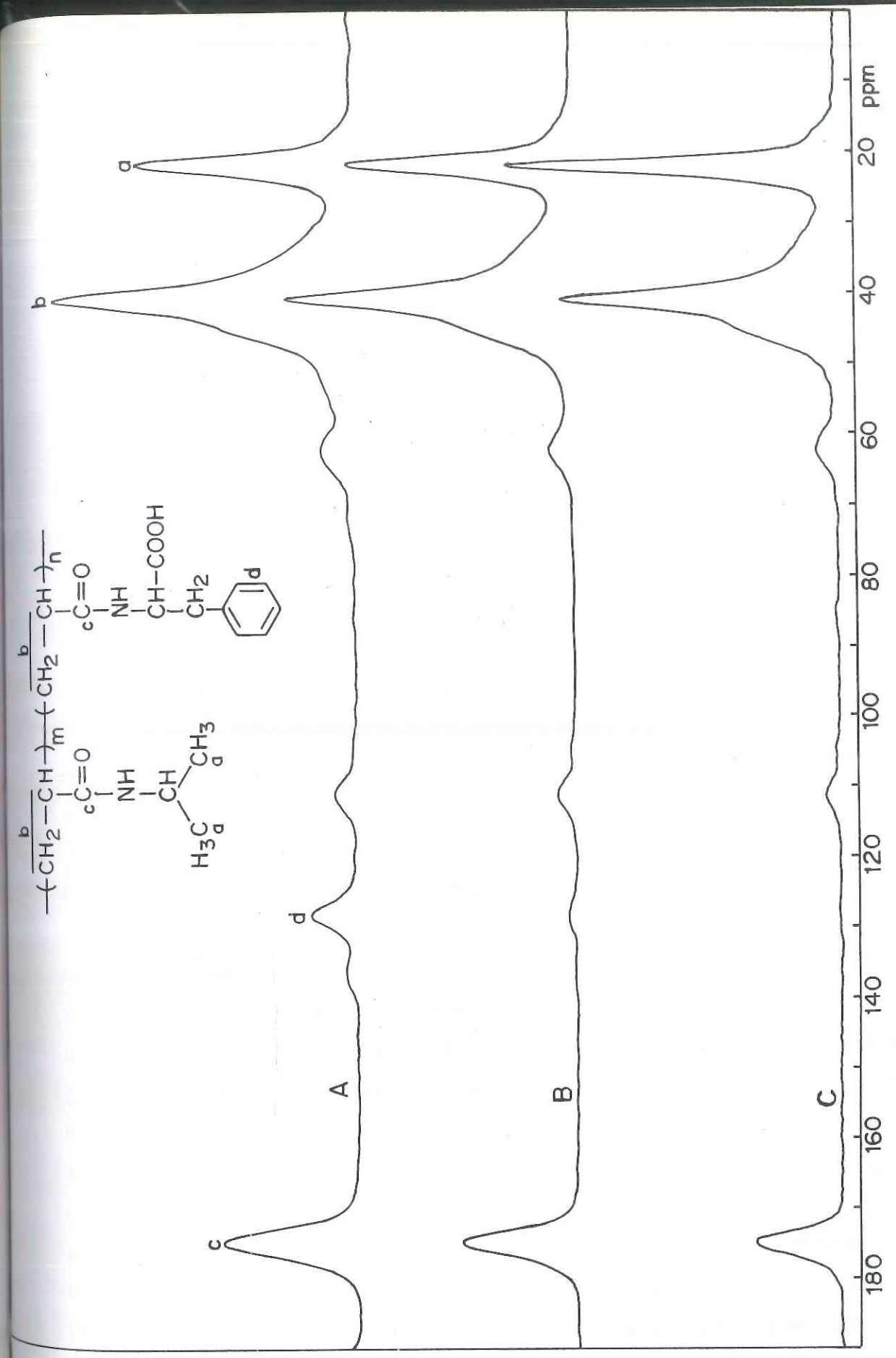


Figure 4.2: Comparison of ¹³C NMR spectra of homopolymer [PNIPAm] (2C) and copolymer gels [PNIPAm-co-PAPA] [95:5 (2B), 80:20 (2A)]

Table 4.2

Composition of copolymer gels by ^{13}C NMR spectroscopy

Sample code	Mole ratio in copolymers	
	PNIPAm	PAPA
PNIPAm	100.0 (100.0)	0.0 (0.0)
PNIPAm-co-PAPA	96.02 (95.0)	3.98 (5.0)
PNIPAm-co-PAPA	75.9 (80.0)	24.1 (20.0)

(molar feed ratios are given in parentheses)

4.8.2 Swelling characteristics of gels in SDS solution

The copolymers were so designed that different hydrophilic and hydrophobic balances could be obtained in the chemical structure of gels, which strongly influence the swelling properties. We show in Figure 4.3 the swelling ratios of PNIPAm homopolymer gel as a function of temperature in different concentration of SDS solutions. It can be readily seen that both the transition temperature and the equilibrium swelling ratio of PNIPAm gel increased remarkably in SDS solutions. PNIPAm homopolymer gel with a swelling ratio of around 10 was found to undergo a discontinuous transition at temperature between 31 to 32°C in the absence of surfactant. The volume phase transition was also discontinuous for all the SDS concentrations studied. Both volume phase transition temperature and the net volume change at transition increased with increasing SDS concentration. At 0.1% SDS concentration, the transition temperature was found to be in between 38 and 40 °C, which was accompanied by an increased swelling ratio of around 17. This increase in transition temperature and swelling ratio was seen only upto a certain concentration of SDS, and above this concentration there was a negligible change in transition temperature. Further addition of surfactant results in a large increase in the amount of bound surfactant, while the concentration of free surfactant remains constant. Upon further increase in surfactant concentration, the binding levels off and a point is reached, where surfactant micelles co-exist in solution with negligible effect on the transition temperature. For PNIPAm homopolymer gel, this concentration was found to

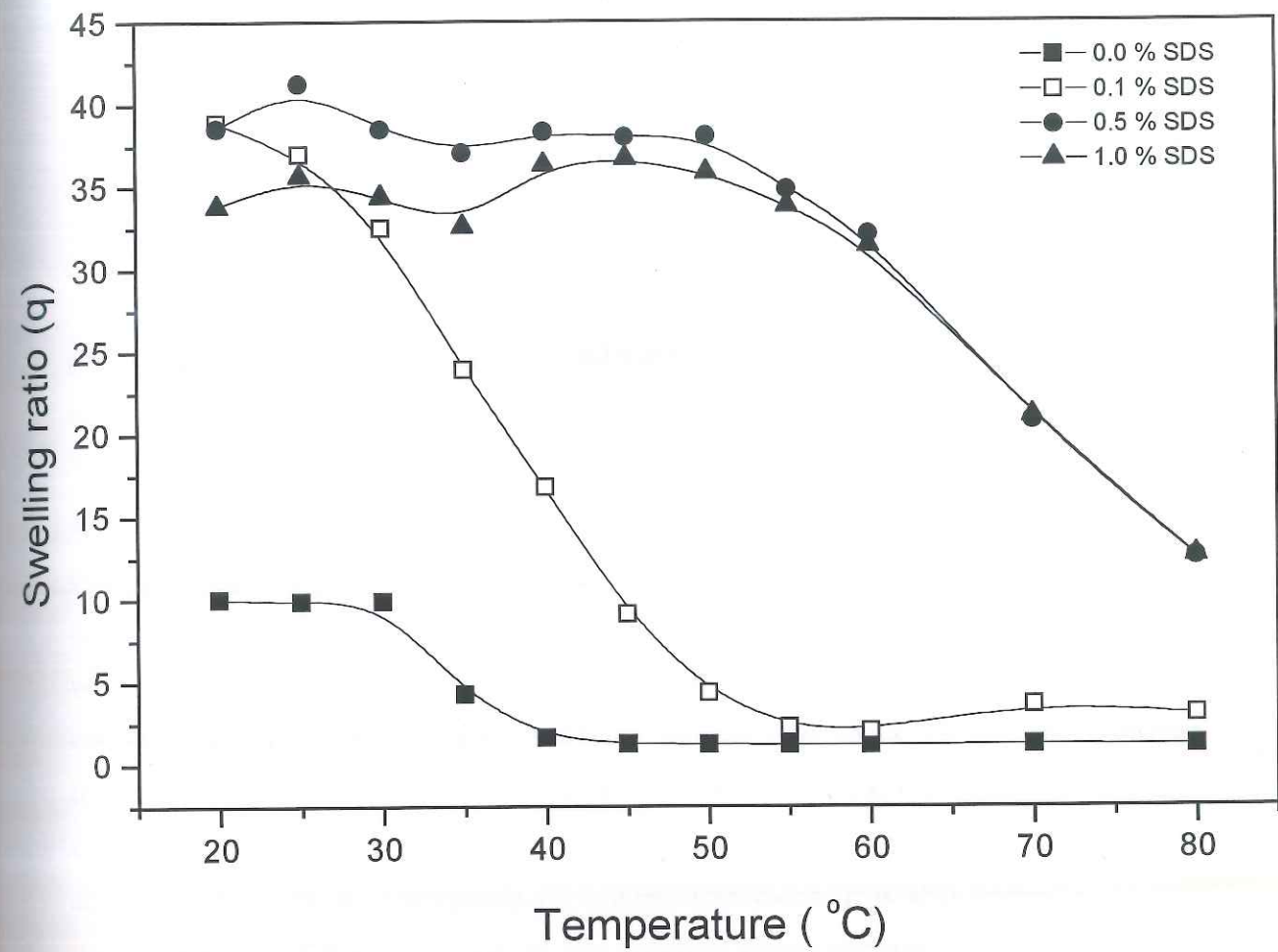


Figure 4.3: Swelling ratios of PNIPAm homopolymer gel as a function of temperature in different concentrations of SDS solutions

be around 0.5% (~20.0 mM). This is in good agreement with the earlier reports.^{3,4} The surfactant SDS binds to the PNIPAm gel through hydrophobic interactions between the isopropyl groups of the polymer and the long chain alkyl groups of the surfactant, thereby converting the neutral gel into a polyelectrolyte gel. This prevents the intermolecular hydrophobic associations upon increasing the temperature, which is otherwise the driving force for the phase transition in the absence of surfactant. These acquired charges on the gel along with the counter ions associated with the charges exert an extra osmotic pressure on the gel. As a result, both the transition temperature and swelling ratio at the transition are increased.

We show in Figure 4.4 the swelling ratios of copolymer gel, PNIPAm-co-PAPA [80:20] as a function of temperature in different concentrations of SDS solutions. It can be seen that the gels remain in a completely collapsed form in water between 20 and 80 °C. This is due to the dominance of the hydrophobic character arising from the phenyl alanine groups in the copolymer gel. This clearly suggests that the LCST of this copolymer gel is at subzero temperatures, which is not in the observable range. This is in agreement with our earlier report that the LCSTs of PNIPAm copolymer gels decrease with the incorporation of hydrophobic comonomers.¹⁰ However, at 0.5% SDS concentration, the swelling ratios suddenly increases to about 15 and the transition temperature increases to about 37 °C. This is due to the fact that the surfactant molecules sequester the hydrophobic groups in the chain and prevent the interchain hydrophobic associations, which are responsible for volume transitions. It is also interesting to note that with rise in SDS concentration, the swelling ratios increase further and the gels exhibit two discontinuous volume transitions, one at 38 °C and another at 60 °C. The observation of two transitions, which is intriguing at a first glance, will be explained later on the basis of heterogeneous interactions between the gels and surfactants.

4.8.3 *Core-Shell Morphology in Copolymer gels*

We show in Figure 4.5(a), the pictures of swollen PNIPAm and PNIPAm-co-PNBAm gels in 1% SDS solution at 40 °C. It can be seen that the swelling of these gels is uniform throughout the bulk, indicating a homogeneous interaction of surfactant with these gels. Furthermore, these gels do not contain ionisable groups in their chemical structure and hence the electrostatic repulsion does not arise from the polymer chains.

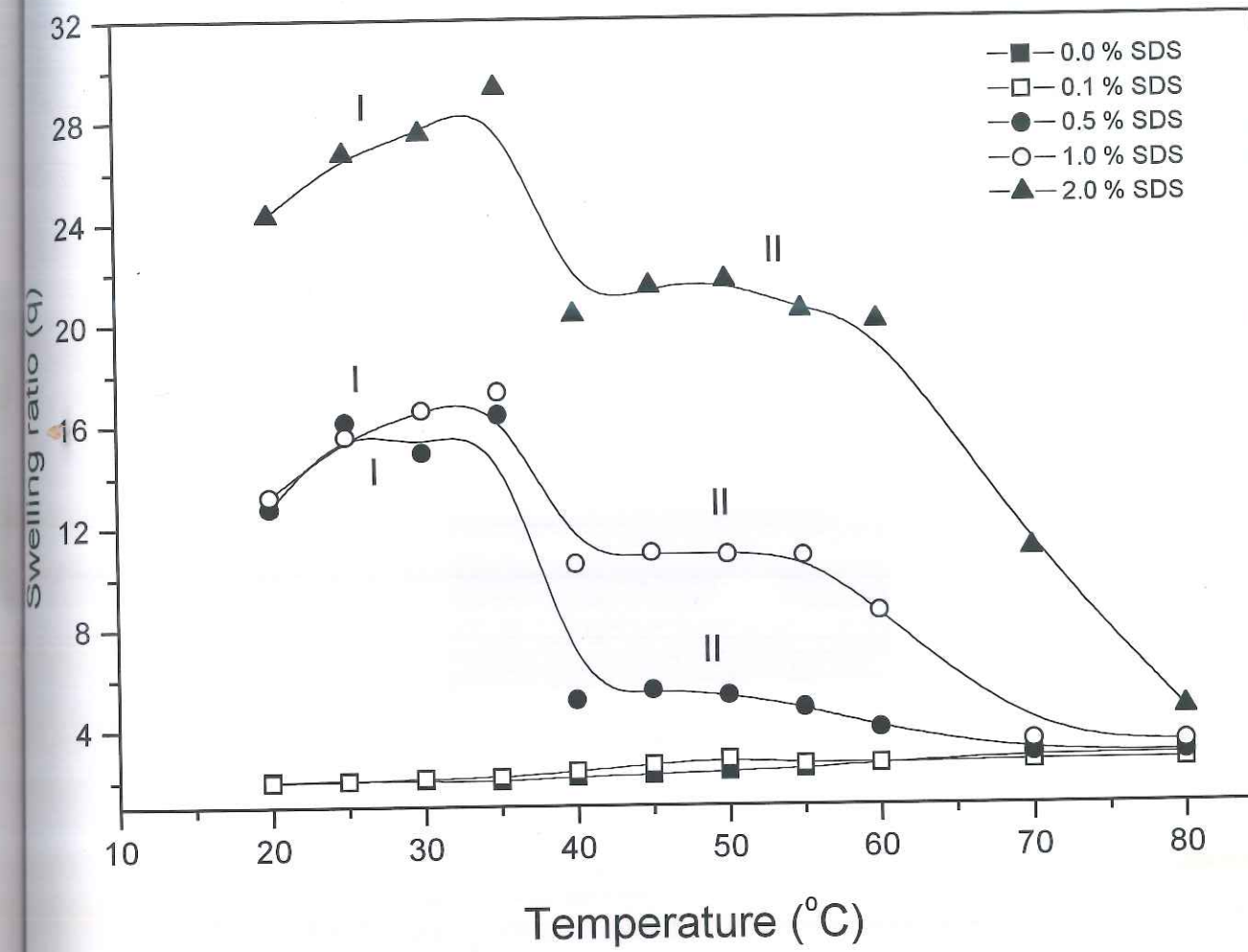
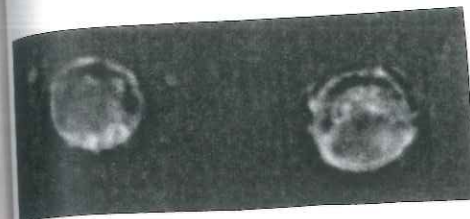
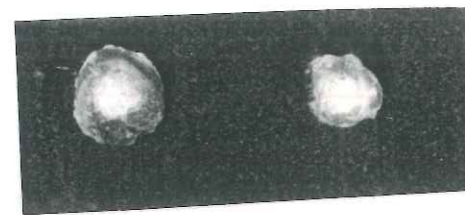


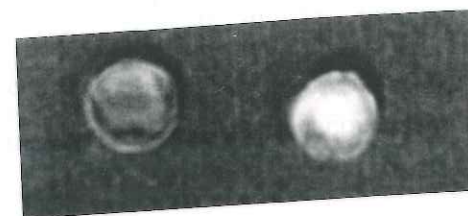
Figure 4.4: Temperature-dependent swelling ratios of PNIPAm-co-PAPA (80:20) copolymer gel in different concentrations of SDS solutions.



(a)



(b)



(c)

Figure 4.5: Pictures of swollen homopolymer and copolymer gels.
(a) PNIPAm homopolymer gel (left) and PNIPAm-co-PNBAm [80:20] copolymer gel (right) swollen in 1.0% SDS solution at 40 °C
(b) PNIPAm-co-PAPA [80:20] copolymer gel (left) and PNIPAm-co-P6ACA [80:20] copolymer gel (right) swollen in 1.0 % SDS solution at 40 °C.
(c) PNIPAm-co-PAPA [95:5] copolymer gel swollen in 1.0% SDS solution at 10 °C (left) and at 40 °C (right)

The SDS interacts with polymer through hydrophobic interactions and the distribution of SDS is likely to be uniform through out the bulk of the swollen gel. Therefore, the swollen gels are transparent and do not exhibit core-shell morphology. On the contrary, the copolymer gels of PNIPAm-co-PAPA and PNIPAm-co-PA6ACA, contain ionizable -COOH groups and show an interesting feature of core-shell morphology when swollen in 1% SDS solution at 40 °C. [Figure 4.5(b)]. The core is collapsed and opaque in nature where as the shell is swollen and transparent. The observation of core-shell morphology is indicative of an uneven binding of surfactant molecules to the gel network. Due to this uneven binding, there exists a local distribution of charge density in the gel network. Although our efforts to identify the constituents of core and shell by IR spectroscopy was unsuccessful (due to undistinguishable spectra between the core and the shell), the very fact that the shell is highly swollen in SDS solution indicates that the surfactant molecules interact only at the surface.

The observation of two plateau in the temperature dependent swelling measurements of copolymer gels in SDS solution (I and II in Figure 4.4) can be understood in the light of uneven binding of surfactant molecules, which gives rise to local microphases having phase transition temperatures of around 36-38 °C. These microphases undergo deswelling at this temperature and exhibit first order volume transition at 36- 38 °C. The outer layer of the gel, which has large concentration of surfactant is still swollen and undergoes volume transition at around 60-65 °C. Therefore, the observation of two plateau followed by two volume transitions in the swelling ratio measurements can be explained in terms of the presence of heterogeneous phases as a result of uneven binding of surfactant molecules.

Numerous studies on the interaction of various surfactants with PNIPAm gel have been reported.^{3,4,11} Recently, Kokufuta *et al.*¹² have reported on the quantitative uptake of surfactant, sodium dodecyl benzene sulfonate [NaDBS] by PNIPAm gel and subsequently its effect on the phase transition of the gel. The surfactant, NaDBS is also an anionic type, but contain an additional phenyl ring in the chemical structure as compared to SDS. Their comparative study of SDS and NaDBS uptake by PNIPAm gel clearly indicate that SDS exhibited a stronger effect than NaDBS with 20 mol % increase in the uptake level. While the binding of SDS with PNIPAm gel is more, they demonstrated an inhomogeneous local binding of NaDBS to PNIPAm gel by using a microscopy technique. Their

experimental observations suggested that surfactant molecules are bound only to the gel surface but are unable to penetrate into the core of the gel phase. The authors claim that this happens because the negative charges of the surfactant bound layer seem to hinder further diffusion of surfactant molecules having similar charge into the internal parts of the gel through the electrostatic repulsion. According to this hypothesis, if the bound surfactant layer in PNIPAm-NaDBS system exhibits electrostatic charge repulsion, then it is reasonable to expect a similar uneven/surface binding of surfactant in PNIPAm-SDS system also. However, we have observed a homogeneous swelling of PNIPAm gel in SDS solutions and to our knowledge there are no such reports in the literature on the uneven binding of SDS with PNIPAm.

Our copolymer gels contain hydrophobic *N*-isopropyl and phenyl groups and hydrophilic ionisable -COOH groups on the chain. The interaction of anionic surfactants with the polymer chains by hydrophobic associations induces charges in the polymer chains. Furthermore, the ionisable -COOH groups on the chain further enhance the electrostatic charges on the chains. Therefore, the presence of large electrostatic charges on the chain creates a barrier at the surface for further diffusion of surfactant molecules to the core. Hence the core remains collapsed and the outer shell, which has interacted with the surfactant, becomes highly swollen. This hindered diffusion of surfactant molecules inside the bulk of the gel gives rise to a core-shell morphology. We also noticed that when a dry gel piece (5mm diameter, 1mm thickness) was immersed in 1% SDS solution, the core-shell morphology which developed in about four hours, disappeared after a long period of three months. Therefore, we believe that the core-shell morphology occurs due to the competition between the kinetics of diffusion of surfactant molecules into the gel and kinetics of surfactant binding to the gel. A faster rate of surfactant diffusion and slow binding leads to a uniform distribution of surfactant into the gel resulting in homogeneous interaction. On the other hand, slow diffusion and rapid binding of surfactant molecules gives rise to uneven distribution of surfactant molecules, which results in core-shell morphology. The observation of core-shell morphology also depends on the hydrophobic content of the copolymer gel, which, in turn determines the initial LCST of the gel.

A possible mechanism for the observed core-shell morphology in our copolymer gels can be proposed qualitatively. The copolymer gel PNIPAm-co-PAPA contains about 20 % of acryloyl phenylalanine. At this composition, the LCST of copolymer gel in water

is below 0 °C and hence the gels are completely collapsed in water at room temperature (25°C)(Figure 4.4). However, in the presence of a surfactant, the surfactant molecules interact at the surface and the swelling ratios at the surface increase remarkably along with an increase in the LCST of the polymer chains at the surface. Our observation suggests that the LCST at the surface (shell) increases to about 70 °C, which is well above our measurement temperature of 40 °C. Due to this local binding of surfactant at the surface and the presence of ionisable -COOH groups on the chain, there exists a strong hindrance to the further diffusion of surfactant molecules towards the inner core of the hydrogel. With a lack of interaction between the surfactant molecules and the core, the LCST of the core region of the hydrogel remains unchanged. As a result, the core region remains collapsed at 40 °C and the shell is swollen due to surfactant induced increase in LCST thereby exhibiting the core-shell morphology.

In order to verify this hypothesis, we undertook similar swelling measurements on a copolymer gel PNIPAm-co-PAPA, which contains only 5% acryloyl L-phenylalanine. The hydrophobic content of the copolymer gel was kept low so that the LCST shifts to the higher observable temperature range. This copolymer gel was found to have an LCST of 15 °C. Hence, a dry gel when immersed in 1 % SDS solution at 10 °C [Figure 4.5(c), left] did not show core-shell morphology. This is due to the fact that at 10 °C, which is below the LCST, the inner core, although not having interacted with the surfactant is still swollen and the shell, which has interacted with the surfactant, is also swollen. As a result, there is a uniform swelling through out the gel although there will be higher concentration of surfactant at the surface. However, at 40 °C a core-shell morphology was distinctly seen [Figure 4.5(c), right]. This clearly indicates that the occurrence of core-shell morphology also depends on the initial LCST of the copolymer gel, which is dictated by the hydrophobic content of the gel and the temperature of observation.

4.8.4 Effect of degree of ionization of -COOH groups on the equilibrium swelling ratios of the copolymer gel

Although, it is difficult to determine the localized pH of the gels experimentally, we have attempted to see the influence of the degree of ionization of -COOH groups in the copolymer gels on the swelling ratios. We have undertaken the swelling measurements of neutralized PNIPAm-co-PAPA gels in 1.0 % SDS solutions at 25 °C.

The PNIPAm-co-PAA (80: 20) copolymer gel pieces (with 5mm diameter and 1mm thickness) were neutralized to different extents by immersing them in 1N sodium hydroxide solution for different times. Then the gel pieces were removed, washed with distilled water and dried in oven at 25 °C under reduced pressure. The dry gel pieces were subsequently taken for measurement of swelling ratios in 1.0 % SDS solution as a function of degree of ionization. The results are shown in Figure 4.6. It is evident that, the swelling ratios in 1.0 % SDS solution increase considerably as the degree of ionization increases. This clearly suggests that the ionization of -COOH groups in the copolymer gel increase the hydrophilicity of the gel, which in turn enhances the LCST of the gel. As a result the swelling capacity of the gel increases significantly. From the Figure 4.6, it can be seen that, the unneutralized sample with a swelling ratio of 15.8 increases to 50.2 when it is completely neutralized. Due to the enhanced LCST, increased swelling capacity of the gel and the corresponding increase in diffusion rates of the surfactant inside the swollen gel, the core-shell morphology is not seen in the completely ionized gels. This is once again in line with our earlier observation of dependence of core-shell morphology on the initial LCST of the copolymer gel. The observation of core-shell morphology also depends on the hydrophobic content of the copolymer gel, which, in turn determines the initial LCST of the gel.

4.9 Conclusions

Interaction of surfactant, SDS, with hydrophobically modified copolymer gels enhanced the swelling ratios and LCSTs remarkably. The slow/hindered diffusion and uneven distribution of surfactant molecules in the gel gave rise to a new type of core-shell morphology and two unusual volume transitions. The swelling capacity and the initial LCST of the copolymer gel plays vital role in the observation of the core-shell morphology. Such observed core-shell morphology in thermosensitive hydrogels can have potential applications in controlled drug delivery systems wherein the hydrophobic drugs can be incorporated in the inner core of the hydrogel and released through the hydrated outer layer at a controlled rate.

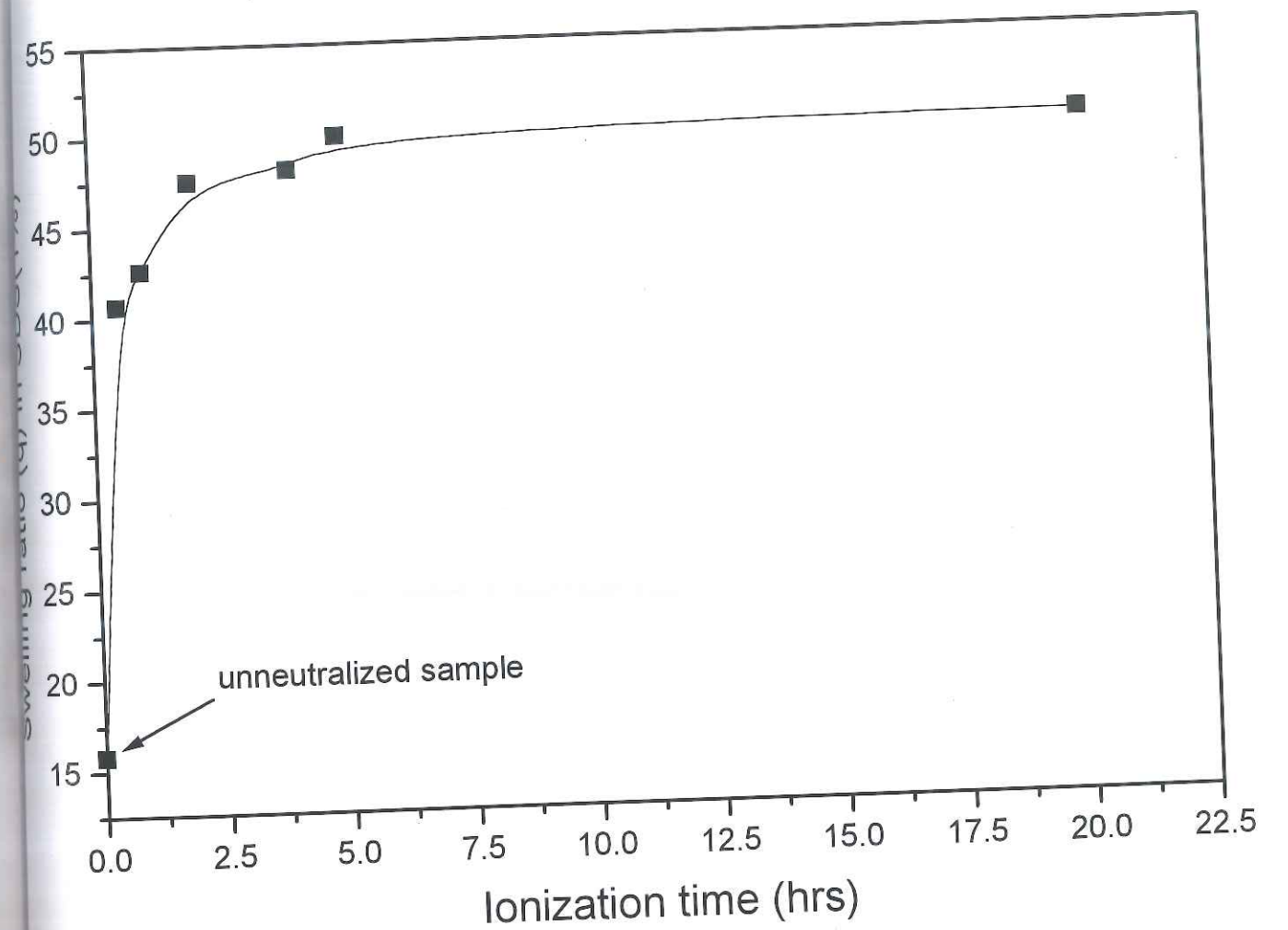


Figure 4.6: Influence of ionization of -COOH groups on the swelling ratios of PNIPAm-PAPA (80:20) copolymer gels in 1.0 % SDS solution.

4.10 References

1. E. D. Goddard, *Colloids Surf.*, **19**, 255 (1986).
2. J. Xia, P. L. Dubin, Y. Kim, *J. Phys. Chem.*, **96**, 6805 (1992).
3. H. G. Schild, D. A. Tirrell, *Langmuir*, **7**, 655 (1991).
4. E. Kokufuta, Y. Q. Zhang, T. Tanaka, A. Mamada, *Macromolecules*, **26**, 1053 (1993).
5. K. C. Tam, X. Y. Wu, R. H. Pelton, *Polymer*, **33**, 436 (1992).
6. F. Zeng, X. Zheng, Z. Tong, *Polymer*, **39**, 1249 (1998).
7. H. G. Schild, *Prog. Polym. Sci.*, **17**, 163 (1992).
8. J. J. Eliassaf, *Appl. Polym. Sci.*, **22**, 873 (1978).
9. V. S. Shinde, M. V. Badiger, A. K. Lele, R. A. Mashelkar, *Langmuir*, **17**, 2585 (2001).
10. M. V. Badiger, A. K. Lele, V. S. Bhalerao, S. Varghese, R. A. Mashelkar, *J. Chem. Phys.*, **109**, 1175 (1998).
11. F. M. Winnik, H. Ringsdorf, J. Venzmer, *Langmuir*, **7**, 905 (1991).
12. E. Kokufuta, H. Suzuki, D. Sakamoto, *Langmuir*, **13**, 2627 (1997).

Chapter 5

The influence of experimental conditions on the mesoscopic morphologies developed during the phase transitions of thermosensitive polymers

5.1 Introduction

PNIPAm is known to exhibit an LCST of 32°C in water.¹ A crosslinked PNIPAm hydrogel exhibits a discontinuous volume transition at a temperature close to the LCST. At lower temperature, water molecules form hydrogen bonds with the amide groups of the NIPAm units and also shield the isopropyl hydrophobic groups by the so-called 'caging' effect. At the transition temperature, the polymer-water hydrogen bonds are replaced by the polymer-polymer hydrogen bonds and the hydrophobic interactions between polymer chains also increase substantially. This results in phase separation of the system.

PNIPAm-water solution can phase separate by either nucleation-growth mechanism or spinodal decomposition mechanism depending on whether the system is in the metastable region or the unstable region of the phase diagram. In the metastable region, the formation of a polymer-rich phase is initiated through large concentration fluctuations called the critical nuclei, which overcome the energy barrier associated with the excess surface energy of the new phase. Often, particulate mesoscopic morphologies are formed by the subsequent growth of the critical nuclei. In the unstable region, the energy barrier is negligible and concentration fluctuations grow spontaneously to form network-like mesoscopic morphologies.²

PNIPAm gel, when synthesized by the conventional route in a non-aqueous solvent or in water at sub-ambient temperature, shows transparency to visible light below the volume transition temperature. On heating, the gel becomes opaque due to the formation of phase separated domains by spinodal decomposition mechanism.³ This optical transition of the gel, which accompanies the volume transition, is reversible, i.e.; the gel becomes transparent again on lowering the temperature. However, if the PNIPAm gel is synthesized in water at temperatures above the transition temperature, the gel becomes irreversibly hazy or opaque, i.e., it retains its opacity at lower temperatures. In this work we show that the gels so synthesized show a wide range of mesoscopic structures depending on the experimental conditions. We show that the morphologies are formed by phase separation of the polymerizing mixture and subsequent "pinning down" of the mesoscopic structures by gelation. We show theoretically and experimentally that by controlling the gelation kinetics it is possible to freeze the morphology of the gel in the

metastable or the unstable regions of the phase diagram. We show that the gels so produced show rapid swelling compared to the conventionally synthesized gels. Finally, we also show that the phase separation kinetics can be strongly coupled with the gelation kinetics under certain experimental conditions.⁴

5.2 Theory

In this section we discuss the phase diagram of PNIPAm-water system, the polymerization kinetics of NIPAm in water and the influence of the mode of polymerization, namely, adiabatic or non-adiabatic. We show how the formation of different morphologies can be explained by simply superimposing the polymerization paths on the phase diagram. The assumption here is that the polymerization and phase separation processes are decoupled, which need not hold true for all experimental conditions. Nonetheless, this approach gives sufficient insight into the formation of various morphologies in the PNIPAm gel.

5.2.1 Phase diagram

Lattice-Fluid-Hydrogen-Bond (LFHB) model⁵ can quantitatively predict the temperature driven thermodynamic volume transition of crosslinked PNIPAm gel in water. We summarize the model in the following for predicting the phase diagram of an aqueous solution of uncrosslinked PNIPAm. The details of the free energy of mixing terms⁶ are described in chapter 1 and 3. From the free energy of mixing, the chemical potentials of the solvent and the polymer can be calculated as

$$\frac{\mu_1}{RT} = \ln(\phi_1 / \omega_1) + \left(1 - \frac{r_1}{r_2}\right) \phi_2 + r_1 \tilde{\rho} \phi_2^2 X_{12} + r_1 \left\{ -\frac{\tilde{\rho}}{\tilde{T}_1} + \frac{\tilde{P}_1 \tilde{v}}{\tilde{T}_1} + (\tilde{v} - 1) \ln(1 - \tilde{\rho}) + \frac{1}{r_1} \ln \tilde{\rho} \right\} +$$

$$r_1 \sum_i^m \sum_j^n v_{ij} - \sum_i a_i^1 \ln \frac{v_d^i}{v_{io}} - \sum_j a_j^1 \ln \frac{v_a^j}{v_{oj}} - \sum_j a_j^1 \ln \frac{v_a^j}{v_{oj}} \quad (5.1)$$

and

$$\frac{\mu_2}{RT} = \ln(\phi_2 / \omega_2) + \left(1 - \frac{r_2}{r_1}\right) \phi_1 + r_2 \tilde{\rho} \phi_1^2 X_{12} + r_2 \left\{ -\frac{\tilde{\rho}}{\tilde{T}_2} + \frac{\tilde{P}_2 \tilde{v}}{\tilde{T}_2} + (\tilde{v} - 1) \ln(1 - \tilde{\rho}) + \frac{1}{r_2} \ln \tilde{\rho} \right\} + r_2 \sum_i^m \sum_j^n v_{ij} - \sum_i d_i^2 \ln \frac{v_d^i}{v_{io}} - \sum_j a_j^2 \ln \frac{v_d^j}{v_{oj}} - \sum_j a_j^2 \ln \frac{v_d^j}{v_{oj}} \quad (5.2)$$

where,

$$X_{12} = \frac{\varepsilon_1^* + \varepsilon_2^* - 2\zeta_{12}(\varepsilon_1^* \varepsilon_2^*)^{1/2}}{RT} \quad (5.3)$$

and $\tilde{\rho}$ is the reduced density of the mixture which is related to the reduced pressure $\tilde{P} = P/P^*$ and reduced temperature $\tilde{T} = T/T^*$ by the equation of state

$$\tilde{\rho}^2 + \tilde{P} + \tilde{T} \left\{ \ln(1 - \tilde{\rho}) + \tilde{\rho} \left[1 - \left(\frac{1}{r} - \sum_i^m \sum_j^n v_{ij} \right) \right] \right\} = 0 \quad (5.4)$$

In the first line of eq (5.1, 5.2), the first two terms are the combinatorial entropy contribution, the third term is energetic (effective hydrophobic) contribution and the fourth term in brackets represents the effect of the pure component properties. The terms in the second line represent the hydrogen bonding contribution.

The binodal curve, which separates the single-phase region from the two-phase region of the phase diagram, can be calculated by solving

$$\mu_1' = \mu_1'' \quad \text{and} \quad \mu_2' = \mu_2'' \quad (5.5)$$

where, the superscripts ' and '' indicate the polymer-rich and solvent-rich phases and the chemical potentials are given by equations (5.1) and (5.2).

The spinodal curve, which demarcates the unstable region and the metastable region of the phase diagram, can be calculated from $\frac{\partial^2 G}{\partial \phi^2} = 0$. Substituting from equations (5.1, 5.2), the equation for spinodal is

$$\left(\frac{1}{\phi_1} - 1 + \frac{r_1}{r_2} - 2r_1 \tilde{\rho} \phi_2 X_{12} \right) + \frac{1}{r_1 \phi_2} \left(\sum_i \sum_j \left(-r_i^2 + \frac{d_i^2}{v_d^i v_{io}} + \frac{a_j^2}{v_a^j v_{oj}} \right) v_{ij} \right) = 0 \quad (5.6)$$

5.2.2 Polymerization kinetics

NIPAm monomer undergoes a free radical polymerization in water in the presence of a redox initiator such as ammonium persulfate $[(\text{NH}_4)_2\text{S}_2\text{O}_8]$ and an accelerator such as N,N,N',N'-tetramethylethylenediamine (TEMED). However, experimental data on the kinetics of this polymerization has not been reported so far. Polyacrylamide undergoes similar polymerization to NIPAm and its kinetics has been well documented. In view of this, we assume that the polymerization kinetics of NIPAm is the same as that for acrylamide monomer.

The rate of free radical polymerization is given by

$$-\frac{dM}{dt} = k_p \left(\frac{fk_d[I]}{k_t} \right)^{1/2} [M] \quad (5.7)$$

where, $[M]$ is the concentration of unreacted monomer, k_p , k_d , and k_t are rate constants of propagation, dissociation (of initiator) and termination reactions. f is the efficiency of the initiator, whose dissociation is assumed to be a first order reaction given by $I = I_0 e^{-k_d t}$. Using Arrhenius forms for rate constants, the rate of polymerization can be written in dimensionless form as follows,

$$\frac{dM^*}{dt^*} = \gamma M^* \exp \left[-\frac{2\alpha_p + 2\alpha_d - \alpha_t + t^* T^* e^{(\alpha_d/T^*)}}{2T^*} \right] \quad (5.8)$$

where,

$$\begin{aligned} \alpha_{p,d,t} &= \frac{E_{p,d,t}}{RT_o} & T^* &= \frac{T}{T_o} \\ \gamma &= A_p \left(\frac{A_d A_t}{I_o} \right)^{-1/2} & M^* &= \frac{M}{M_o} \\ \beta &= \frac{\Delta H M_o}{\rho C_p T_o} & t^* &= t A_d \end{aligned} \quad (5.9)$$

The degree of polymerization is given by

$$\frac{1}{X_n} = \frac{k_t}{k_p^2} \frac{R_p}{[M]^2} + C_M + C_S \frac{[S]}{[M]} + \frac{C_I k_t}{k_p^2 f k_d} \frac{R_p^2}{[M]^3} \quad (5.10)$$

where, C_M , C_S , C_I are the chain transfer coefficient to monomer, solvent and initiator, respectively. R_p is the rate of propagation given by equation (5.8) and $[S]$ is the solvent concentration.

Since polymerization is an exothermic process, the net heat accumulated in the reaction mixture determines the rise in temperature of the mixture. Depending on whether the reaction occurs under near-adiabatic or near-isothermal conditions the temperature rise of the polymerizing mixture crucially determines whether the reaction path would cross into the two-phase boundary of the phase diagram. For a general non-adiabatic reaction path in which polymerization is carried out in a thin film with controlled wall temperatures, the temperature rise accompanying the polymerization is given in non-dimensional terms by

$$\frac{\partial T^*}{\partial t^*} = \xi \frac{\partial^2 T^*}{\partial x^{*2}} + \beta \frac{\partial M^*}{\partial t^*} \quad (5.11)$$

where,

$$\xi = \frac{K}{\rho C_p A_d a^2} \quad (5.12)$$

K is the thermal conductivity, ρ is the density and C_p is the specific heat of the reaction mass. A_d is the area of heat transfer (surface area of film) and a is the thickness of the

film. If the rate of heat removal is slow compared to the rate of heat generation ($\xi \ll \beta$), then the reaction is adiabatic and the temperature rise is given by

$$T^* = 1 + \beta(1 - M^*) \quad (5.13)$$

5.3 Experimental Section

5.4 Materials

N-isopropylacrylamide was purchased from PolySciences Inc. (Warrington, PA, USA). The crosslinking reagents, N,N'-methylenebisacrylamide (Bis-A) and ethyleneglycol dimethacrylate (EGDMA) were obtained from Aldrich Chemical Company Inc., USA. Ammonium persulfate $[(\text{NH}_4)_2\text{S}_2\text{O}_8]$, 2,2'-azobisisobutyronitrile (AIBN) and N,N,N',N'-tetramethylethylenediamine (TEMED) were all of reagent grade. The AR grade 1,4-dioxane was obtained from J.T.Baker Chemical Co. (Philipsberg, NJ, USA). Deionized distilled water used for all synthesis was prepared in the laboratory using standard procedures.

5.5 Preparation of PNIPAm gel films

Method 1: NIPAm and crosslinker Bis-A (1.3%) were dissolved in distilled water. Nitrogen gas was bubbled through the solution in order to remove any dissolved oxygen. This monomer solution was kept at three different temperatures, 6°C, 27°C, and 50°C. After attaining the temperature, ammonium persulfate and TEMED were added to the solution, which was poured in between two glass plates separated by 1 mm. Polymerization was carried out at the three temperatures for 24 hours to form films of 1mm thickness. The gel films were washed with distilled water for one day for removing any unreacted monomers and dried in oven at 40°C till constant weights were obtained. The films prepared at the three temperatures are coded as P6, P27 and P50, respectively. A part of each films were equilibrated in water at room temperature and then freeze dried using Freeze dryer ALPHA 1-4 model (Christ Co., Germany). The code numbers for the freeze-dried gel films were FP6, FP27 and FP50, respectively.

Method 2: NIPAm and crosslinking agent EGDMA were dissolved in 20 ml 1,4-dioxane. Nitrogen gas was bubbled through the solution. Then AIBN initiator was added. This solution was kept for polymerization at 70°C for 24 h. Gel film was kept in water for another 24 h to remove unreacted monomers and dried in oven at 40°C till constant weight was obtained. A part of film was equilibrated in water at room temperature and then freeze dried. The sample code for the oven-dried film and the free-dried film are P70 and FP70, respectively.

5.6 Morphology studies

The oven-dried and freeze-dried films were fractured, sputtered with gold and observed by scanning electron microscope (Leica-stereoscan 440 model, Leica Co. Cambridge, UK).

5.7 Swelling ratio measurement

The gel films were immersed in deionized water at given temperatures for 24 h. Excess water on the gel surface was wiped off by filter paper and then the gels were weighed. The swelling ratio was calculated by

$$q \text{ (g/g)} = \frac{W_s}{W_o} \quad (5.14)$$

where, W_s and W_o denote the weights of swollen and dried gel samples, respectively.

For measurement of swelling kinetics, the gel films were removed from water at pre-determined time intervals and weighed to calculate the swelling ratio.

5.8 Results and Discussion

We begin by discussing the predictions of the phase diagram of PNIPAm-water by the LFHB model. We then discuss the polymerization pathway for NIPAm and show how different phase-separated morphologies can be achieved when the reaction pathway intersects the phase diagram.

Prediction of the phase diagram of PNIPAm-water mixture from equations (5.1 to 5.5) and (5.6) for the binodal and the spinodal curves, respectively, requires information on the various parameters in the LFHB model. We have already chosen appropriate values of the parameters in our earlier work on predicting the volume transitions of PNIPAm gel. These values are tabulated in Tables 5.1 to 5.2.

Table 5.1 gives the characteristic pure component parameters, which fit the P-V-T properties of pure PNIPAm and water. Table 5.2 gives the hydrogen bonding parameters for all types of H-bonds formed in the mixture. The only other parameter left in the model, namely the binary interaction parameter, was assumed to be temperature dependent.⁵

$$\zeta = 1.5 - 1.75 \times 10^{-3} T \quad (5.15)$$

Table 5.1
Pure component characteristic parameters

Component	P^* (MPa)	T^* (K)	ρ^* (kg/m ³)	MW (g/mol)
PNIPAM	503	699	1269	10,000
Water	475	578	853	18

Table 5.2
Hydrogen Bonding Parameters

H-bonding parameters	Donors \longrightarrow	-NH	-OH
	Acceptors \downarrow	$d_1^2 = 80$	$d_2^1 = 2$
E_{ij}^0 (J/gmol)		-3.24×10^3	-16.0×10^3
S_{ij}^0 (J/gmolK)	-C=O	-9.9	-25.8
V_{ij}^0 (cm ³ /gmol)	$a_1^2 = 80$	-0.85	--0.85
E_{ij}^0 (J/gmol)		-12.5×10^3	-16.595×10^3
S_{ij}^0 (J/gmolK)	-OH	-17.8	-26.6
V_{ij}^0 (cm ³ /gmol)	$a_2^1 = 2$	-0.85	-4.2

Figure 5.1 shows the predicted spinodal curves for different molecular weights (MW) of PNIPAm dissolved in water. The spinodals become increasingly skewed for higher molecular weight polymer. Figure 6.1 also shows the binodal curve (broken line) for a MW of 1,00,000.

Figure 5.2 shows that the predicted critical temperature decreases with increasing molecular weight but saturates after a molecular weight of 10,000. The region in Figure 5.2, which is below the T_c -MW curve represents the single-phase solution, while that above the curve represents the two-phase region of the phase diagram.

Figure 5.2 also shows the reaction pathways in temperature-MW coordinates for adiabatic polymerization reactions starting from different initial temperatures. The reaction paths are predicted from equations (5.8-5.10 and 5.13) and the various parameters required therein are listed in Table 5.3. It is seen from Figure 5.2 that as the polymerization proceeds, the increase in MW is accompanied by a rise in temperature, which takes the reaction mixture into the two-phase region depending on the initial temperature. The entry into the two-phase region occurs above a certain MW.

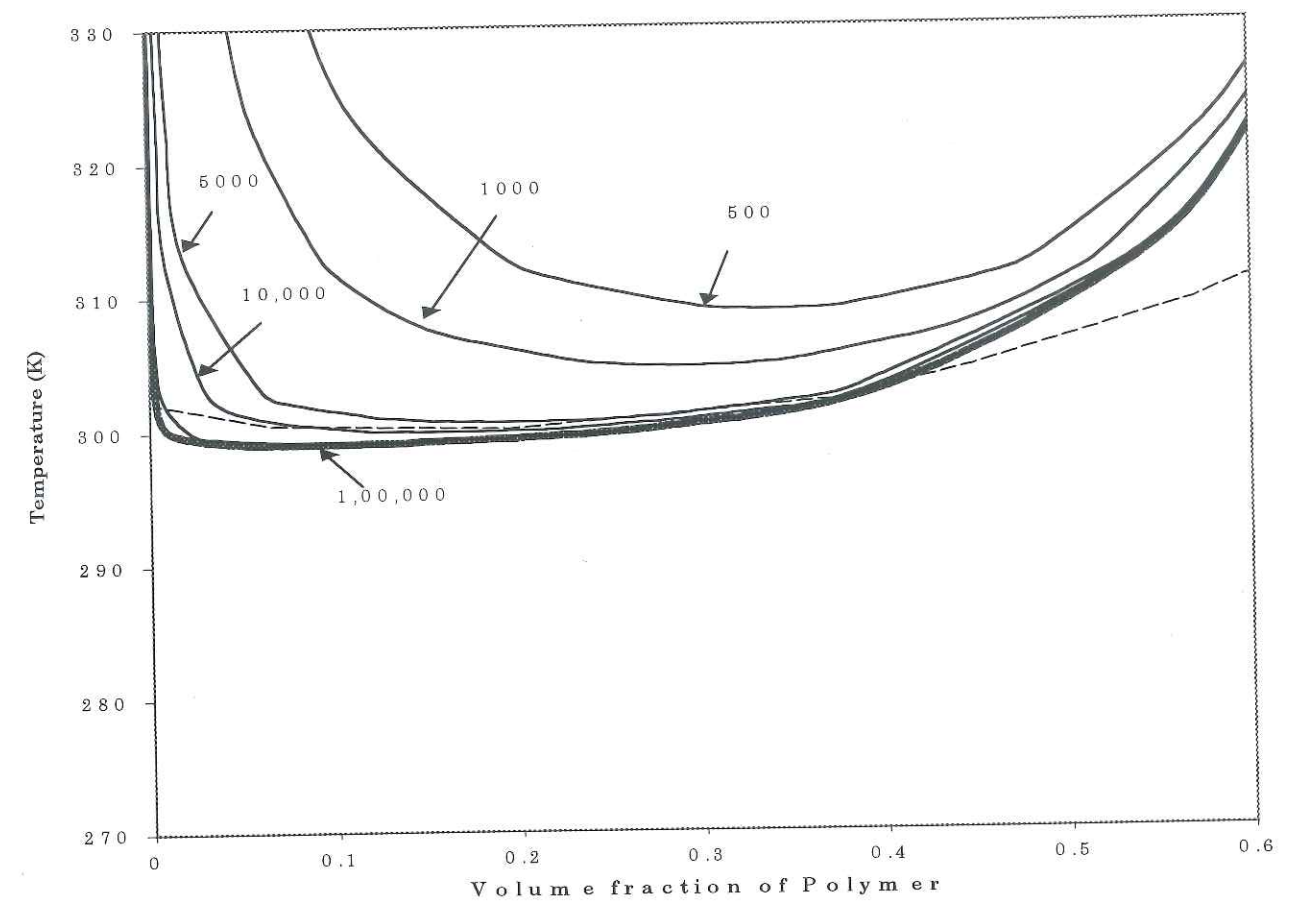


Figure 5.1: Predicted phase diagram of PNIPAm of different molecular weights

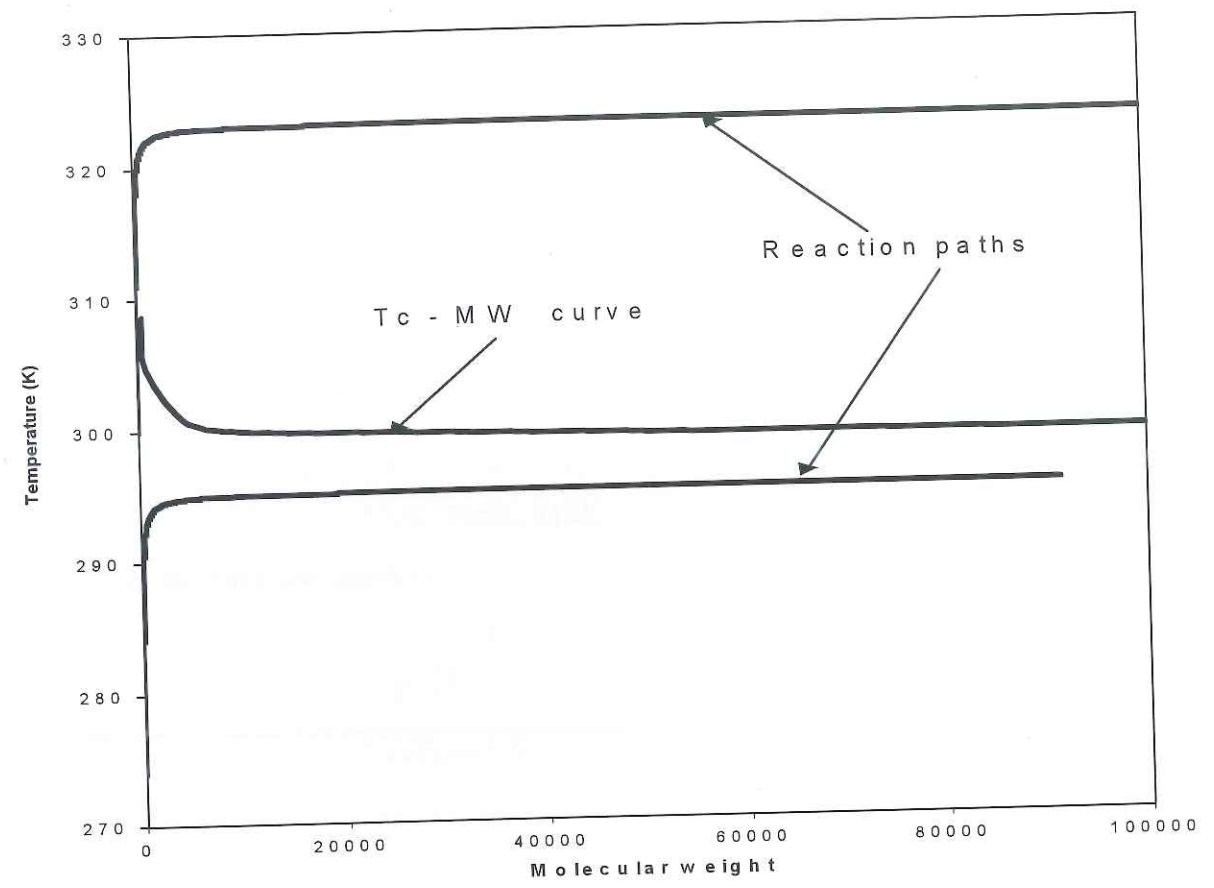


Figure 5.2: Tc-MW phase diagram superimposed on reaction paths showing phase separation

Table 5.3
Parameters for kinetics of polymerization

Rate constants	
k_d	$3.845 \times 10^{16} \exp.(-140.2 \times 10^3/RT)$
k_p	$2.024 \times 10^6 \exp.(-12.95 \times 10^3/RT)$
k_t	$1.630 \times 10^9 \exp.(-69.34 \times 10^3/RT)$
Initial conditions	
I_o	$8.5 \times 10^{-6} \text{ gmol/cm}^3$
M_o	$8.85 \times 10^{-4} \text{ gmol/cm}^3$
T_o	279K, 300K, 318K
Reaction mixture parameters	
ΔH	24.2 kcal/gmol
ρ	1 g/cm ³
C_p	1 cal/gmol-K

The reaction paths can enter different parts of the two-phase region, which is more clearly seen in Figure 5.3 where the phase diagram is superimposed on the reaction pathways. Depending on the initial temperature and the initial monomer concentration, the reaction path can either remain in the single-phase region, or can enter the two-phase region from the polymer-lean side or the polymer-rich side. If the two-phase region is never crossed, as in path (1) of Figure 5.3, the reaction mixture will remain as a single-phase system and the gel so formed will be transparent. If the reaction path just enters the two-phase region and remains in the metastable region as in path (2), the reaction mixture could phase separate by the nucleation and growth mechanism to form polymer-rich domains. Reaction paths (3) and (4) provide deep quenches into the two-phase region such that the phase separation would occur most probably by the spinodal decomposition mechanism. For the case of path (3), a continuous network-like morphology of the polymer-rich phase could be anticipated by rapid spinodal decomposition. The initial temperature in path (3) is the same as in path (2); however, the initial monomer concentration is higher. For path (5), where the reaction mixture enters the two-phase region from the polymer-lean side of the phase diagram, a combination of particulate and network morphologies could be anticipated.

Figure 5.4 shows the SEM micrographs of PNIPAm 1mm thick gel films synthesized at initial temperatures of 6°C (a) and 27°C (b) and an initial monomer concentration of 10% by weight. Also, shown is a gel film synthesized at 6°C but at double the initial monomer concentration (c). It is easy to show from typical numbers in Table 5.3 that for these films the time scale for heat transfer is larger than the reaction time scales, hence near-adiabatic conditions can be assumed. It is seen from Figure 5.4 that the gel synthesized at 6°C and 10% monomer initial concentration contains very fine particles of about 100 nm size. This morphology is similar to that expected by path (2) in Figure 5.3. For the gel synthesized at 27°C, a large-scale morphology is seen in which water-rich droplets of 10-20 μm are dispersed in a polymeric network. The droplets are formed from the water-rich phase, while the supporting network is most probably formed by spinodal decomposition of the polymer-rich phase. This morphology is similar to that obtained by path (3) in Figure 5.3.

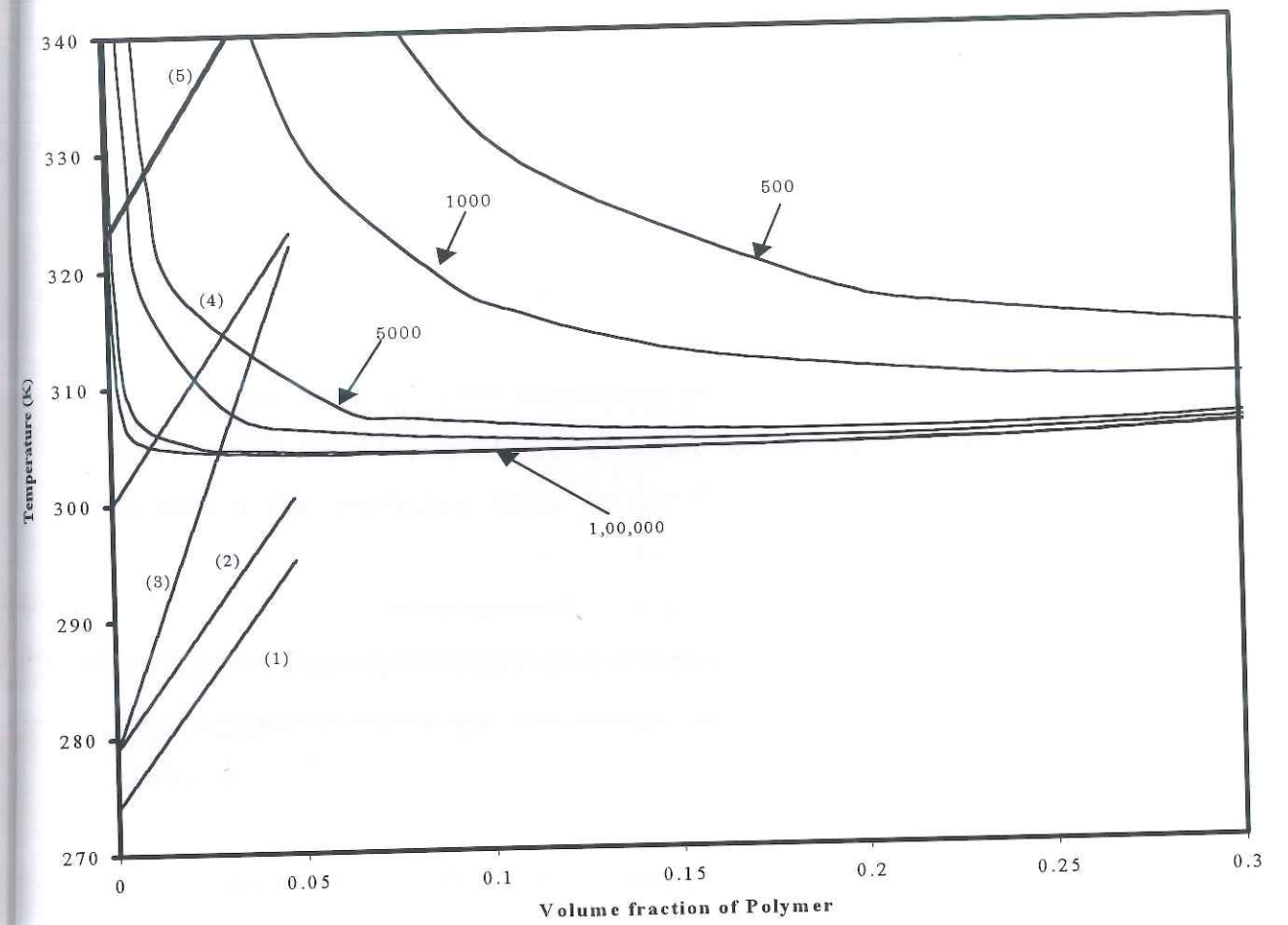
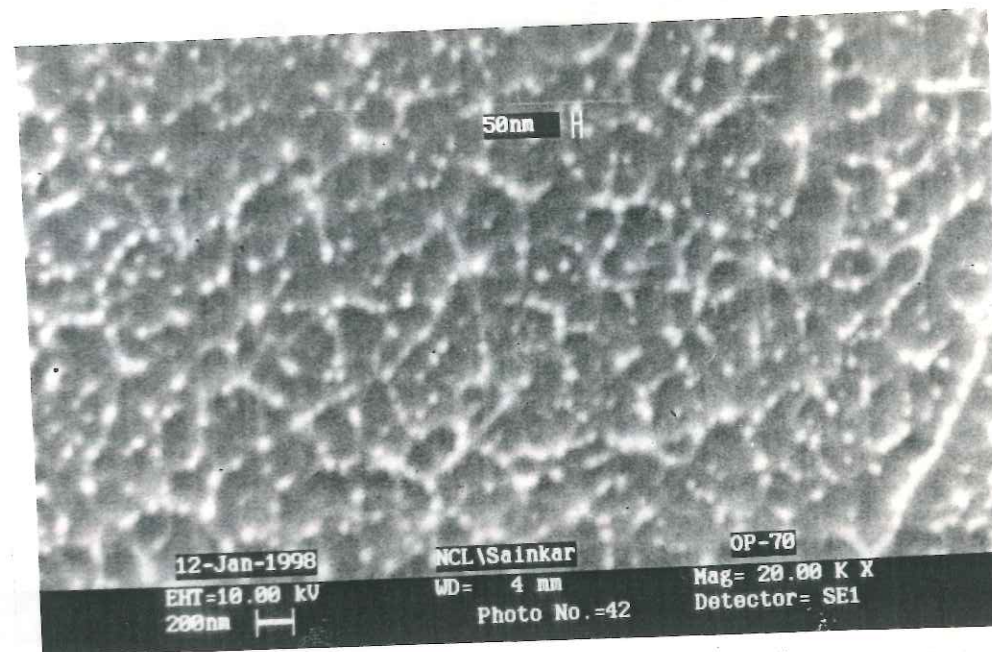


Figure 5.3: Various reaction paths entering the phase diagram in different regions

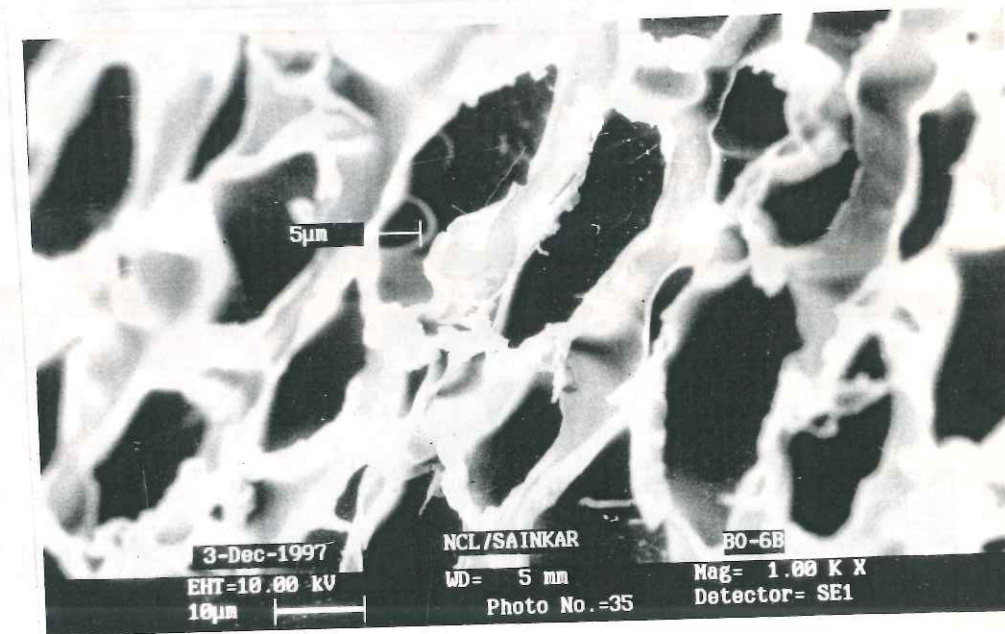
The gel synthesized at 6°C but at double the initial monomer concentration shows a combination of particulate and network morphologies, which is similar to that obtained from path (3) in Figure 5.3. Gels synthesized at an initial temperature of 50°C also show similar morphology since the reaction path starting from this temperature will also enter the two-phase region from the polymer-lean side (Figure 5.3). Finally, if the gels are synthesized in a non-adiabatic process, wherein one side of the gel is kept at 10°C during synthesis and the other side is open to air, then the gel shows a variation in the microstructure along its thickness as seen in Figure 5.4 (d).

Figure 5.5 predicts the temperature rise in the film assuming a constant wall temperature at one side (cooled side) and a zero heat flux on the other side (air-side). The variation in the temperature across the film thickness correlates with the variation in morphology. The lower temperatures on the cooler side causes shallower quench into the two-phase region, while the accumulated heat near the air interface causes deeper quench into the two-phase region. Hence the microstructure at this side consists of larger pores. Thus, a variety of mesoscopic morphologies are obtained starting from different initial conditions.

Gels with these different morphologies show different swelling behavior in water. In Figure 5.6 we have compared the equilibrium swelling of gels prepared at 6°C, 27°C and 50°C in water with that prepared by the conventional procedure in 1,4-dioxane at 70°C. The gel synthesized in dioxane shows a large volume transition in which the swelling capacity decreases from about 20 g/g to almost dry state (~1 g/g) at 30°C, which is close to the LCST of PNIPAm. In contrast, the swelling capacity of the gels prepared in water show a decrease in swelling ratio, a reduced magnitude of volume transition and a slightly higher transition temperature. The gel prepared at 50°C, which has a sponge-like in appearance, shows the most reduced swelling capacity and magnitude of volume transition.

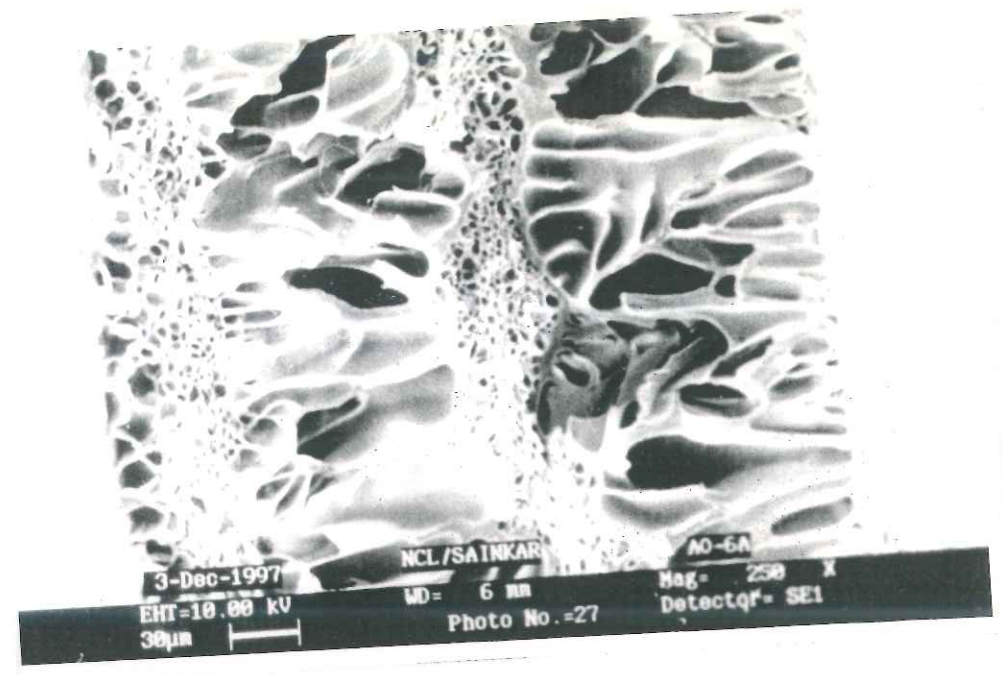
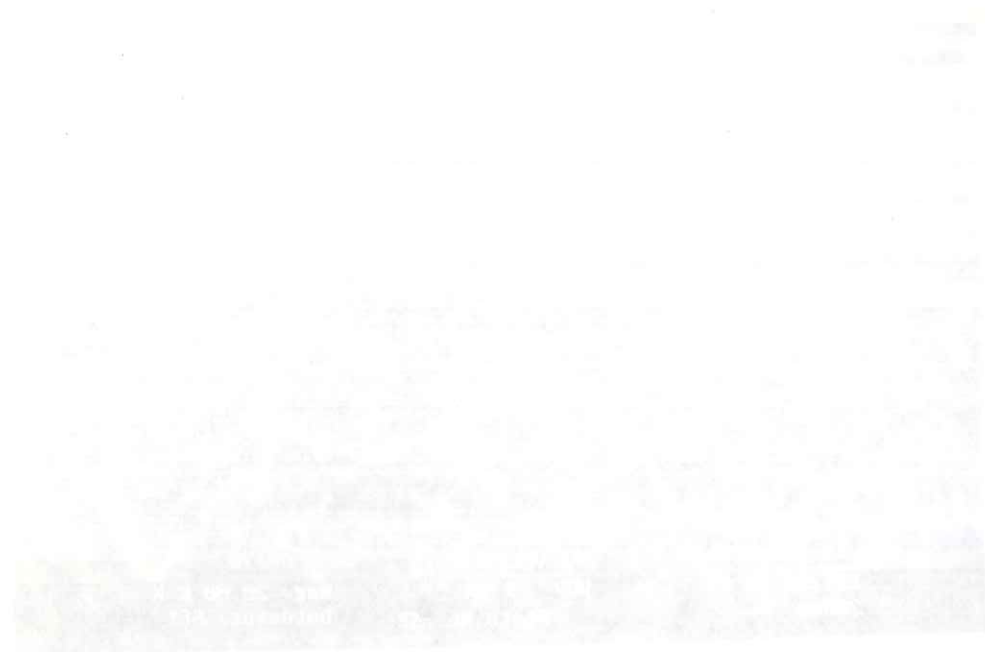


(a)



(b)

Figure 5.4: Scanning Electron Microscopy of PNIPAm gel films prepared at different initial conditions. (a) $T_0=6^\circ\text{C}$, $M_0=10\%$ by wt, (b) $T_0=27^\circ\text{C}$, $M_0=10\%$ by wt.



(c)



(d)

Figure 5.4: Scanning Electron Microscopy of PNIPAm gel films prepared at different initial conditions. (c) $T_0=6^\circ\text{C}$, $M_0=20\%$ by wt, (d) non-adiabatic with one side of the film at 10°C and other side exposed to air.

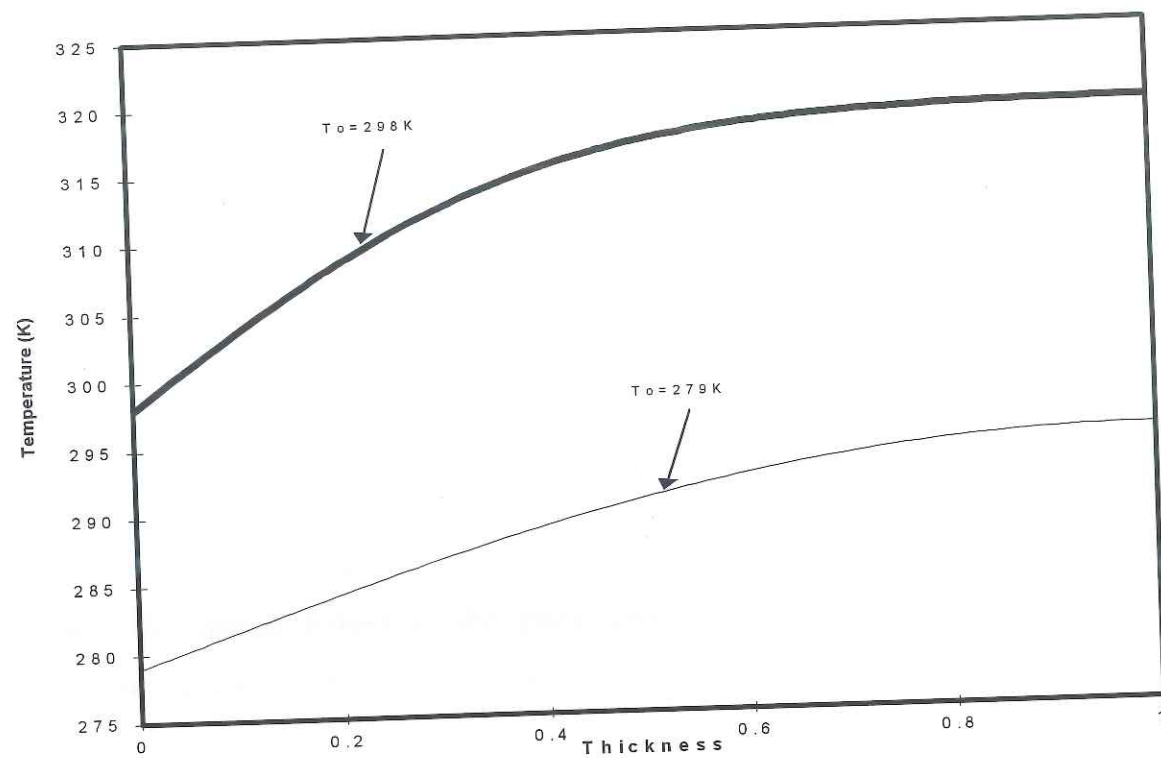


Figure 5.5: Prediction of temperature rise in a non-adiabatic polymerization process in a film with one side cooled and the other exposed to air

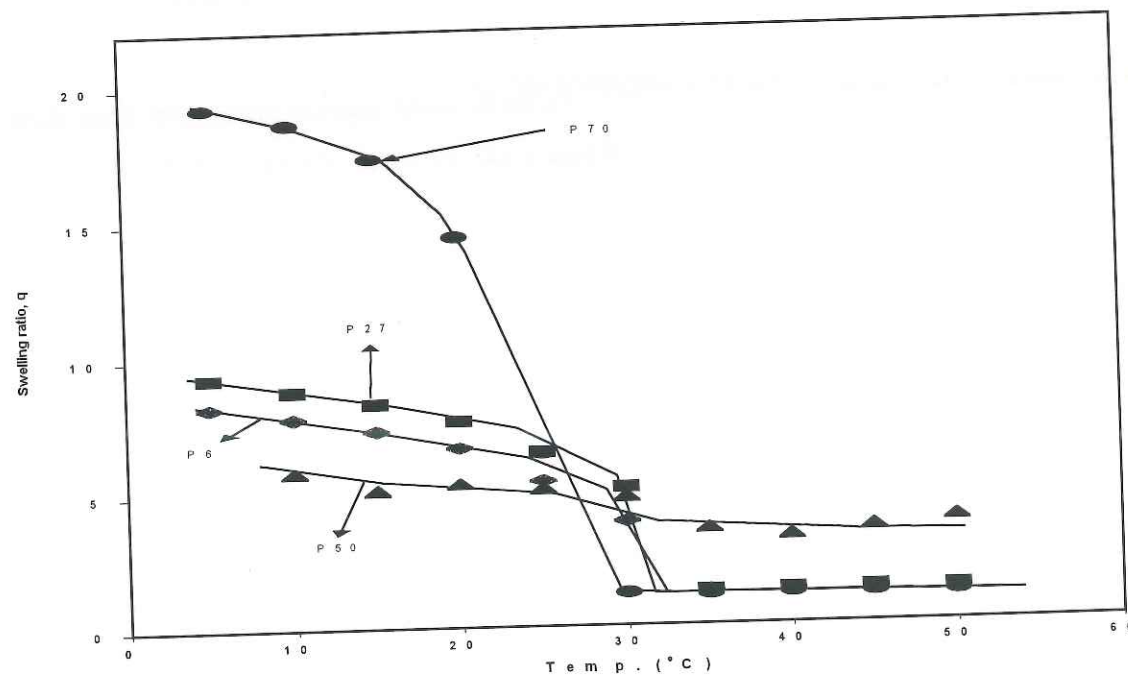


Figure 5.6: Swelling capacities of gels having different heterogeneous morphologies

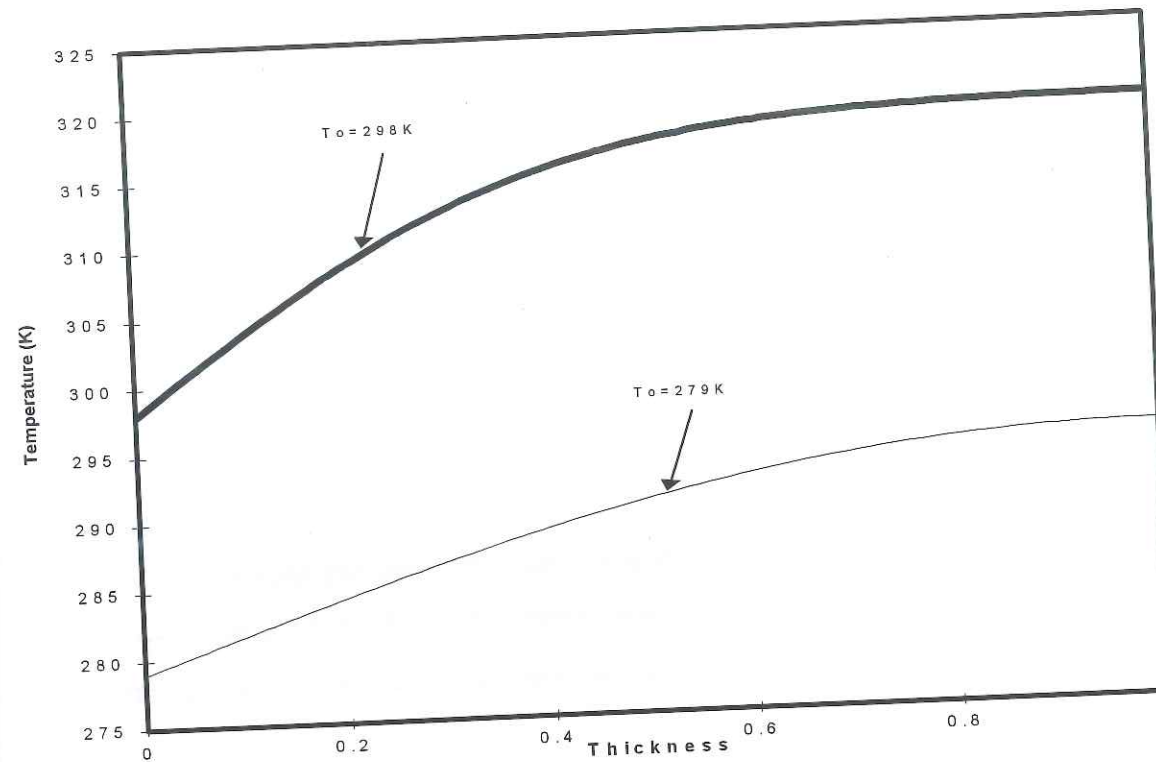


Figure 5.5: Prediction of temperature rise in a non-adiabatic polymerization process in a film with one side cooled and the other exposed to air

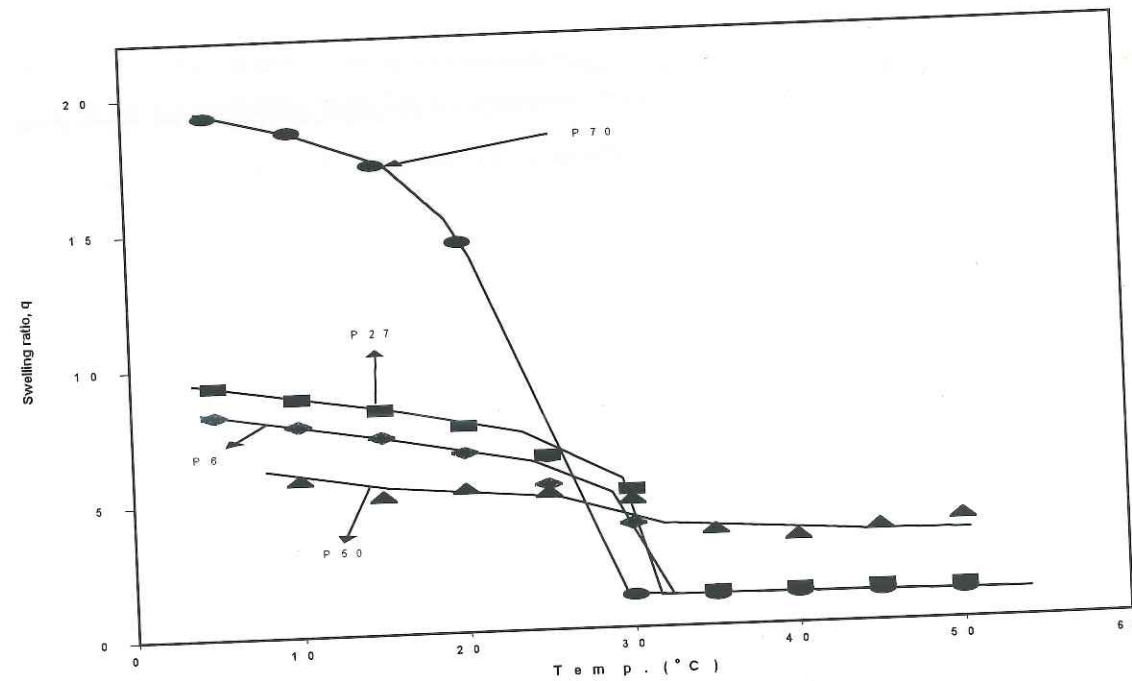


Figure 5.6: Swelling capacities of gels having different heterogeneous morphologies

It is important to realize that the water absorbed by the gels, which show heterogeneous morphologies, exists in two different states in the gel. A large part of the water exists as water-filled domains, which are created during the phase separation process. A relatively smaller amount of water is osmotically absorbed in the gel walls forming the network, which holds the water-filled domains. Since the polymer-rich network formed by phase separation occupies only a part of the total volume of the mixture, it would contain a larger crosslink density than that in a non-phase-separated gel (such as that prepared by conventional route). Therefore, the absorption capacity of the gel is reduced as compared to the conventionally synthesized gel. Similarly, if the gel has an extremely porous and open structure (as is the 50°C gel), then significant amount of water can remain lodged in the pores even at temperatures above the transition temperature. Hence, the gel shows a reduced magnitude of volume transition compared to other gels.

The heterogeneous microstructure of the gel also affects its swelling kinetics as shown in Figure 5.7. The gel synthesized in 1,4-dioxane (P70) and which does not contain any heterogeneous morphology has the slowest rate of water absorption. Water absorption in this gel takes place by diffusion of water inside the gel followed by cooperative swelling of the polymer chains of the gel. Compared to the non-porous P70, the gels P6, P27 and P50 have increasing rates of water absorption, which correlates well with their increasing porous microstructure. The larger the pore size, the smaller is the size scale of the network structure. As a result, the length scale over which water has to penetrate to swell the gel wall is smaller. Hence the absorption rates are faster.

Swelling of P6 gel also results in an optical transition in the gel from an initial transparent state to an opaque gel. As shown in Figure 5.8, the gel remains transparent till a swelling ratio of 4, after which it becomes transparent and opaque above a swelling ratio of 6. The change in transparency of the gel is caused by swelling of the pores with water to a size above the wavelength of visible light so that the incident light is scattered thus, rendering the gel opaque.

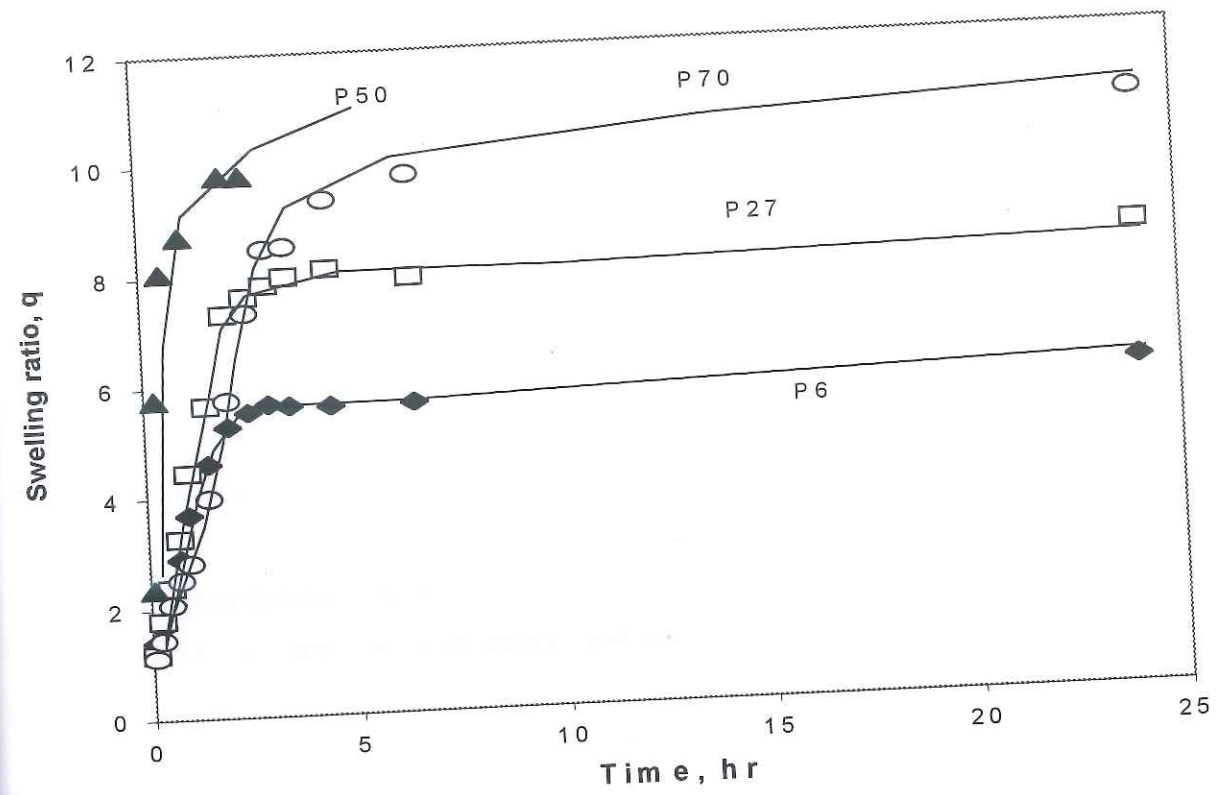


Figure 5.7: Swelling kinetics of gels showing heterogeneous morphologies.

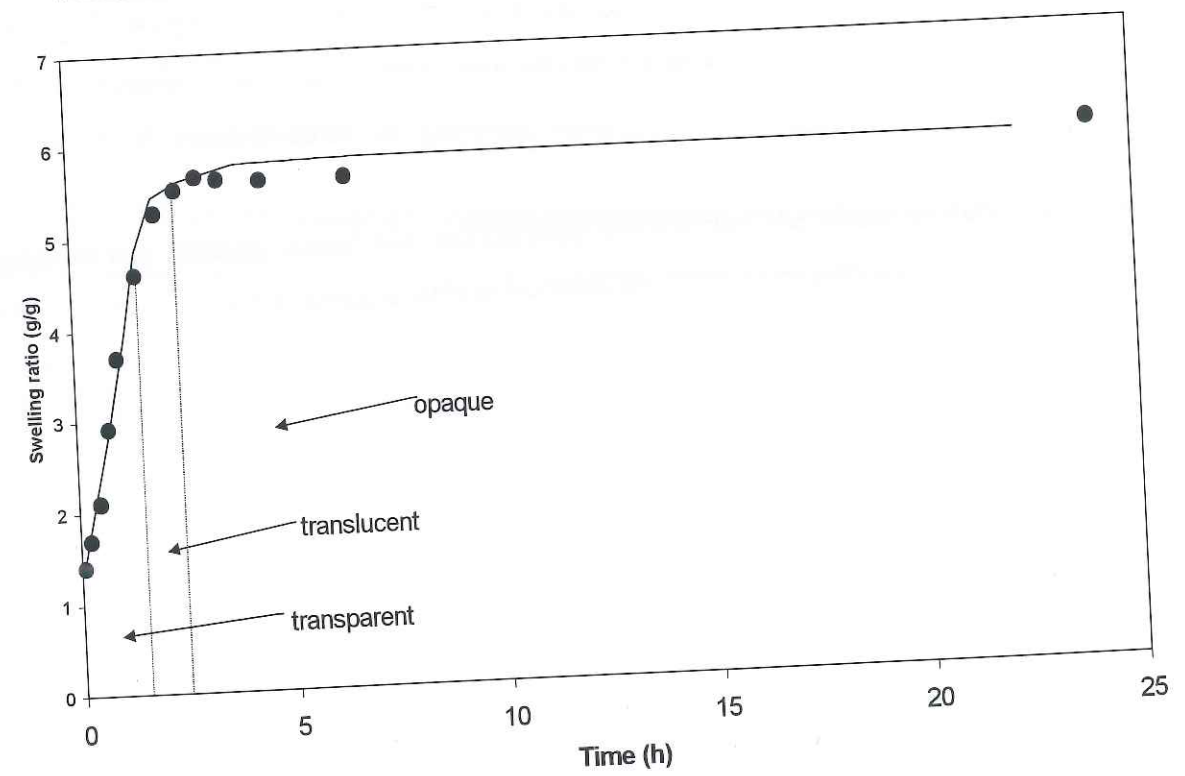


Figure 5.8: Optical transition of P6 gel during swelling

We have seen so far that a simple model, in which the phase diagram and the polymerization pathways are decoupled and superimposed, can predict the formation of different morphologies in PNIPAm gel. However, once the reaction mixture enters the two-phase boundary of the phase diagram, the rate processes of polymerization and phase separation occur simultaneously and are actually coupled. The coupling is clearly demonstrated in Figure 5.9, which shows the absorbance of a light of wavelength 555 nm through a polymerizing sample at room temperature (25°C) as a function of time measured on a Shimadzu UV-Vis spectrophotometer. For the case of polymerization of linear PNIPAm, the absorbance increases rapidly after an initial time of 300 seconds, then saturates at a high value till about 500 seconds and finally decreases gradually again. The rapid increase in absorbance indicates rapid polymerization of PNIPAm accompanied by phase separation and the gradual decrease of absorbance indicates the redissolution of PNIPAm in water as the solution cools down below the LCST. For the case of NIPAm polymerization in the presence of a cross-linker, there are two distinct differences seen in Figure 5.9. Firstly, the rapid rise in the absorbance occurs consistently at about 20 seconds earlier than that for linear PNIPAm, which indicates, that gelation influences the phase separation process. Phase separation in turn, will also influence the gelation kinetics since the reaction rates will be enhanced in the polymer-rich phase due to increased concentration of growing chains. Secondly, the absorbance remains permanently at a high value, contrary to that for linear PNIPAm. This suggests that the gelation has "pinned down" the morphology by freezing the phase separation process. Thus, there is in fact a strong coupling between the kinetics of polymerization and phase separation.

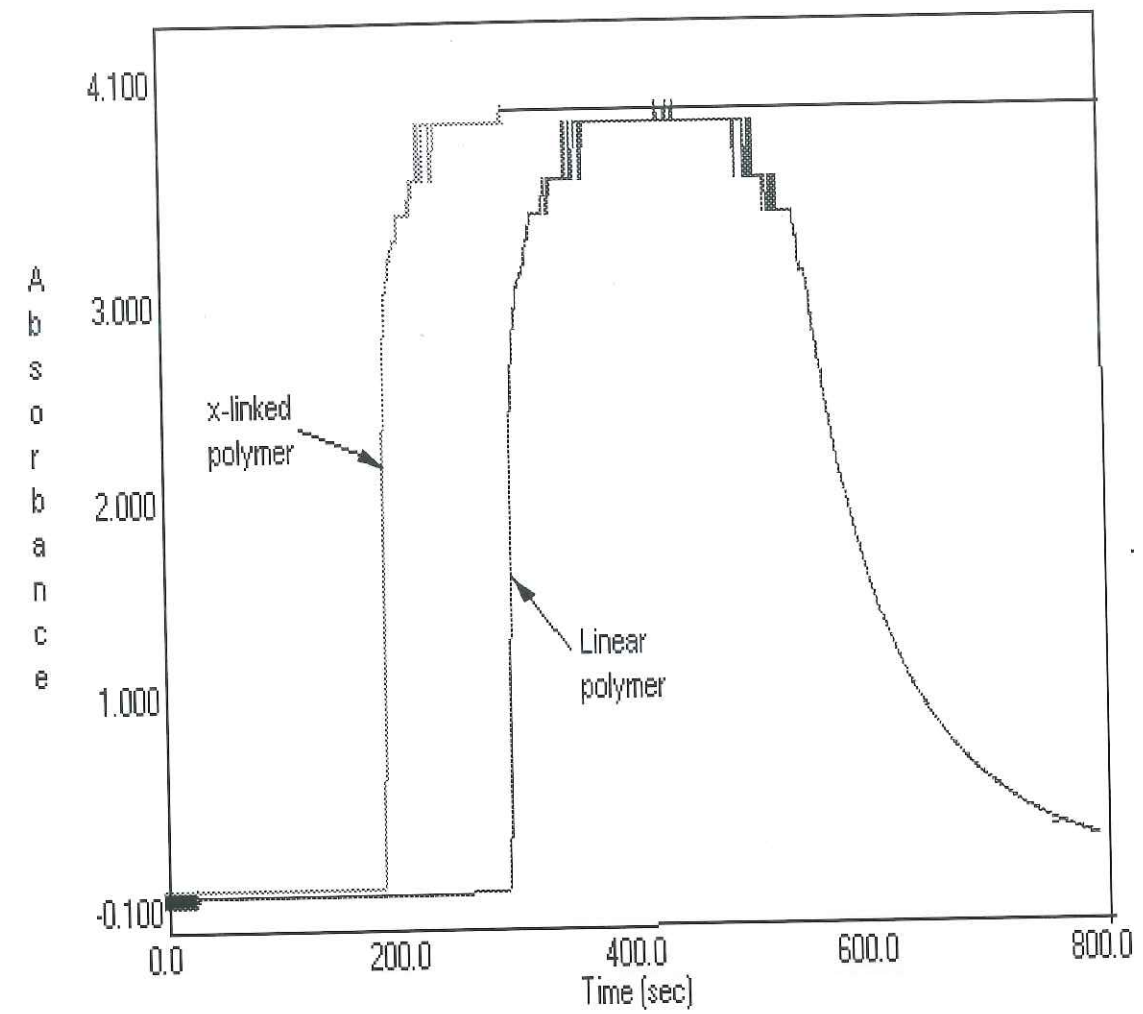


Figure 5.9: Absorbance of PNIPAm versus time measured in UV-Vis spectrophotometer (Shimadzu, UV-1601PC) at constant $\lambda=555$ nm

5.9 Conclusions

We have shown that a wide variety of mesoscopic morphologies can be obtained in a stimuli-responsive gel such as poly (N-isopropylacrylamide) by synthesizing the gel under conditions wherein phase separation of the reaction mixture occurs during polymerization and gelation. It is possible to predict qualitatively the type of morphology, which will be created under a given set of experimental synthesis conditions, by predicting the phase diagram of the polymer solution and superimposing on it the predicted reaction path.

The mechanism of phase separation depends on the region in the two-phase diagram in which the reaction mixture enters during polymerization. We have predicted the phase diagram of PNIPAm in water using the LFHB model. The polymerization kinetics were assumed to be those of acrylamide monomer in water under similar conditions. Predictions of adiabatic polymerization paths, when superimposed on the phase diagram showed that phase separation could occur by deep or shallow quenches into the two-phase region depending on the initial conditions of temperature and monomer concentration. The predicted type of morphologies agreed with those obtained by SEM. Thus, it is possible to control the morphology in a stimuli-responsive gel. Gels with such morphologies have different swelling capacities and swelling kinetics.

Finally, we have shown that there exists a strong coupling between the kinetics of phase separation and gelation. A comprehensive theory for predicting morphologies in a more quantitative manner should account for this coupling.

5.10 References

1. H. G. Schild, *Prog. Poly. Sci.*, **17**, 163 (1992).
2. J. D. Gunton, M. San Miguel, P. S. Sahni, in "Phase transitions and critical phenomena", C. Domb and J. L. Lebowitz (Eds) Vol. 8, Academic Press, London, p-267 (1983).
3. K. Otake, H. Inomata, Y. Yagi, M. Konno, S. Saito, *Polym. Commun.*, **30**, 203 (1989).
4. A. K. Lele, M. V. Badiger, V. S. Bhalerao, S. N. Sainkar, R. A. Mashelkar, in "Structure and Dynamics of Materials in the Mesoscopic Domain", M. Lal, R. A. Mashelkar, B. D. Kulkarni, V. M. Naik, (Eds.), Imperial College Press and the Royal Society, London, p119-138 (1999).
5. C. Parayiotou, I. C. Sanchez, *J. Phys. Chem.*, **95**, 10090 (1991).
6. A. K. Lele, M. V. Badiger, M. M. Hirve, R. A. Mashelkar, *Chem. Eng. Sci.*, **50**, 3535 (1995).

6.1 Conclusions

In view of the increasing demand for thermosensitive polymers for various applications, there is a need to develop newer thermosensitive polymers. Therefore, this work focused on the design and synthesis of new hydrophobic comonomers and the consequent development of novel thermosensitive polymers by incorporating these new comonomers. The influence of chemical structure and various additives on the transition properties of these polymers has been corroborated.

The conclusions of this work can be summarized as follows,

- Hydrophobically modified copolymer gels were synthesized by copolymerizing N-isopropylacrylamide with vinyl comonomers having increasing length of alkyl chain. These hydrogels showed lower LCST and lower heat of transition when compared to pure PNIPAm gel. The reduction in the transition temperature was found to increase with the length of the alkyl chain and the concentration of the hydrophobic comonomers. The experimental results were compared with the theoretical calculations based on the lattice-fluid-hydrogen-bond [LFHB] model. A linear correlation between the transition temperature and the number of alkyl groups was found to exist in these gels. Such a correlation could be useful in designing/tailoring gels with specific transition temperatures.
- The copolymer gels were synthesized based on poly(ethylene oxide) and PNIPAm by γ -radiation technique. The temperature dependent swelling ratio measurements of these gels in water showed that, the PEO homopolymer do not exhibit a well defined first order transition eventhough PEO belongs to a type of LCST polymer. On the other hand copolymer gels of PEO and PNIPAm showed clear LCST behavior. The LCSTs of the gels were found to be dependent on the composition of the copolymers. Since these gels are synthesized by γ -radiation technique they are free from impurities and can have potential biomedical applications.
- The thermosensitive copolymer gels based on poly(N-isopropylacrylamide) and poly(acryloyl aminoacids) were synthesized and their interactions with an anionic surfactant namely, sodium dodecyl sulfate (SDS) was studied. Binding of SDS with copolymer gels enhanced the swelling ratios and LCSTs remarkably. This study led to an interesting observation of core-shell morphology in the swollen gels along with two unusual discontinuous volume phase transitions. Such core-shell morphology in

Chapter 6
Conclusions and Directions for future work

thermosensitive hydrogels can have potential applications in controlled drug delivery systems.

- Influence of various experimental conditions on the synthesis of PNIPAm gels were studied. The gels showed a wide range of mesoscopic structures. The mesoscopic structures in these morphologies were formed as a result of the phase separation of the polymerizing mixture into polymer-rich and water-rich domains, which were simultaneously frozen into a permanent morphology due to gelation. It has been shown theoretically and experimentally that by controlling the gelation kinetics it was possible to freeze the morphology of a gel in the metastable or the unstable regions of the phase diagram.

6.2 Directions for the future work

The present work was an attempt to synthesize tailor-made thermosensitive hydrogels with specific LCSTs by changing the chemical structure of hydrogel by introducing hydrophobic groups in the chain or by changing the ratio of two monomers concentrations in the copolymerization. This work also describes influence of surfactant and experimental condition on the swelling behaviour of thermosensitive polymers.

This work could be further extended to the following systems,

1. We have studied the effect of hydrophobicity on the LCST of thermosensitive polymers. If we incorporate hydrophilic comonomers in NIPAm, the LCST of a copolymer gel should increase. But there are certain monomer systems such as dimethyl aminoethyl methacrylate (DMAEMA) and acrylamide, which form internal hydrogen bonding with other comonomers and both collectively act as hydrophobe, which would lead to a decrease in LCST, instead of increasing it. Study of such systems, which influence LCST of copolymer in opposite direction, could be interesting.
2. There is great scope for the design of thermosensitive microgels and latexes based on the above type of copolymer gels. They can create unique temperature dependent fluid properties when they are suspended in aqueous media. Strictly speaking, microgels are insoluble and do not form solutions as such, but may be considered to form colloidal dispersions.

3. We have seen core-shell morphology in the copolymer gels in the presence of surfactant, SDS. This morphology could be useful for designing novel drug delivery systems in which the drug can be loaded in the inner core part of the gel and its release in response to temperature can be controlled.
4. We have examined the mesoscopic morphologies developed during the phase transition of thermosensitive polymers. The theoretical framework of coupling between the kinetics of phase separation and gelation developed, although was successful in giving mechanistic insights, is still somewhat qualitative. A more comprehensive theory should take into account such a coupling. This would require solving the equations (5.8 to 5.13) for polymerization simultaneously with equations describing phase separation kinetics such as for example, the linear regime of spinodal decomposition process given by

$$\frac{\partial \phi}{\partial t} = M \nabla^2 \mu_2 + \eta$$

where, M is the mobility of phase separating polymer chains, μ_2 is the polymer chemical potential given by equation (5.2) and η is a thermal noise term.

The relative time scales of gelation and phase separation would finally decide the formation of specific morphologies in the gel. Thus,

$$\frac{\tau_{gel}}{\tau_{SD}} < 1 \quad \Rightarrow \quad \text{Fine morphology (smaller length scale domains)}$$

$$\frac{\tau_{gel}}{\tau_{SD}} > 1 \quad \Rightarrow \quad \text{Coarse morphology (larger scale domains)}$$

where, the time scale for spinodal decomposition is approximately given by, $\tau_{SD} \approx |T - T_c|^{-1.75}$ and the gelation time scale is related to, $\tau_{gel} = f(k_t, M_o, R_G^2 / D_p)$ [Ref. R. Bansil, G. Liao, Trends in Polym. Sci., 5, 146 (1997)].

Besides early spinodal decomposition a complete theory should also incorporate other phase separation processes such as non-linear hydrodynamic regimes in spinodal decomposition, ripening mechanism and nucleation and growth mechanism.

Finally, the mechanisms responsible for "pinning down" of morphologies by gelation such as a rapid rise in viscosity of the polymer-rich phase by gelation, which will retard the hydrodynamic spinodal process or the ripening process, will also have to be incorporated in a comprehensive theory.



5 AUG 2002

NATIONAL CHEMICAL LABORATORY
REFERENCE BOOK
(NOT TO BE CHECKED)